A.G.Venkatesh

Novel Platform for DNA Alignment and Studying DNA-Protein Interaction in Realtime

Bielefeld University

Examining Committee

Prof. Dr. Günter Reiss (Thesis Review)

Prof. Dr. Walter Pfeiffer (Thesis Review)

Prof. Dr. Anke Becker

Prof. Dr. Peter Reimann

submitted to bielefeld university

Printed, October 2011

Declaration

I hereby declare that this thesis is my own work and that, to the best of my knowledge and belief, it contains no material previously published or written by another person nor material which to a substantial extent has been accepted for the award of any other degree or diploma of the university or other institute of higher learning, except where due acknowledgement has been made in the text.

A.G.Venkatesh
Bielefeld University

Abstract

Recreating DNA-protein interaction *in vitro* could unravel the relationship between their structure and function, which necessarily requires transforming the DNA from its coiled state to a linear form. In this work, two main techniques were developed to realize this aim namely, orientation-defined DNA alignment and realtime monitoring of polymerase movement.

Orientation-defined alignment of DNA was performed by bifunctionalization of DNA with two different pairs of chemical groups namely, thiol and biotin or thiol and silane at the termini. The terminal functionalized DNA was dropped on a nanofabricated electrode and aligned across the gold and silicon dioxide surface using electrokinetic force.

The Movement of polymerase in realtime was monitored using molecular-beacons as reporters. The molecular beacons bind at regular intervals on a DNA that contains highly repeated sequences called homopolymer DNA. The homopolymer DNA will act as a template for the polymerase. The total fluorescence intensity decreases as the polymerase copies the second strand of DNA, due to removal and closing of molecular beacons. *E. coli* DNA polymerase I, T7 DNA polymerase, T7 RNA polymerase, and N4 virion RNA polymerase were used to validate this new technique.

Contents

1 Introduction **9**
2 Basic Background **11**
2.1 Lithography and Fabrication 11
2.2 Manipulation of DNA 14
2.3 Molecular Biological Techniques 17
3 Experimental Procedure **25**
3.1 Alignment of DNA 25
3.1.1 Fabrication of Electrode 25
3.1.2 Synthesis and Modification of DNA 27
3.1.3 Pre-preparation and Alignment of DNA 31
3.1.4 DNA Visualization 32
3.2 Homopolymer DNA Synthesis 33
3.2.1 Synthesis of Homopolymer DNA 33
3.2.2 Concatemerization of DNA with Repeated Sequence 35
3.2.3 Preparation of Single-Stranded DNA 39
3.2.4 Molecular Beacon: Design and Characteristics 40
3.2.5 DNA Template for DNA Polymerase Analysis 40
3.2.6 DNA Template for RNA Polymerase Analysis 42
3.2.7 Optimization of Parameter Settings for Fluorescent Analysis 42
3.2.8 Data Analysis 44
4 Results **45**
4.1 Alignment of DNA 45
4.1.1 DNA Bifunctionalized with Thiol and Biotin 45
4.1.2 DNA Bifunctionalized with Thiol and Silane 51

4.2 Synthesis of Homopolymer DNA 53
4.2.1 Synthesis of 239bp DNA 53
4.2.2 Synthesis of 773bp DNA 53
4.2.3 Rolling Circle Amplification 55
4.2.4 Synthesis of DNA with Specific Insertion Sequences 55
4.3 Real time analysis of DNA/RNA polymerase activity on homo polymer DNA 58
4.3.1 Optimization of Realtime Fluorescence Method 60
4.3.2 Analysis of DNA Polymerases 62
4.3.3 Analysis of RNA Polymerases 66
5 Discussion 67
5.1 Alignment of DNA 67
5.1.1 Immobilization and Visualization of DNA 67
5.1.2 Alignment of DNA Functionalized with Thiol and Biotin 68
5.1.3 Alignment of DNA Functionalized with Thiol and Silane 73
5.1.4 Compared to Literature 75
5.2 Synthesis of Homopolymer DNA 76
5.2.1 239 bp and 773 bp DNA 77
5.2.2 Synthesis of DNA with Specific Insertion sequences 79
5.3 Molecular-Beacon Characteristics 81
5.3.1 Thermodynamics 81
5.3.2 Specificity and Stability 84
5.4 Polymerase Activity 84
5.4.1 *E. coli* DNA Polymerase I 84
5.4.2 T7 DNA Polymerase 86
5.4.3 RNA Polymerases 89
5.4.4 Compared to Literature 92
5.5 Conclusion 94
5.6 Outlook 96
6 Summery 99
7 References 101
8 Appendix 111
9 List of Publications 115
10 Acknowledgement 117

1
Introduction

Evolution of life began on earth with an unicellular organisms and over a period of millions of years they evolved into multicellular organisms. During the course of this evolutionary process they adapted to the environment and acquired more complexity in their genetic constitution. All the information regard to their basic characteristics are enshrined in **nucleic acids**.[1] These nucleic acids are later found to be **Deoxyribonucleic acid (DNA)** in almost all organisms and **Ribonucleic acid (RNA)** in some viruses.

[1] A. Hershey et al., J Gen Physiol **36**, 39 (1952)

While *genotype* represents the entire genetic information of an organism, the *phenotype* represents all the visible expressions of the genetic information. In a molecular sense this is called **Central dogma of molecular biology**, where the information passes from DNA to RNA to Protein. During the life cycle of an organism, the DNA is copied to another set of DNA called *DNA Replication* for the offspring, information in DNA is transferred to mRNA called *Transcription*, and synthesis of proteins using the information in mRNA called *Translation*.

mRNA
messenger RiboNucleic Acid

Understanding the important stages in DNA-protein interaction during cellular processes, such as replication, transcription and translation, which involves orchestration of many macromolecules could lead to designing novel drugs. In *in vivo* conditions, there are mechanisms to unwind and maintain the DNA in linearised state, but in *in vitro* conditions an external force is required to transform the DNA from coiled to linearised state.

The aim of this research work is to develop an experimental set-up that could recreate the biological process *in vitro*. A tool that can be employed in either bulk or single-molecule assay. In order to attain the objective, two main independent innovative techniques are developed namely, *Orientation defined alignment of DNA* and *Realtime analysis of DNA-Protein interaction*.

The orientation defined alignment is achieved by bifunctionalizing the DNA with *thiol* and *silane* and aligned between *gold* and *silicon dioxide* layers by electrokinetic technique, respectively.[2] Similarly, the realtime DNA-protein interaction analysis is a molecular beacon based fluorescence technique. In this technique, the change in total fluorescence as a function of time is directly correlated to the effect of DNA-protein interaction. A DNA template is synthesized consisting highly repeated sequence complementary to the molecular beacon and a specific insertion site for analysing DNA-protein interaction.

[2] E. Braun et al., Nature **391**, 775 (1998); V. R. Dukkipati et al., Appl. Phys. Lett. **90**, 083901 (2007); and H.-Y. Lin et al., Nanotechnology **16**, 2738 (2005)

The framework and contents of this thesis are briefed as follows. The chapter *Basic Background* explains all the underlying principles governing the performed experiments. The methods followed to attain the desired research goal are given in chapter *Experimental Procedure*. Chapter *Results* enlists the outcome of experimental research and the results are discussed in chapter *Discussion*. The thesis is concluded with a chapter *Summary* to give a final overview.

2
Basic Background

An interdisciplinary research requires a better understanding of basic concepts from related scientific domains. This chapter is a primer for understanding the principles behind the experiments presented in this thesis.

2.1 Lithography and Fabrication

Fabrication of micro- and nano-structures involves few important steps such as, material deposition, selection of resist, lithography and etching. Techniques used to fabricate electrode for orientation-defined alignment of DNA is given below.

2.1.1 Magnetron Sputtering

Sputtering is a form of physical vapour deposition process used for materials coating in semiconductor industry. In principle, a vacuum chamber filled with argon gas produces Ar^+ ions under an applied high DC voltage. This Ar^+ ions in plasma were accelerated towards the target (cathode) causing the target atom to eject. The high velocity imparted by ejection force will accelerate the target atom to hit the substrate (anode) to form a film with high density. The deposition rate can be increased by increasing the ionization density of argon gas by adding magnetic field in the system (fig 2.1). This magnetic field will influence the electron to follow the magnetic lines causing an increase in ion density to 10^{13} ions/cm^3 due to a higher degree of collision.

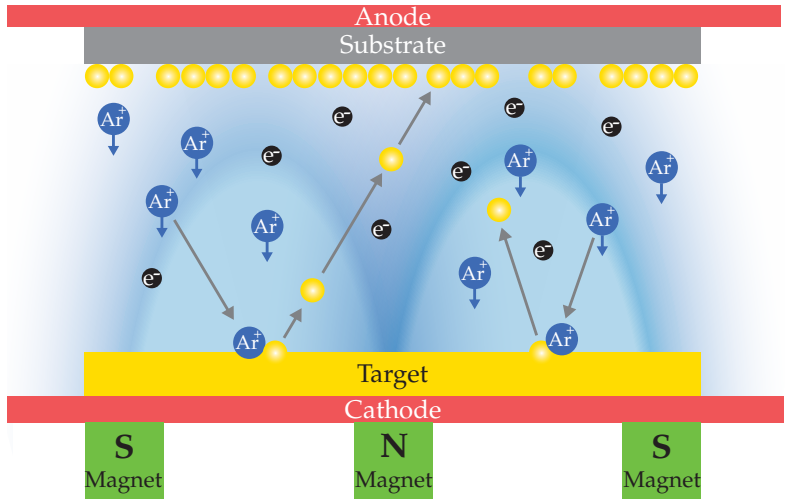

Figure 2.1: Schematic illustration of DC magnetron sputtering. Ar^+ ions in the plasma hits the target and ejects the atom. The ejected atom forms a thin film at the positive-biased substrate.

Unlike coating conductive materials, DC magnetron sputtering is not suitable for coating insulating materials, which requires 10^{12} volts resulting in arc formation. An alternative voltage current in radio frequency range of 13.56 MHz was applied to trap the positive charge in plasma zone and preventing accumulation at the cathode for a successful sputtering of insulating materials.

2.1.2 *Resist Chemistry*

Resist is a polymer used for transferring the pattern to substrate in a fabrication process. Resists are classified in two groups called tone, namely positive and negative. A positive resist becomes soluble in developer upon exposure, whereas the exposed region becomes insoluble in case of negative resist. Chemically, an exposure causes either a breakdown of high molecular weight polymer in to lower ones (positive) or a polymerization of monomers to high molecular weight polymer (negative). The resist for electron-beam lithography requires a sensitivity of 1 to 5 μC cm^{-2} at 20 kV.[1]

[1] E. Reichmanis et al., Annu. Rev. Mater. Sci. **23**, 11 (1993)

2.1.3 *Electron Beam Lithography*

This technique is performed by computer controlled scanning of a highly focused electron beam on resist-coated substrate. The amount of electron exposure per unit area is calculated by equation 2.1.

$$Area\ dose = \frac{Beam\ current \times Area\ dwell\ time}{(Area\ step\ size)^2} \tag{2.1}$$

In principle, the primary ionizing radiation generates secondary electrons with sufficient energies to breakdown of molecules in positive resist and polymerization in negative resist. Backscattered electrons is the major source of energy to dissociate or associate a chemical bond rather than forward scattering (fig 2.2). In the due process, the scattering electrons comes to a rest in the polymer after depositing all its kinetic energy. Electron-beam lithography offers high resolution due to the highly focussed electron source.

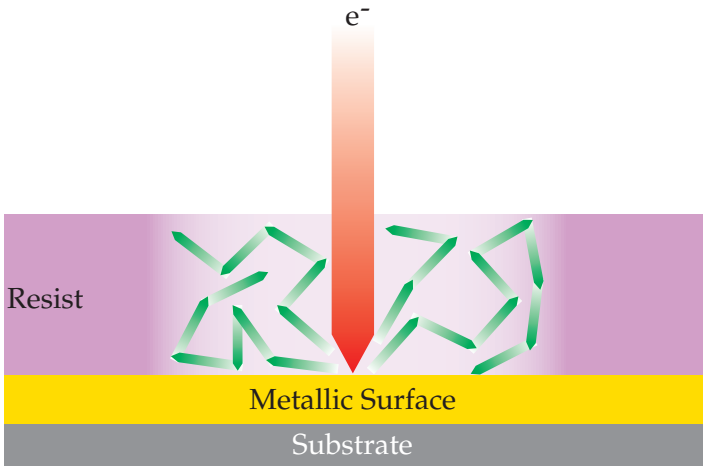

Figure 2.2: Schematic illustration of role of forward scattering (red) and back scattering (green) electrons altering the chemical nature of resist.

2.1.4 *Argon Ion Milling*

Ar^+ ions are used for removing unwanted thin film portion from the substrate after lithography. Argon is chemically inactive, heavy and readily ionised by applying a voltage. It is a reverse process of sputtering, where the substrate will be the target. The Ar^+

ions are accelerated by an electric field, will physically and chemically attack the atoms on the substrate's surface. The rate of atom removal can be monitored by mass spectrometer. This etching process delivers micro and nano structures with high aspect ratio compared to isotropic chemical etching.

2.2 *Manipulation of DNA*

The process of stretching DNA enables the spatial resolution, which is essential for investigating DNA-protein interaction[2] and DNA mapping.[3] The orientation of the DNA becomes significant, when its intrinsic electronic properties have to be investigated[4] as in molecular electronics,[5] for DNA templated nano-cargos,[6] or for an investigation of other physical properties of DNA.

The stretching of DNA can be achieved by exerting an applied force namely, *mechanical*, *Hydrodymanic*, *confinement elongation* and *Electrokinetic*, which yield different degree of stretching from under- to over-stretching.

[2] R. Riehn et al., Proc. Natl. Acad. Sci. USA **102**, 10012 (2005)

[3] T. R. Strick et al., Nature **404**, 901 (2000)

[4] V. Bhalla et al., EMBO reports **4**, 442 (2003)

[5] D. Porath et al., Nature **403**, 635 (2000)

[6] S. Sahu et al., Nano Lett. **8**, 3870 (2008)

2.2.1 *Mechanical Force*

DNA stretching by mechanical force include optical-tweezers, magnetictweezers etc., which yield either a single or few stretched molecules. To facilitate stretching, one or both ends of DNA were liked to bead or surface. Optical tweezer techniques are primarily used for quantifying force driving the DNA-protein interactions[7] where, one end of DNA is fixed to a surface and another end linked to the trapped bead is moved by a laser beam.[8] The trapping of bead by laser is caused by two forces namely gradient and scattering, when the laser is transmitted and reflected from the bead respectively. Both these forces attain equilibrium, when the bead is centered at the point of maximum light intensity; any change in this equilibrium is measured as a molecular event. Magnetic tweezers are similar to optical tweezers but magnetic field is applied on a magnetic bead.[9].

[7] K. C. Neuman et al., Rev. Sci. Instrum **75**, 2787 (2004)

[8] A. Ashkin et al., Optics Lett. **11**, 288 (1986)

[9] S. B. Smith et al., Science **258**, 1122 (1992)

2.2.2 *Hydrodynamic Force*

DNA can be stretched by fluid-flow or air-liquid interface causing a velocity gradient that exert a drag force on the coiled DNA. The process is called **molecular combing**,[10] which yields hundreds of stretched DNA. This type of stretching method is usually done on a substrate after surface treatment, which facilitates immobilization by hydrophobic interaction or net charge. The surface treated substrate is dipped into the DNA solution and retracted back slowly, during this time the DNA binds to the substrate and get stretched by moving air-liquid interface. This technique is good for DNA mapping but not for DNA-protein interaction studies because, most part of the DNA backbone is bound to the surface preventing the binding of protein. The force of receding meniscus exerted on the DNA is strong enough to overstretch the DNA beyond its physical length and prevent binding of proteins.[11]

[10] A. Bensimon et al., Science **265**, 2096 (1994); and J. Allemand et al., Biophys J **73**, 2064 (1997)

[11] Z. Gueroui et al., Proc. Natl. Acad. Sci. USA **99**, 6005 (2002)

2.2.3 *Confinement Elongation*

It is a physical entrapment technique, the dimensions of nano-channel will constrain the DNA to be stretched. This technique is referred as **entropy stretching**.[12] The DNA is forced to enter the nano-channel by an applied electric field and the magnitude of stretching increases with decreasing width of nano-channel. DNA mapping and protein interaction can be performed with this technique, since the stretched DNA is free from any interaction with the surface.[13]

[12] W. Reisner et al., Phys. Rev. Lett. **94**, 196101 (2005); M. Krishnan et al., Nano Lett. **7**, 1270 (2007); and Y. Kim et al., Lab Chip **11**, 1701 (2011)

[13] Y. M. Wang et al., Proc. Natl. Acad. Sci. USA **102**, 9796 (2005)

2.2.4 *Electrokinetic Force*

This technique exploits the polarizing property of DNA under the influence of an applied electric field. The behavior of DNA in an electric AC field is a function of frequency (f) and based on its dielectric properties. At low frequencies below 1 kHz, the DNA would follow the direction of electro-osmotic fluid flow due to the pronounced formation of a double layer[14] and at higher frequencies (1 kHz $\leq f \leq$ 1 MHz), DNA is attracted towards the high electric field region and hence trapping of DNA dominates rather than stretching due to a dielectrophoretic phenomenon.[15]

[14] H.-Y. Lin et al., Nanotechnology **16**, 2738 (2005)

[15] S. Tuukkanen et al., Nanotechnology **18**, 295204 (2007)

Dielectrophoresis

The dieletrophoretic force exerted on a particle of radius r due to an induced-dipole in an non-homogeneous electric field is given by,

$$\boldsymbol{F}_{DEP} = \Gamma \times \varepsilon_m Re[\boldsymbol{K}(\omega)] \nabla |\boldsymbol{E}|^2 \tag{2.2}$$

where, Γ is dependent on particle geometry, ε_m is the medium permittivity, $|\boldsymbol{E}|$ is the magnitude (rms) of the applied field and $Re[\boldsymbol{K}(\omega)]$ is the real component of the Clausius-Mossotti factor is given by,

$$\boldsymbol{K}(\omega) = \frac{\varepsilon_p^* - \varepsilon_m^*}{\varepsilon_p^* + 2\varepsilon_m^*} \tag{2.3}$$

where, ε_p^* and ε_m^* are the complex permittivity of the particle and surrounding medium, respectively. For a real dielectric, the complex permittivity is defined as $\varepsilon^* = \varepsilon - i(\sigma/\omega)$, where ε is the permittivity, σ is the conductivity of the dielectric, and ω is the angular frequency of the applied electric field. DNA is a long polymer and can be characterized as a cylindrical shape, hence the equation 2.2 can be redefined as,[16]

[16] M. Dimaki et al., Nanotechnology **15**, 1095 (2004)

$$\boldsymbol{F}_{DEP} = \frac{\pi}{6} r^2 l \varepsilon_m Re[\boldsymbol{K}_w(\omega)] \nabla |\boldsymbol{E}|^2 \tag{2.4}$$

where r is the radius and l is the length of the cylinder and $\boldsymbol{K}_w(\omega)$ is given by,

$$\boldsymbol{K}_w(\omega) = \frac{\varepsilon_p^* - \varepsilon_m^*}{\varepsilon_m^*} \tag{2.5}$$

Apart from particle's volume and shape, its behaviour in the solution in an applied electric field depends on real part of the Clausius-Mossotti factor ($\boldsymbol{K}_w(\omega)$), which is proportional to the permittivity and conductivity of the particle and medium. When $\mathrm{Re}[\boldsymbol{K}_w(\omega)] > 0$, the particle is more polarizable than the medium and hence moves toward the high electric field region, termed as *positive dielectrophoresis*. Similarly, if $\mathrm{Re}[\boldsymbol{K}_w(\omega)] < 0$, the particle is less polarizable than the medium and moves away from high electric field region, termed as *negative dielectrophoresis*. No dielectrophoresis is observed, if $\mathrm{Re}[\boldsymbol{K}_w(\omega)] = 0$. The DEP force increases linearly with the strength and gradient of the applied electric field.

But the electric field gradient decays exponentially away from the electrode edge, hence it is a short range force for particle manipulation. The DNA molecule possess an intrinsic negative charge due to the phosphate back-bone. When suspended in an non-ionic buffer, it will experience positive dielectrophoresis.

ELECTROHYDRODYNAMIC FLOW

Electrohydrodynamic flow is a frequency dependent motion of bulk liquid induced by an applied non-homogeneous electric field. At frequencies between 100 Hz and 1 kHz, the charged ions build-up near the electrode surface. This build-up of ions will eventually get attracted towards counter ions fixed on the electrode surface, forming an electric double layer. This movement of charged ions causing the bulk liquid to move in a cyclic motion is called AC electro-osmosis and can be expressed as[17]

[17] H.-Y. Lin et al., Nanotechnology **16**, 2738 (2005)

$$v = \lambda_D E_t \sigma / \rho \tag{2.6}$$

where, ρ is the viscosity, and σ is the surface charge density in the electric double layer. E_t tangential electric field. Both the E_t and σ are frequency dependent and the Debye length (λ_D) is given by

$$\lambda_D = \sqrt{\frac{\varepsilon_r \varepsilon_0 k_B T}{2 N_A e^2 I}} \tag{2.7}$$

where, ε_r is the dielectric constant, ε_0 is the permittivity of free space, k_B is the Boltzmann constant, T is the absolute temperature, N_A is the Avogadro number and e is the electron charge (1.602×10^{19} C), and I is the ionic strength of the electrolyte (mole/m^3).

2.3 *Molecular Biological Techniques*

2.3.1 *Structure of Nucleic acids*

The nucleic acid is made up of three basic components namely, a nucleobase, a ribose sugar and a phosphate group. The nucleobase linked with ribose sugar moiety is called **nucleoside** and further addition of a phosphate group is called **nucleotide**. The nucleobase is derived from a hetrocyclic compound called purine or

pyrimidine. Purine forms the basis for adenine and guanine, similarly, cytosine, thymine and uracil are derived from pyrimidine. The nature of ribose moiety will determine the final destination of nucleobases in nucleic acid polymer ie., a native ribose sugar containing nucleotide will be part of an RNA polymer, whereas nucleotide with ribose lacking hydroxyl group in the second carbon position called **deoxyribose** forms DNA polymer. Guanine and cytosine complements in both DNA and RNA, but adenine complements either thymine in DNA and uracil in RNA.

Deoxyribonucleic acid (DNA) is a double helical molecule having two complimentary strands running in anti-parallel direction. Three different helical forms are believed to be present in nature (table 2.1). B-DNA is more prevalent helical form proposed by Watson and Crick (fig 2.3).

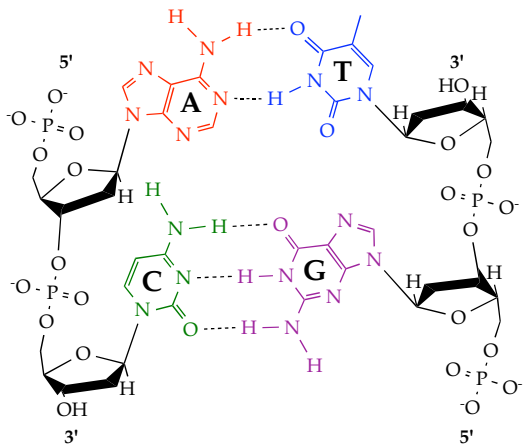

Figure 2.3: DNA base pairing: adenine (A) complements thymine (T) with two hydrogen bonds and guanine (G) compliments cytosine (C) with three hydrogen bonds

Table 2.1: Different forms of DNA double helix. *Source: Wikipedia.org*

	A-DNA	**B-DNA**	**Z-DNA**
Helix sense	Right-handed	Right-handed	Left-handed
bp/turn	11	10.5	12
Diameter	23 Å	20 Å	18 Å

2.3.2 *Amplification of DNA*

IN VITRO DNA AMPLIFICATION is a process for synthesizing DNA in a large amount. There are different types of methods such as Polymerase Chain Reaction (PCR), Ligase Chain Reaction (LCA), Rolling Cycle Amplification (RCA), Homogeneous Real-Time Strand Displacement amplification, Multiple-Displacement Amplification (MDA) etc. Irrespective of the method used, they all require a template DNA, primer, DNA polymerase in appropriate buffer and 4 deoxynucleotide triphosphate (dNTP).

POLYMERASE CHAIN REACTION is a cell free *in vitro* amplification technique developed by Kary Mullis in 1983 based on thermal-cycling. In principle, the DNA double helix is melted at high temperature >94^{o}C and annealed with short oligo nucleotides called primers. The temperature of the reaction mixture is increased to 72^{o}C so that the thermostable DNA polymerase can synthesize the second strand using 4 dNTPs. This process of DNA melting-annealing-extention is repeated several times to yield a desired amount of DNA. This technique requires optimization and pure template for good results.

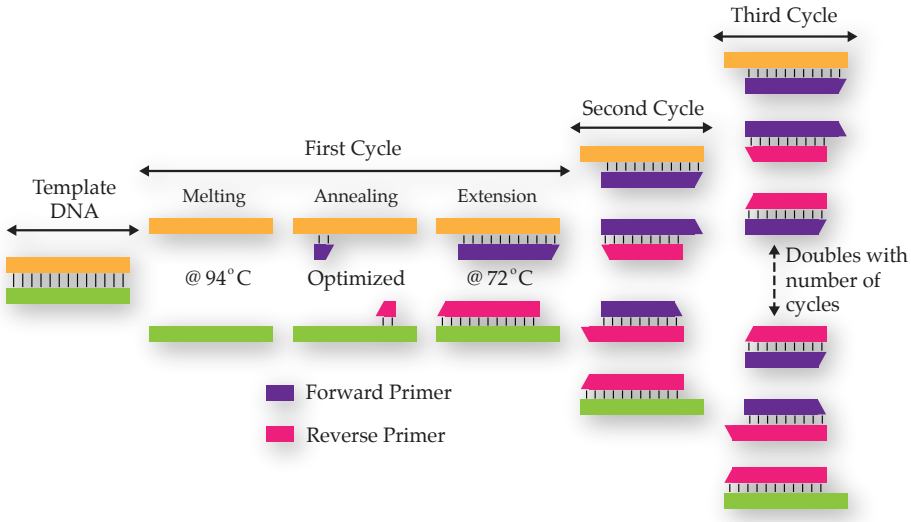

Figure 2.4: Schematic illustration of Polymerase Chain Reaction technique

2.3.3 *DNA Modifying Enzymes*

DNA modifying enzymes are a class of enzymes that alter the physical and chemical nature of nucleic acids that includes *nucleases*, *polymerases*, *Ligases*, *phosphotases* etc.

Nucleases are group of enzymes altering the physical length of DNA in a random or sequence specific manner by breaking the phosphodiester backbone. Enzymes that remove the nucleobases from the DNA terminals are termed **exonuclease**, and **endonucleases** break the phosphodiester bond in the internal region of the DNA.

Endonuclease

Endonucleases are class of enzymes also known as restriction enzyme that cuts double standard or Single strand DNA sequences internally at a specific manner called as **recognition site**. There are three classes of restriction endonucleases, but only class II is explained further due to its relevance to this work.

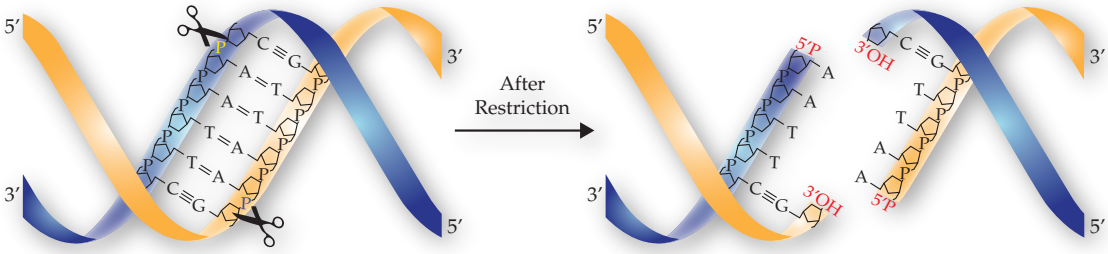

Figure 2.5: Schematic illustration of DNA Replication: A polymerase (green) adds a nucleotide (pink) at 3′-OH end of the new strand

Type II restriction enzymes have been the key to molecular biology, because they cut the DNA at definable sites within or short distance from the recognition site. Type II restriction endonucleases recognize a palindrome (i.e., symmetrical) sequence of four, six, or eight bases (i.e., 4-, 6-, or 8-cutters) consequently identical in both strands in 5′ → 3′ direction. Enzymes of this class cleave DNA within their recognized sequence and generate fragments

with a 5′-phosphate and a 3′-OH end that could be either smooth (blunt ends) or sticky (cohesive ends) as shown in figure 2.5.

DNA Polymerase

DNA polymerase is an enzyme that synthesizes DNA by a process called replication (fig 2.6). The enzyme polymerizes the new strand by incorporating deoxynucleotides complimentary to the template strand in the 5′ → 3′ direction. They need a free 3′-OH group to initiate the process of new strand synthesis. In *in vivo* conditions, the enzyme is assisted by many other proteins for successful polymerization of DNA, they include primase (synthesizing RNA to provide 3′-OH group), helicase (unwinding the DNA double helix) and single-stranded binding proteins (SSB) to maintain the single strandedness until copied. Most of the DNA polymerases possess proof-reading activity to correct the mistakes in newly-synthesized strand. They move in the opposite direction 3′ → 5′ to rectify an misincorporated base and proceed forward (5′ → 3′) after incorporating the correct base.

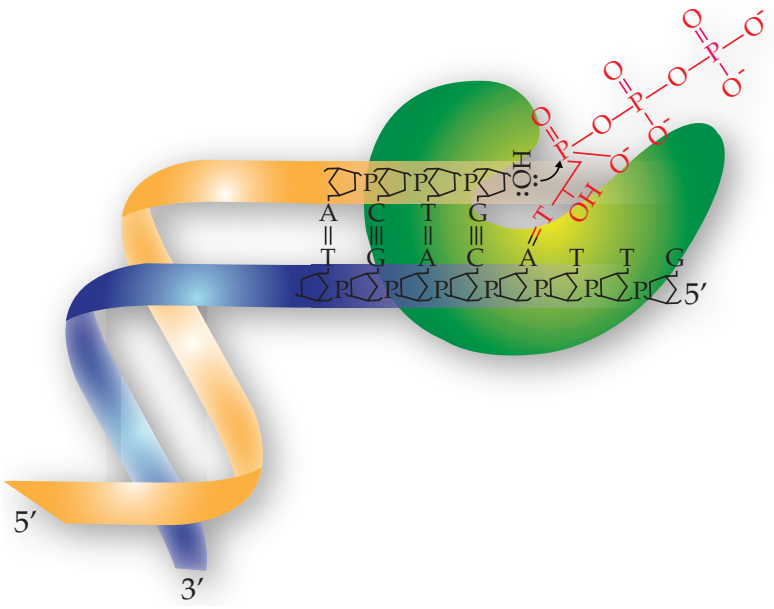

Figure 2.6: Schematic illustration of DNA Replication: A polymerase (green) adds a nucleotide (red) at 3′-OH end of the new strand

DNA ligase

DNA ligase is an enzyme that repairs single-stranded discontinuities in double-stranded DNA molecules. It requires ATP for establishing phosphodiester bond between 5′ end of donor nucleotide and 3′-OH end of acceptor nucleotide. This bond formation involves three steps, namely adenylation (addition of AMP) of a residue in the active center of the enzyme, transfer of the AMP to the 5′ phosphate of the donor nucleotide, and finally, formation of a phosphodiester bond with 3′-OH of the acceptor nucleotide.[18] Ligases are extensively used in molecular biology for linking two different DNA strands.

[18] I. R. Lehnman, Science **186**, 790 (1974)

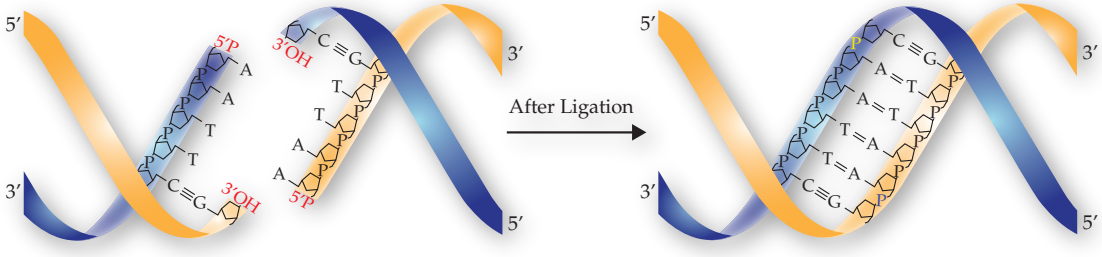

Figure 2.7: Schematic illustration of DNA Ligation

2.3.4 *Agarose Gel Electrophoresis and Visualization of DNA*

An analytical technique used for separation of biomolecules based on sieving principle using agarose, a polysaccharides extracted for sea weeds. The negatively charged nucleic acid migrates through the gel-pores under an applied electric field. The shorter nucleic acid moves faster compared to longer ones and gets sorted at different distances. Ethidium bromide is a common intercalating dye used to visualize the separated nucleic acids. Stained Nucleic acids become visible under ultra violet illumination.

2.3.5 *Molecular Beacon*

Molecular beacons (MB) are single stranded oligonucleotides labeled with fluorophore and a quencher molecule at the termini ca-

pable of forming a stem-loop structure in the absence of target.[19] The fluorescence increases, when the MB interact with complimentary nucleic acids or thermal denaturation caused by opening of the stem region that prevents the proximity of fluorophore-quencher pair.

[19] S. Tyagi et al., Nat. Biotechnol. **14**, 309 (1996)

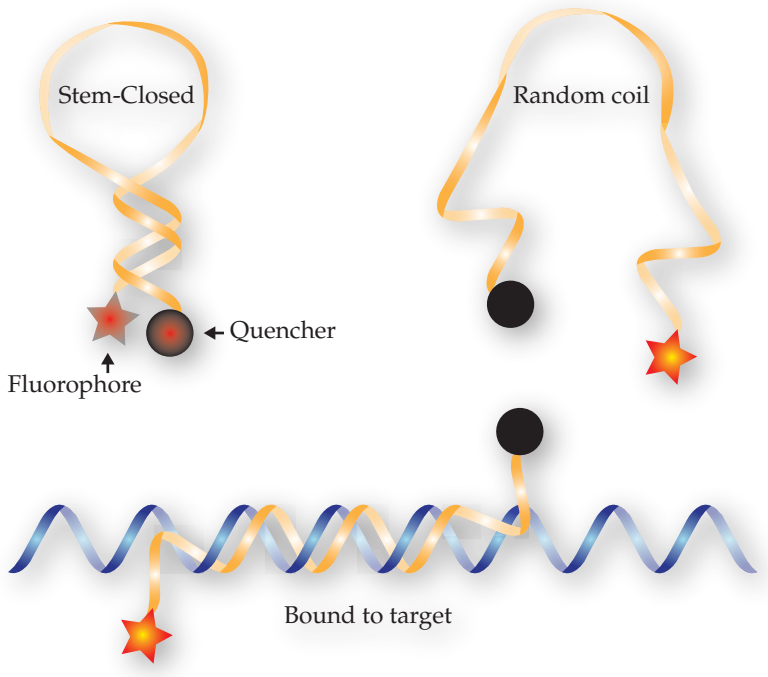

Figure 2.8: Three states of molecular beacon

3
Experimental Procedure

This chapter explains the steps of methods used in stretching DNA and homopolymer DNA for DNA-Protein interaction studies. It is divided into two sections such as *Alignment of DNA* and *Homopolymer DNA*. Enzymes for molecular biology experiments were procured from Fermentas GmbH and primers for DNA amplification were supplied by Eurofins MWG Operon, unless otherwise specified.

3.1 Alignment of DNA

Orientation-defined alignment and fixing of DNA at specific location requires terminal modification of DNA, fabrication of the electrode and the alignment by electrokinetics. Electron-beam lithography was employed to fabricate electrodes (Figure 3.1) with dimensions less than few micrometers, which is much harder to achieve with optical lithography. DNA was synthesized by molecular biological techniques and terminal modification by chemical methods. The alignment was performed by an applied AC electric field and visualized with different methods such as fluorescence, glutaraldehyde fixing and metallization.

AC
Alternating Current

3.1.1 Fabrication of Electrode

Preparation of Substrate: Silicon wafer (Good Fellow) have been used as the substrate for electrode fabrication. A substrate

of desired dimension was cut and cleaned with acetone followed by ethanol in ultra-sonic bath and finally dried with nitrogen.

Physical Vapour Deposition: The metallic layers such as platinum, gold and tantalum required for DNA alignment were coated using DC magnetron sputtering in the presence of an Argon plasma. Insulating layers such as SiO_2 and TaO_x were coated using RF magnetron sputtering in a combination of Oxygen and Argon plasma.

DC
Direct Current
SiO_2
Silicon dioxide
TaO_x
Tantallum Oxide
RF
Radio Frequency

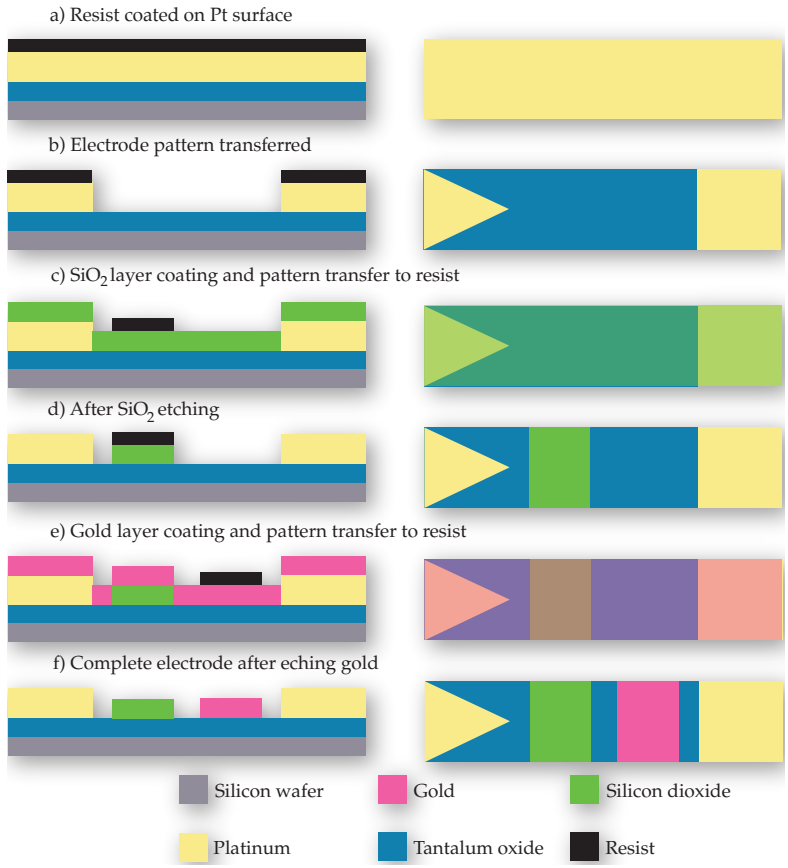

Figure 3.1: Steps involved in fabrication of electrode for stretching DNA: **(Left)** Cross-sectional view with resist and **(Right)** Top view after resist removal.

Electron Beam Lithography: Elphy Raith eLine Lithography system was used for patterning the electrode layout on the sub-

strate containing metallic layer coated with negative resist (AR-N 7520.018 from Allresist). Contact pads for the electrode were patterned using positive resist (AR -P 610.03 from Allresist). The lithography was performed at a gun voltage of 20 kV and a working distance of 15 mm. Different sized apertures were used to control the intensity of the beam current depending on the structure being patterned. The fine structure of DNA stretching region was patterned with 30 µm aperture and contact pads with 120 µm aperture. In order to prevent over exposure of fine electrode structures, the dose values were optimized separately for every shape of the electrode region. After lithography the negative resist was developed with AR-300.47 (AllResist) for 5 minutes followed by rinsing with water and dried with nitrogen. Incase of positive resist, the resist was developed in AR 600-55 for 2 minutes and in stopping solution AR 600-60 for 30 seconds and finally dried with nitrogen.

Argon Ion Milling: Once the electrode pattern was transferred to the substrate, the metallic layer other than the electrode was removed by Argon ion milling. The progress of etching was monitored through a mass-spectrometer. Etching was terminated once the desired layer is reached. The resist was removed by ultrasonication in 1-Methyl-2-Pyrolidinone at 70^0C

Bonding and Storage: The fabricated electrode was placed in a ceramic IC socket and wire bonded for providing external contact. The electrode setup was then stored in the vacuum to prevent carbon contamination on the gold surface as well as accumulation of dust.

3.1.2 Synthesis and Modification of DNA

pUC19 plasmid[1] was used as a model DNA in this study. The plasmid was linearized by restriction enzyme PfoI and used as template for DNA amplification. Two different types of terminal modification schemes were performed namely Thiol-Biotin and Thiol-Silane.

[1] C. Yanisch-Perron et al., Gene **33**, 103 (1985)

PCR
Polymerase Chain Reaction

Amplification of DNA: The linearized plasmid was amplified by Polymerase Chain Reaction (PCR). The primers were designed to yield 2673 bp DNA, which has a physical length of about 890 nm. The amplified DNA was cleaned with Qiagen PCR purification kit to remove enzyme and excess primers before proceeding to the next functionalization step.

Reaction Components		**Thermocycling Conditions**	
10x *Taq* DNA Pol buffer	5µl		
10mM dNTP	1µl	Initial Melting	95^oC/ 2 min
Forward primer (5 pM/µl)	1µl	—32 Cycles—	
Reverse primer (5 pM/µl)	1µl	Melting	94^oC/ 20 sec
pUC19 plasmid (10 ng/µl)	1µl	Annealing	55^oC/ 20 sec
Taq DNA Pol (5 u/µl)	0.2µl	Extension	72^oC/ 2 min 30 sec
H_2O	40.8µl	———————-	
Total volume	50µl	Final extension	72^oC/ 10 min

Table 3.1: Reaction components and thermocycling conditions for pUC19 DNA amplification

Functionalization of DNA with Thiol and Biotin: The Thiol-Biotin scheme was straightforward by amplifying the DNA using the forward primer with 5′ thiol and reverse primer with 5′ biotin as mentioned in table 3.1. The thiol group is protected during the amplification process and will be activated before the alignment experiments. Figure 3.2 shows the chemical composition of the primers.

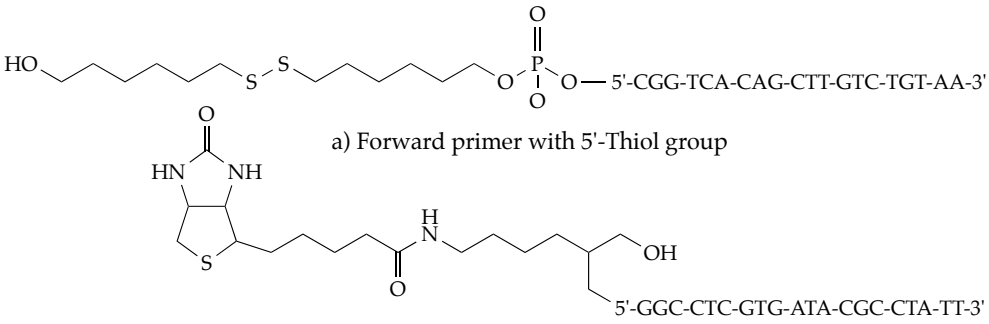

Figure 3.2: Forward and reverse primers functionalized with thiol and biotin at 5′ termini respectively

FUNCTIONALIZATION OF DNA WITH THIOL AND SILANE: In case of Thiol-Silane scheme the DNA was amplified with 5′ thiol forward primer and 5′ amine reverse primer with as mentioned in table 3.1. The 5′ primary amine of the reverse primer (fig. 3.3) was used to link the silane moiety using heterobifunctional crosslinkers. A detailed schematics of silane functionalization is illustrated in figure 3.4.

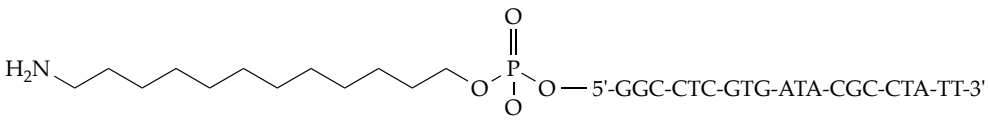

Figure 3.3: Reverse primer with 5′- Amino group

In principle, the Bioconjugate Toolkit Reagent procured from Piercenet Biotech contains *N*-hydroxysuccinimide ester (NHS ester) and either a hydrazide or an aldehyde group such as succinimidyl 4-hydrazidoterephthalate hydrochloride and succinimidyl 4-formylbenzoate respectively. The amine functionalized DNA was coupled with SFB and the silane moiety APTES was coupled with SHTH based on NHS-ester moiety to form stable amide bonds with primary amino groups. In the second phase, the DNA-SFB and SHTH-APTES intermediate complexes were conjugated by formation of a hydrazone bond.

Experimentally, the coupling of DNA and SFB was carried out in phosphate buffer (pH 7.2) at 37^0C for 3 hours and desalted in Zeba column (Piercenet Biotech) to remove excess crosslinkers. Since, silane is unstable in aqueous solution the conjugation was carried out in ethanol[2] at 37^0C for 3 hours and excess of SHTH was not desalted due to their smaller molecular weight. Both the intermediates DNA-SFB and SHTH-APTES were stored at -20^0C. Before the DNA alignment experiment, DNA-SFB and SHTH-APTES were mixed in 100mM MES buffer pH(5.5) and incubated at room temperature for an hour.

SFB
Succinimidyl 4-formylbenzoate

APTES
(3-Aminopropyl) triethoxysilane

SHTH
Succinimidyl 4-hydrazidoterephthalate hydrochloride

NHS-ester
N-hydroxysuccinimide ester

[2] A. Kumar et al., Nucleic Acids Res. **28**, e71 (2000)

MES
2-(*N*-morpholino) ethanesulfonic acid

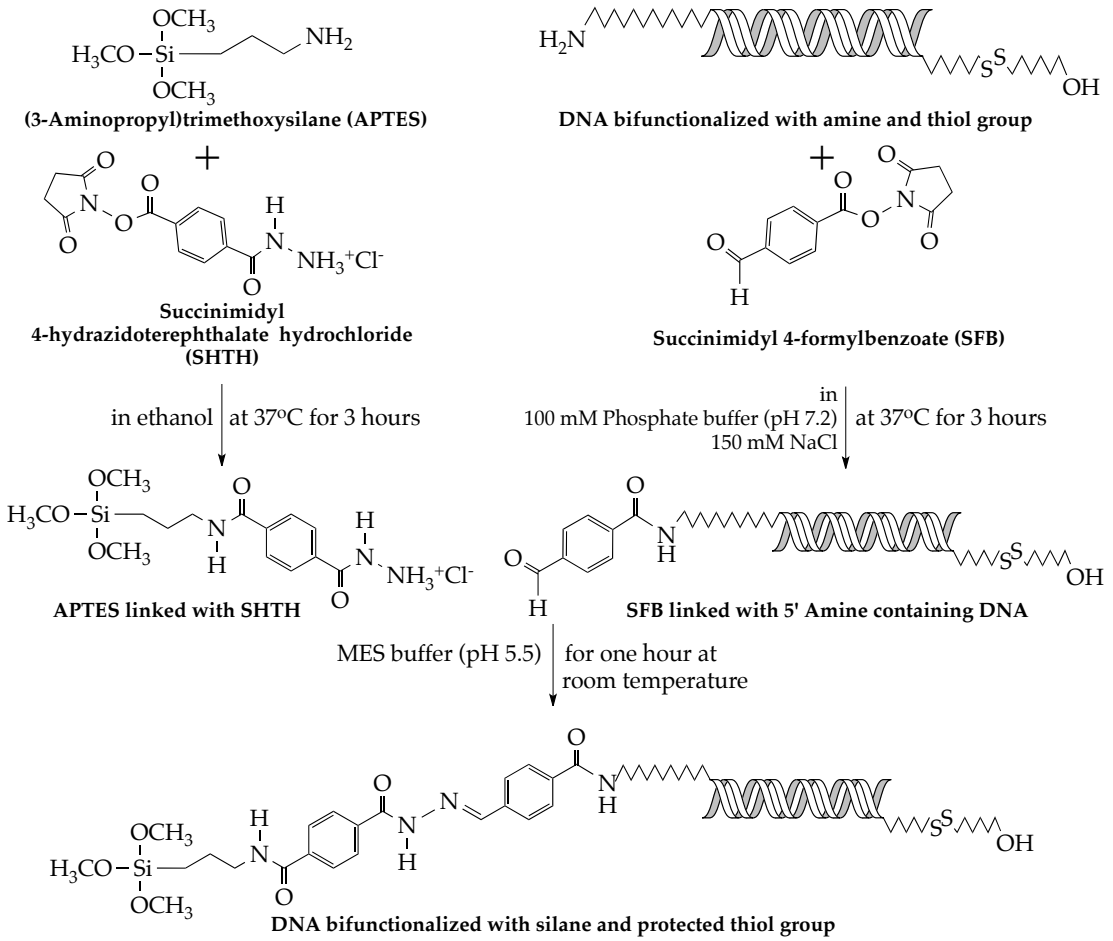

Figure 3.4: Steps involing attachment of silane to DNA

3.1.3 *Pre-preparation and Alignment of DNA*

Before the actual alignment experiment, few preparatory steps were performed, such as activation of the thiol group, cleaning of electrode and placement of PDMS membrane on the electrode to hold the DNA solution during the stretching procedure.

PDMS
Polydimethylsiloxane

ACTIVATION OF THIOL GROUP: The protected thiol group was activated by treating the thiol functionalized DNA with 100mM DTT in 100mM MES buffer (pH 5.5) at room temperature for 30 minutes and desalted in Zeba column (Piercenet Biotech). After desalting, the activated Thiol-DNA-Silane compound was resuspended in 25 mM MES (pH 5.8) and 10mM DTT. Silane is stable at pH 5.8 a well as an optimal pH for DNA stretching.[3]

DTT
Dithiothreitol
MES
2-(*N*-morpholino) ethanesulfonic acid

[3] J. Allemand et al., Biophys J **73**, 2064 (1997)

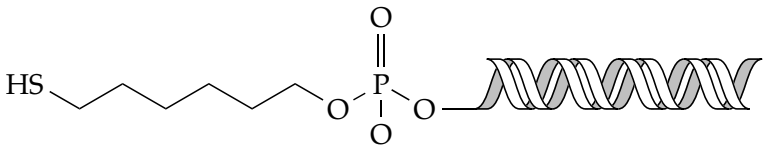

Figure 3.5: DNA with activated thiol group

PIRANHA CLEANING OF ELECTRODE: The carbon content on the gold surface in the electrode was removed if any, by treating with piranha acid (3 parts H_2SO_4 :1 part H_2O_2) for 10 min at 50^oC and rinsing with acetone and ethanol immediately before stretching.

PLACEMENT OF MICROWELL: PDMS was prepared by dispensing a mixture of silicone elastomer - curing agent (Sylgard) in a petridish to a height of one millimeter and allowed to cure at 85^oC for 6 hours. Once cured, a square of 6 mm x 6 mm were cut and the center portion was removed by perforation and placed on the electrode chip.

PDMS
Polydimethylsiloxane

APPLICATION OF AC ELECTRIC FIELD: The thiol activated DNA was dropped on the electrode. The DNA was then stretched by applying AC voltage between the electrodes with a function generator connected in parallel with an oscilloscope. Stretching was

AC
Alternating Current

performed at different frequency domains such as 10 Hz - 1 kHz and 100 kHz - 1 MHz range.

3.1.4 *DNA Visualization*

The event of DNA stretching can be visualized by different techniques such as fluorescence imaging, electron microscope imaging, atomic force microscope imaging, etc. In this work, an Olympus IX70 microscope with 40x oil-immersion objective was used for fluorescent imaging and a Leo-Gemini scanning electron microscope was used for visualizing fixed or metallized DNA. The reason behind different visualization techniques used in this work will be discussed in discussion part of this thesis.

Fluorescent Dye: Before the alignment experiment, DNA was intercalated with YOYO-I (Invitrogen) at the ratio of five bases to one dye molecule. A 10µl of 3M β-Mercaptoethanol was added to 50µl DNA solution to prevent photobleaching of fluorescent dye. With appropriate excitation and emission filters, the images were captured by Princeton CoolSNAP CCD camera and analyzed in WinSpec image viewing software.

Glutaraldehyde Fixing: DNA imaging at the higher resolution can be achieved by using SEM after fixing with cross-linking aldehydes such as glutaraldehyde (fig 3.6). In this study, the aligned DNA was fixed with 2% glutaraldehyde solution and carefully washed with excess of sterile H_2O. The electrode chip was then dried before visualizing the DNA in SEM.

SEM
Scanning Electron Microscope

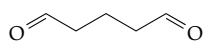

Figure 3.6: Structure of glutaraldehyde

Metallization by Silver Ions: The aligned DNA was also visualized by silver ion metallization as described by Keren *et al*. [4] It is a two step procedure involving aldehyde derivatization and silver metallization. To aldehyde derivatize the DNA, the electrode after applying electric field was incubated in 25 mM HEPES buffer pH 7.5 containing 4 mM MgAc (final DNA concentration 0.1 µg/µl)and 0.2% glutaraldehyde for 20 min at room temperature and then for 20 min on ice and washed with sterile H_2O. The electrode was then incubated in 0.1 M solution of $AgNO_3$ in 25%

[4] K. Keren et al., Nano Lett. 4, 323 (2004)

HEPES
4-(2-hydroxyethyl)-1-piperazineethanesulfonic acid
MgAc
Magnesium acetate
$AgNO_3$
Silver nitrate

ammonia buffer (pH 10.5, titrated with 70% HNO_3) at room temperature overnight in the dark. The electrode was finally washed with sterile H_2O and dried.

HNO_3
Nitric acid

METALLIZATION BY PALLADIUM IONS: The aligned DNA was metallized with palladium ions as reported by Richter *et al.*[5] First, the aligned DNA containing electrode was incubated in saturated palladium acetate solution for 2 hours at room temperature in a humid chamber. The Pd^{2+} ions surrounding DNA was metallized by adding a reducing agent at a concentration ratio of 5:1 for 1 min and the reduction was stopped by adding 50 volumes of sterile H_2O. The saturated palladium acetate solution was prepared by dissolving 5 mg $Pd(CH_3COO)_2$ in 1 ml of 10mM HEPES buffer (pH 6.5). The mixture was ultra-sonicated for 5 min followed by centrifugation at 2000 x*g* for 5 min to get a saturated solution by removing the undissolved salt. The supernatant was diluted eight times to get the working concentration. The reducing solution consists of 2.5 g/l sodium citrate, 2.5 g/l of aqueous 85% lactic acid solution and 0.25 g/l dimethylamine borane and the pH was adjusted to 7.4 with NH_4OH.

[5] J. Richter et al., Appl. Phys. Lett. **78**, 536 (2001)

$Pd(CH_3COO)_2$
Palladium Acetate
HEPES
4-(2-hydroxyethyl)-1-piperazineethanesulfonic acid

NH_4OH
Ammonium hydroxide / Ammonia solution

3.2 *Homopolymer DNA Synthesis*

The homopolymer DNA consists of repeated molecular beacon sites for every 23 base pairs. This repeated DNA was synthesized by Concatemerization of 239 bp DNA, which contains ten MB sites (five for two different MB sequences) and sequences complementary for forward and reverse primers for amplification. The sequence of all oligonucleotides used in this section were listed in appendix.

Concatemerization
A process for synthesizing long continuous DNA molecule that contains multiple copies of the same DNA sequences linked in series.
MB
Molecular Beacon

3.2.1 *Synthesis of Homopolymer DNA*

The 239bp DNA was synthesized by annealing 10 pmol of 129 nt and 131 nt (Eurogentec) and extended with Klenow fragment.

Equimolar ratio of 129nt and 131nt were mixed and annealed by a temperature ramp from 94^{o}C to 37^{o}C at a rate of 2^{o}C/min. 10U of Klenow fragment and 0.2mM dNTP were added to the

nt
nucleotide

Klenow fragment is a large fragment of *E. coli* DNA Polymerase I exhibit 5′ → 3′ polymerase activity and the 3′ → 5′ exonuclease activity but lacks 5′ → 3′ exonuclease activity

annealed oligonucleotide mixture and incubated at 37^0C for 30 min. The resultant 230bp DNA product was purified from other reaction constituents by gel extraction (Qiagen) after agarose gel electrophoresis (AGE).

Stabilization of 239bp DNA:The 239bp DNA was cloned into pGEM-T vector (Promega) for future experiments. The pGEM-T (fig: 3.7) contains 3′T-overhang, which can be used to clone DNA with 3′A-overhangs. Since klenow fragment does not add 3′A to the polymerized DNA, the 3′A tailing for 239bp DNA was added by incubation with 5U *Taq* DNA polymerase and 0.2 mM dATP at 72^0C for 10 min. The 3′A tailed 239bp DNA was ligated with different vector concentrations as given in table 3.2.

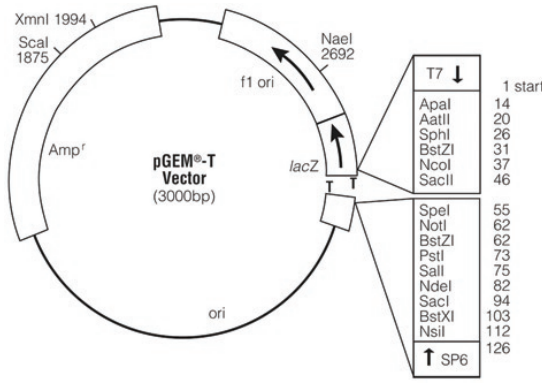

Figure 3.7: pGEM-T vector map. © Promega

Table 3.2: Reaction components for ligation of 239bp DNA into pGEM-T vector

	Vector:Insert		
Reaction components	1:1	5:1	1:3
2x Rapid ligation buffer	5µl	5µl	5µl
pGEM-T (50 ng/µl)	0.6µl	1µl	0.2µl
239bp DNA (10 ng/µl)	3µl	1µl	3µl
Nuclease free water	0.4µl	2µl	0.8µl
T4 DNA ligase (3 Weiss units/µl)	1µl	1µl	1µl
Total volume	10µl each		
The vector-insert ligation mixture was incubated at 12^0C for 16 hours			

TRANSFORMATION, SCREENING AND STORAGE OF CLONES: The ligated product was transformed in to *E. coli* JM109 competent cells prepared with TransformAid^{TM} Bacterial Transformation Kit from fermentas. The transformed cells were plated on LB agar[6] containing ampicillin (100μg/ml), 0.5mM IPTG and X-Gal (80μg/ml), and incubated overnight at 37^{o}C. Positive clones were selected by blue/white screening and further confirmed by PCR amplification of 239bp insert DNA with M13 forward/reverse primers. The positive clones were cryopreserved at -70^{o}C.

LB
Lysogeny broth

[6] G. Bertani, J. Bacteriol. **62**, 293 (1951)

IPTG
Isopropyl β-D-1-thiogalactopyranoside

X-Gal
5-bromo-4-chloro-3-indolyl-β-D-galactopyranoside

3.2.2 *Concatemerization of DNA with Repeated Sequence*

The 239bp DNA consists of 5 MB sites. The number of such sites were increased by concatemerizing the 239bp DNA in a defined direction, so that the strand complimentary to the MB is part of intra-strand of DNA.

MB
Molecular beacon

ADDITION OF RESTRICTION SITES TO 239BP DNA ENDS: The 239bp DNA does not contain any restriction sites. Different restriction enzyme sites were added to the ends by PCR. The characteristic structure of forward and reverse primer are shown in figure 3.8. The basic design consists of sequences for secondary amplification at 5′end, a restriction site and complimentary sequence at 3′end, which binds to the DNA during annealing step of PCR. The 239bp DNA was amplified with three pairs of primers yielding individual DNA fragments with XbaI–KpnI / KpnI–HindIII / HindIII–Kpn2I restriction enzyme sites and are named fragment A, B and C respectively. The reaction setup and thermocycling parameters were listed in table 3.3.

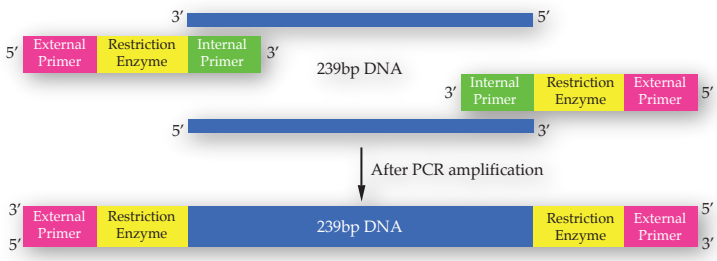

Figure 3.8:
Illustration represneting addition of restriction enzyme sites to 239bp DNA ends

Reaction Components		Thermocycling Conditions	
10x *Pfu* DNA Pol buffer	5µl		
10mM dNTP	1µl	Initial Melting	95^{o}C/ 2 min
Forward primer (5 pM/µl)	1µl	—32 Cycles—	
Reverse primer (5 pM/µl)	1µl	Melting	94^{o}C/ 20 sec
pGEMT/239bp plasmid (10 ng/µl)	1µl	Annealing	55^{o}C/ 20 sec
Pfu DNA Pol (2.5 u/µl)	0.5µl	Extension	72^{o}C/ 1 min
H_2O	40.5µl	———————-	
Total volume	50µl	Final extension	72^{o}C/ 5 min

Table 3.3: Protocol for adding restriction sites to 239bp DNA

Restriction and Ligation: The amplified product with restriction sites was cleaned-up with Qiagen PCR purification kit and restriction digested. The fragments A, B and C were pooled up and restricted with KpnI and HindIII (FastDigest Enzyme - Fermentas). The digestion was performed for 2 hours at 37^{o}C and cleaned-up again to remove the restriction enzyme. The fragments with cohesive-ends were ligated with T4 DNA ligase for 16 hours at 12^{o}C to yield a concatemer of three 239bp fragments (fig. 3.9). The detailed protocol is given in table 3.4.

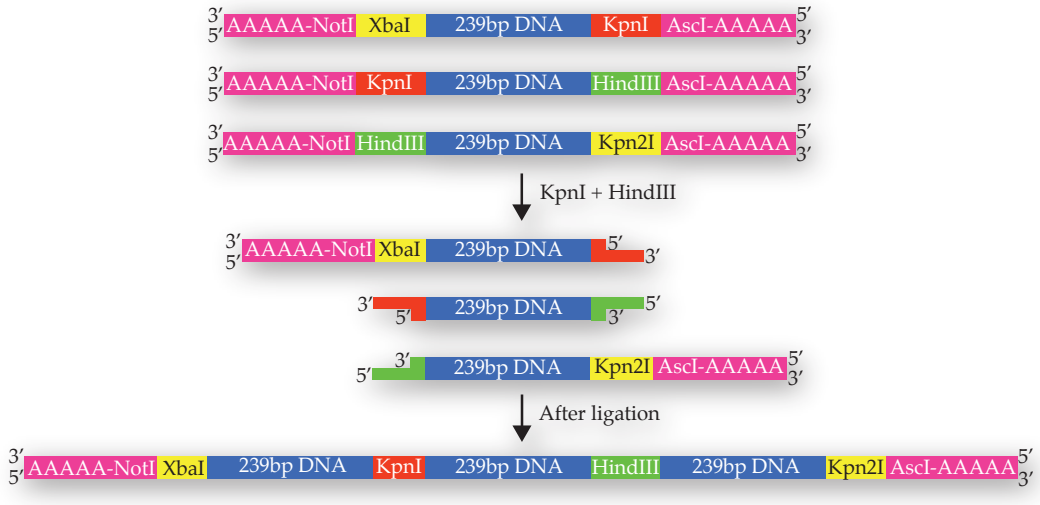

Figure 3.9: Schematic representation of concatemerization of 239bp DNA

Restriction Digestion		**Ligation**	
10x FastDigest Buffer	5µl	10x T4 DNA Ligase Buffer	2.5µl
Template (10 ng/µl)	40µl	Restriction digested DNA	15µl
KpnI (1 u/µl)	2.5µl	24% PEG-6000	5µl
HindIII (1 u/µl)	2.5µl	T4 DNA Ligase (1u/µl)	2.5µl
Total volume	50µ	Total volume	25µ

Table 3.4: Protocol for restriction digestion and ligation of A,B and C 239bp DNA fragment

TRANSFORMATION, SCREENING AND STORAGE OF CLONES: The 773bp concatemerized DNA was separated from ligation mixture by gel-extraction and cloned into pJET1.2/Blunt Vector (fig: 3.10) using CloneJET^{TM} PCR Cloning Kit from Fermentas (table 3.5). The ligated product was transformed in to *E. coli* JM109 competent cells prepared with TransformAid^{TM} Bacterial Transformation Kit from fermentas. The transformed cells were plated on LB agar containing ampicillin and incubated overnight at 37^{o}C. Positive clones were confirmed by PCR amplification of 773bp insert DNA with pJET1.2 forward/reverse primers. The positive clones were cryopreserved at -70^{o}C.

LB
Luria-Bertani

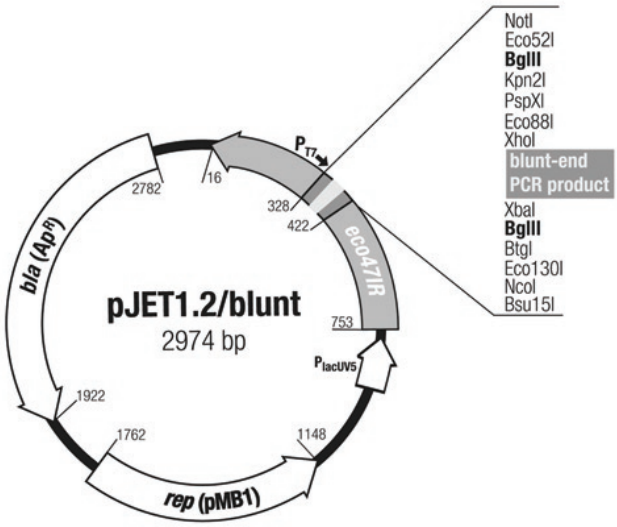

Figure 3.10: pJET1.2/blunt vector map. © Fermentas

Table 3.5: Reaction components for ligation of 773bp DNA into pJET1.2/Blunt vector

	Vector:Insert	
Reaction components	1:1	1:4
2x Rapid ligation buffer	10µl	10µl
pJET1.2/Blunt (50 ng/µl)	1µl	0.2µl
773bp DNA (10 ng/µl)	5µl	4µl
Nuclease free water	3µl	4.8µl
T4 DNA ligase (5U/µl)	1µl	1µl
Total volume	20µl each	
The vector-insert ligation mixture was incubated at 12^oC for 16 hours		

RCA
Rolling Circle Amplification

Rolling Circle Amplification: RCA is a technique used for *in vitro* amplification of target DNA isothermally using Phi 29 DNA polymerase, which has a very high strand-displacement activity. The target DNA was synthesized using exonuclease resistant random hexamer primer, since Phi 29 DNA polymerase posses $3\prime \rightarrow 5\prime$ exonuclease (proofreading) activity degrading the primer that lacks phosphotioate group in the $3\prime$ terminal base.

Table 3.6: Protocol for Rolling Circle Amplification of target DNA

Reaction Components		**Annealing Conditions**	
10x Phi29 DNA Pol Buffer	2µl		
10mM dNTP	2µl		
500mM Exo resistant primer	1µl	Denaturation	95^oC/ 2 min
Template (10 ng/µl)	1µl		
Phi29 DNA Pol (10 u/µl)	2µl	Annealing	65^oC to 30^oC
Pyrophosphatase (0.1 u/µl)	1µl		with a step of
H_2O	11µl		5^oC/ 2 min
Total volume	20µl		

AGE
Agarose Gel Electrophoresis

The reaction mixture was incubated at 30^oC for 6 hours, and the product was analyzed by AGE. The amplified DNA was digested with the appropriate restriction enzyme to release the insert DNA and purified by gel-extraction.

3.2.3 *Preparation of Single-Stranded DNA*

To study the polymerase movement on DNA at the ambient temperature requires single-stranded DNA as the template, since *in vitro* melting of DNA double helix is not possible in the absence of helicase, single strand binding proteins, etc. A modified protocol (fig.3.11) reported by Tai-Chih Kuo[7] was used to prepare ssDNA.

Helicase is a motor protein that separates the two annealed strands by moving along the nucleic acid phosphodiester backbone by ATP hydrolysis

[7] T.-C. Kuo, BioTechniques **38**, 700 (2005)

ssDNA
Single-stranded DNA

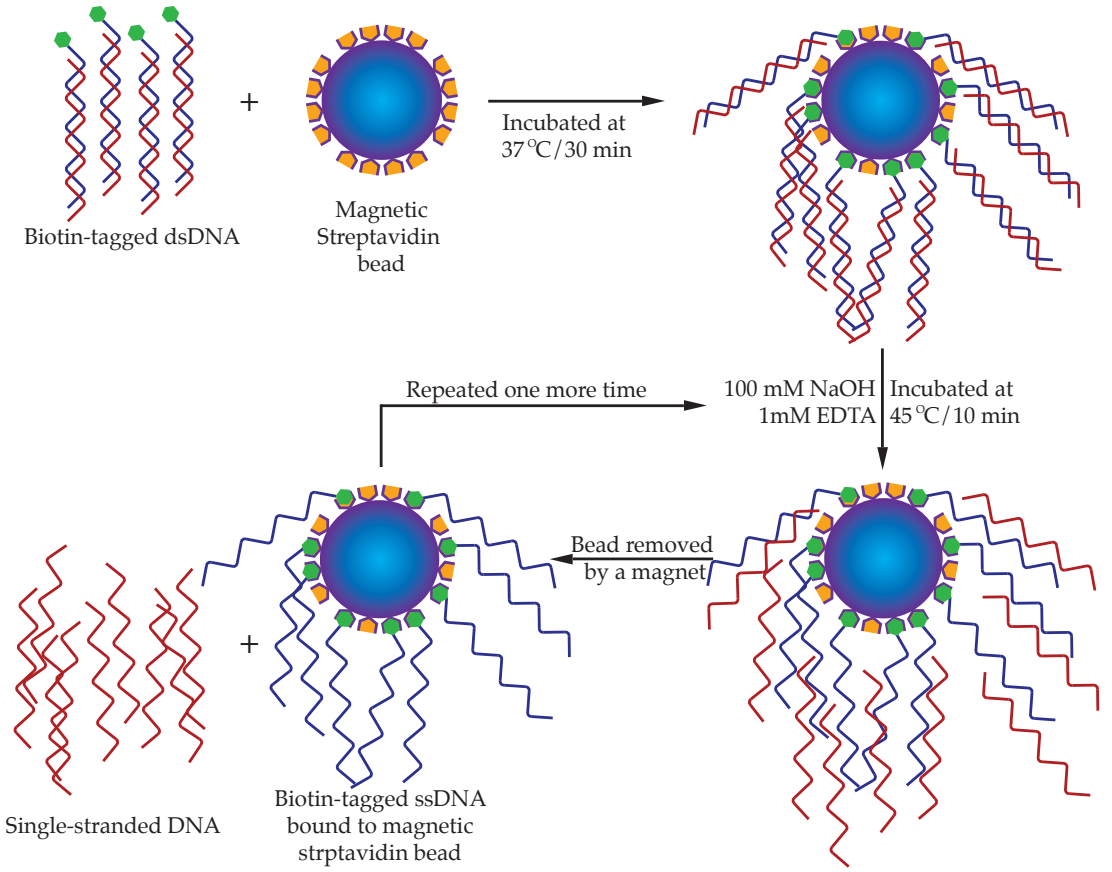

Figure 3.11: Schematic illustration of single-stranded DNA preparation

The DNA was PCR amplified with biotin-tagged primer at one end and resuspended in 1x binding+washing buffer (5 mM Tris-HCl (pH 7.5), 0.5 mM EDTA and 1 M NaCl) containing suspended Dynabeads MyOne^{TM} Streptavidin C1 beads. The unbound DNA was washed three times with 1$\times$ binding+washing buffer and incubated in NaOH solution for 10 minutes at 45^{0}C to melt the DNA double-helix. The beads were concentrated with a magnet and the suspended ssDNA in supernatant was recovered. The procedure was repeated again to recover the remaining ssDNA. The ssDNA in NaOH solution was cleaned by Qiagen PCR cleanup kit and resuspended in 10 mM Tris-HCl buffer (pH 8.0).

3.2.4 *Molecular Beacon: Design and Characteristics*

Molecular beacon was used as reporters for DNA/RNA polymerase movement by monitoring the difference in fluorescence as a function of time. A shared-stem molecular-beacon configuration used as reported by Tsourkas *et al.*,[8] where the part of the sequence hybridizes with stem in the closed state and with target DNA in the open state. The MB contains 5′-Cy5 fluorophore and a 3′-BBQ (Black Berry Quencher) dark quencher was designated as MB1 (fig. 3.12) from TIB MolBiol. A 3′ $\rightarrow$ 5′ exonuclease resistant phosphothioate molecular-beacon was used for analyzing DNA polymerase exhibiting this proofreading activity was designated as MB1-PTO (fig. 3.12). The MB1-PTO contains 5′-Cy5 dye and 3′-BHQ2 (Black Hole Quencher 2).

[8] A. Tsourkas et al., Nucleic Acids Res. **30**, 4208 (2002)

Phosphothioate oligonucleotide contain one sulfur atom in place of an oxygen atom in the phosphate diester linkage of DNA or RNA and becomes resistant to nuclease degradation

3.2.5 *DNA Template for DNA Polymerase Analysis*

The movement of DNA polymerase on ssDNA was observed by annealing the primer, molecular beacon to the DNA template. MB1 was used for polymerases lacking 3′ $\rightarrow$ 5′ exonuclease activity (klenow fragment exo-) and MB1-PTO for polymerase exhibiting 3′ $\rightarrow$ 5′ exonuclease- or proof reading-activity such as Klenow fragment and T7 DNA polymerase. The stoichiometry and annealing steps were given in table 3.7.

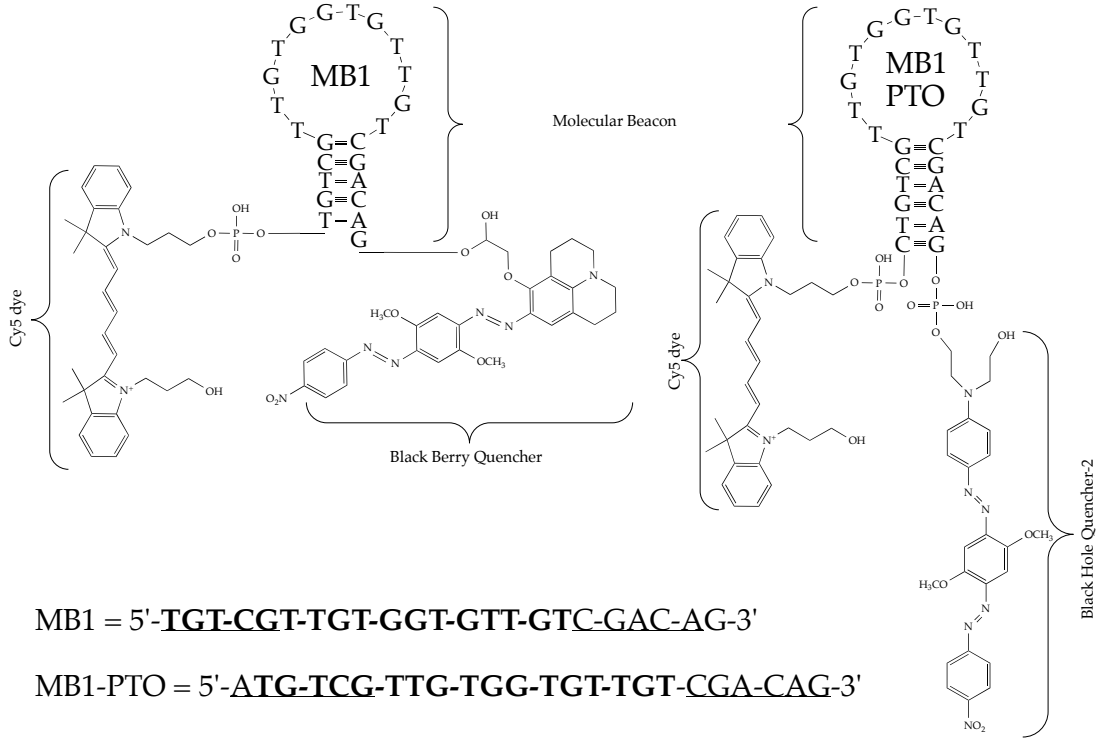

MB1 = 5'-**TGT-CGT-TGT-GGT-GTT-GT**C-GAC-AG-3'

MB1-PTO = 5'-A**TG-TCG-TTG-TGG-TGT-TGT**-CGA-CAG-3'

Figure 3.12:
Schematic structure of shared-stem molecular-beacons. The sequence in boldface hybridizes with target DNA in open state and underlined sequence forms stem structure in closed state.

Reaction Components		**Annealing Conditions**	
10x Enzyme Buffer	1µl		
Primer (5pM/µl)	1µl	Annealing	70^oC to 30^oC
ssDNA	5µl		with a step of
H_2O	variable		
Total volume	10µl		

Table 3.7:
Protocol for annealing primer and molecular beacon on ssDNA.

3.2.6 *DNA Template for RNA Polymerase Analysis*

Unlike DNA polymerase, RNA polymerase requires the promoter and stopping sequences for initiation and termination for RNA transcription. The promoter specific to the RNA polymerase under study, transcription regulators such as ExpR-high affinity, ExpR-low affinity from *Erwinia chrysanthemi*[9], and transcription stopper such as exoP, ropB1 from *Sinorhizobium meliloti*[10] were linked between concatemerized DNA. A detailed strategy will be discussed in the result and discussion part of this thesis.

[9] W. Nasser et al., Molecular Microbiol. **29**, 1391 (1998)

[10] F. Falibert et al., Science **293**, 668 (2001); B. Baumgarth et al., Microbiology **151**, 259 (2005); and M. McIntosh et al., Molecular Microbiol. **74**, 1238 (2009)

3.2.7 *Optimization of Parameter Settings for Fluorescent Analysis*

The time resolved fluorescence (TRF) of polymerase movement on DNA was recorded by Infinite M200, a monochromator-based microplate reader from TECAN GmbH. Different parameters such as excitation- and emission -wavelength, lag time, integration time, and manual gain were optimized to obtain better signal to noise ratio. Figure 3.13 shows the fluorescent behavior of lag *vs* integration time.

The lag time was optimized for different integration times namely 20, 40 and 60 microseconds. The excitation and emission wavelength were held at 650 nm, and the gain of 25. It can be seen that 6µS lag time and 40µS integration time were found optimal.

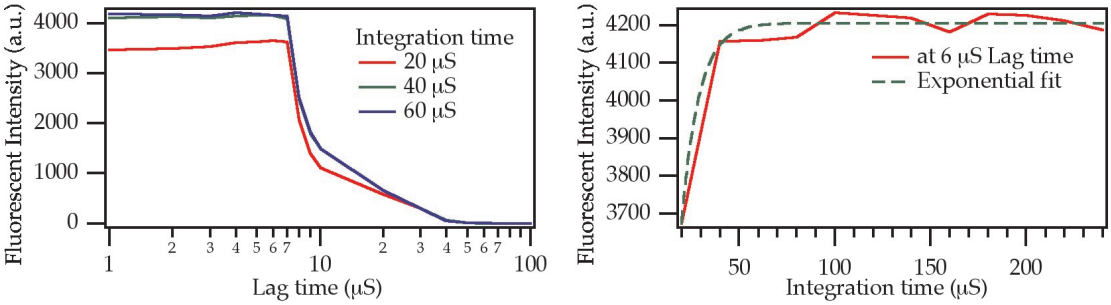

Figure 3.13: Optimization of lag and integration time. The fluorescence value decreases as the lag time increases and fluorescence value increases with increasing integration time.

The Cy5 dye has the excitation maxima at 650 nm and the emission maxima at 670nm. The excitation (Ex) and emission (Em)

bandwidths of Infinite M200 is 9 nm and 20 nm, respectively. The Ex was scanned from 450 nm to 650 nm with Em at 670 nm. Similarly, the Em was scanned from 660 nm to 850 nm with Ex at 650 nm. From the figure 3.14a, it is obvious that the Cy5 dye could be excited at 637 nm and emission read at 672 nm without overlapping Ex-Em bandwidths. Gain is another important parameter in this fluorescence assay, which depicts the amount of signal amplification without lowering the signal-to-noise ratio. Figure 3.14b shows the gain behavior of this instrument. A manual gain of 175 was considered optimal.

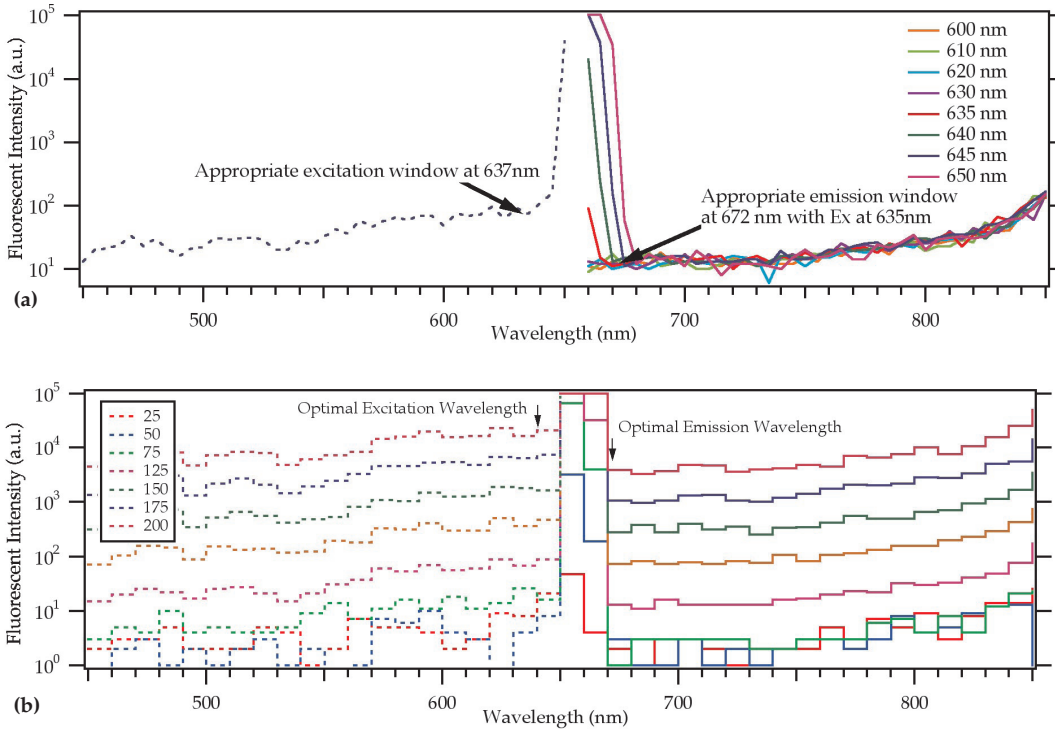

Figure 3.14: **(a)** Scanning of excitation wavelength from 600 nm to 650 nm at 660 nm emission wavelength window for Cy5 dye and **(b)** Optimization of manual gain (insert denotes numerical value). Dotted and solid lines represents excitation and emission regimes, respectively.

Instrumental stability

The stability of the power source and fluorescing capacity of molecular beacon were measured for 3000 seconds (fig 3.15). In the blank test (red) the excitation and emission filters were overlapped to allow a band pass to measure the behaviour of light

source at 37^{o}C. Similarly the behavior of molecular beacon in absence (green) and presence (blue) of ssDNA showed a similar fluorescence decay profile. In photo-bleach test, the decay rate of fluorophore for a 500 second window is too slow, hence, a reduction in fluorescence in experiments with polymerase would be a true reflection of enzymatic activity.

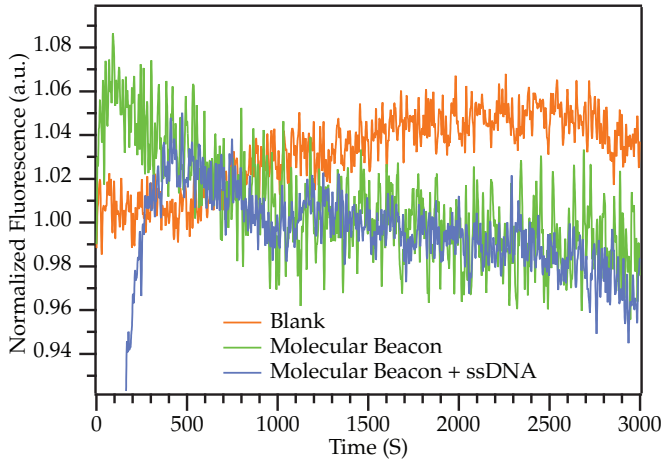

Figure 3.15: Determining the stability of light source and detector of TECAN M200 fluorescence plate reader, and fluorophore stability of molecular beacon for the realtime analysis.

3.2.8 *Data Analysis*

The fluorescent data obtained for the TECAN instrument was smoothed by a 25 point moving average filter and fit with an offset-exponential decay function (eqn 3.1) or offset-two exponential function (eqn 3.2) dependent on the enzymatic properties.

$$I(t) = I_0 + A\ exp\left(\frac{-t-t_0}{\tau}\right) \tag{3.1}$$

$$I(t) = I_0 + A_1\ exp\left(\frac{-t-t_0}{\tau_1}\right) + A_2\ exp\left(\frac{-t-t_0}{\tau_2}\right) \tag{3.2}$$

where, I is the fluorescence intensity (s^{-1}), A is the amplitude, t is time (s) and τ is the characteristic time in seconds. The τ value was used for calculating the relative activity of an enzyme for the given parameter. Data computation such as fitting and plotting was performed using IGOR Pro 6.2 software.

4
Results

This chapter enlists the experimental outcome in a logical way as they evolved during the course of research. It comprises of three main sections, namely (i) *Alignment of DNA* which includes DNA functionalization, fabrication of electrodes and electro stretching of DNA and (ii) *Synthesis of Homopolymer DNA* including synthesis of DNA Concatemer, insertion of transcription -stopping and -regulation sequences and (iii)*Real time analysis of DNA/RNA polymerase activity on homo polymer DNA*, which includes analyzing the activity of different DNA and RNA polymerases using the homo polymer DNA template.

4.1 Alignment of DNA

As a first step towards realizing orientation defined DNA alignment, the DNA terminals were bifunctionalized with different functional groups such as (i) thiol and biotin and (ii) thiol and silane. Electrodes with different dimensions and shapes where fabricated to assist the DNA alignment using electro-kinetic technique and observed by fluorescence microscopy or by metallization.

4.1.1 DNA Bifunctionalized with Thiol and Biotin

The pUC19 plasmid was amplified with forward primer containing 5′ thiol and reverse primer with 5′ biotin by PCR (fig 4.1). The thiol activated DNA was resuspended in 10mM Tris buffer

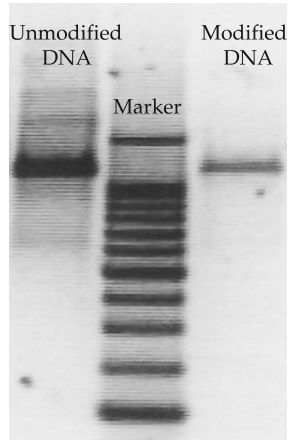

Figure 4.1: Synthesis of bifunctionalized DNA by PCR.

(pH 7.5) containing β-mercaptoethanol, moments before the experiment.

Two different electrode geometries were fabricated to facilitate electrohydrodynamic flow based alignment (fig 4.2a) and dielectrophoresis based alignment (fig 4.2b). The gold and SiO_2 lines are separated by a layer of TaO_x in order to avoid non specific binding of thiol or biotin. The castellated electrode position of DNA at gold and SiO_2 and facilitate alignment.

Figures 4.3 and 4.4 show the alignment of DNA intercalated with YOYO-1 dye recorded at 400× magnification, based on electrohydrodynamic flow due to the presence of electrode with larger surface area. In figure 4.3 and 4.4 the DNA follows the electrohydrodynamic flow (yellow arrows) caused by electrode with larger surface area and gets aligned at gold - SiO_2 region (green arrows).

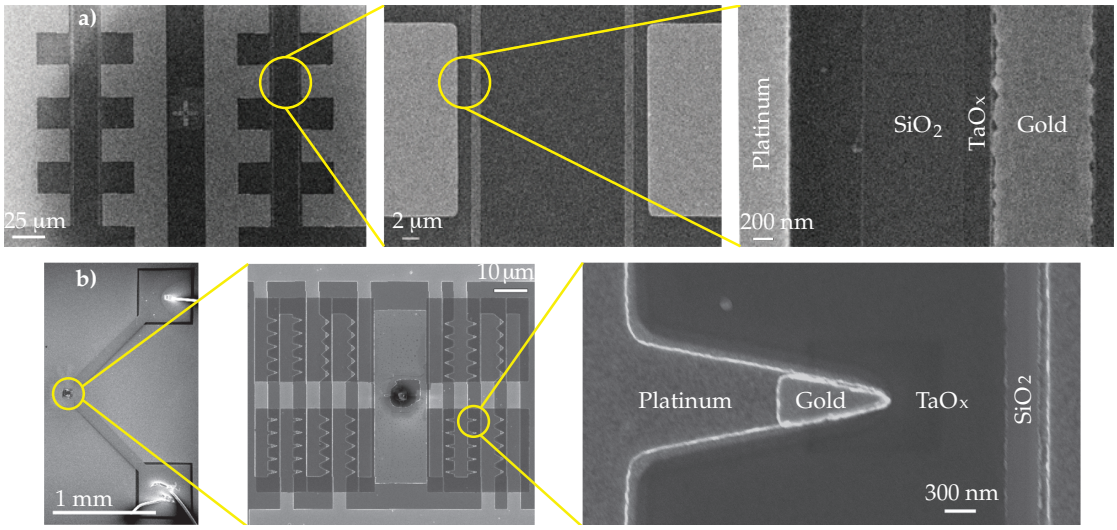

Figure 4.2: Electron michrograph of fabricated electrode: **a)** Interdigitated with oppositely placed castellations and **b)** Interdigitated pointed electrode

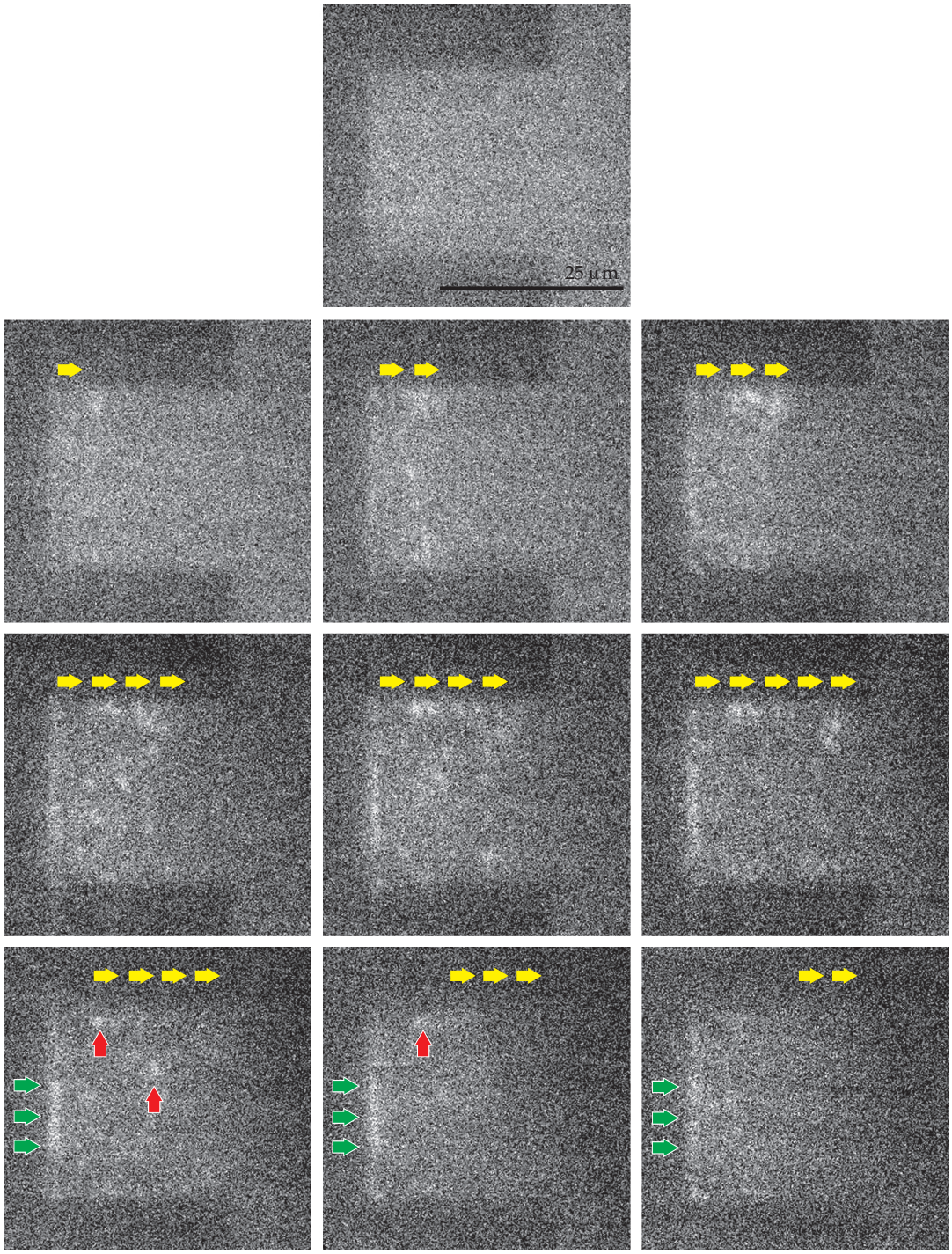

Figure 4.3:
Alignment of thiol-biotin bifunctionalized pUC19 DNA by electrohydrodynamic flow (yellow arrows) at 100 Hz ($2V_{p-p}$). The aligned DNA at the gold-SiO_2 layer and non specific binding on platinum electrode were denoted by green and red arrows respectively.

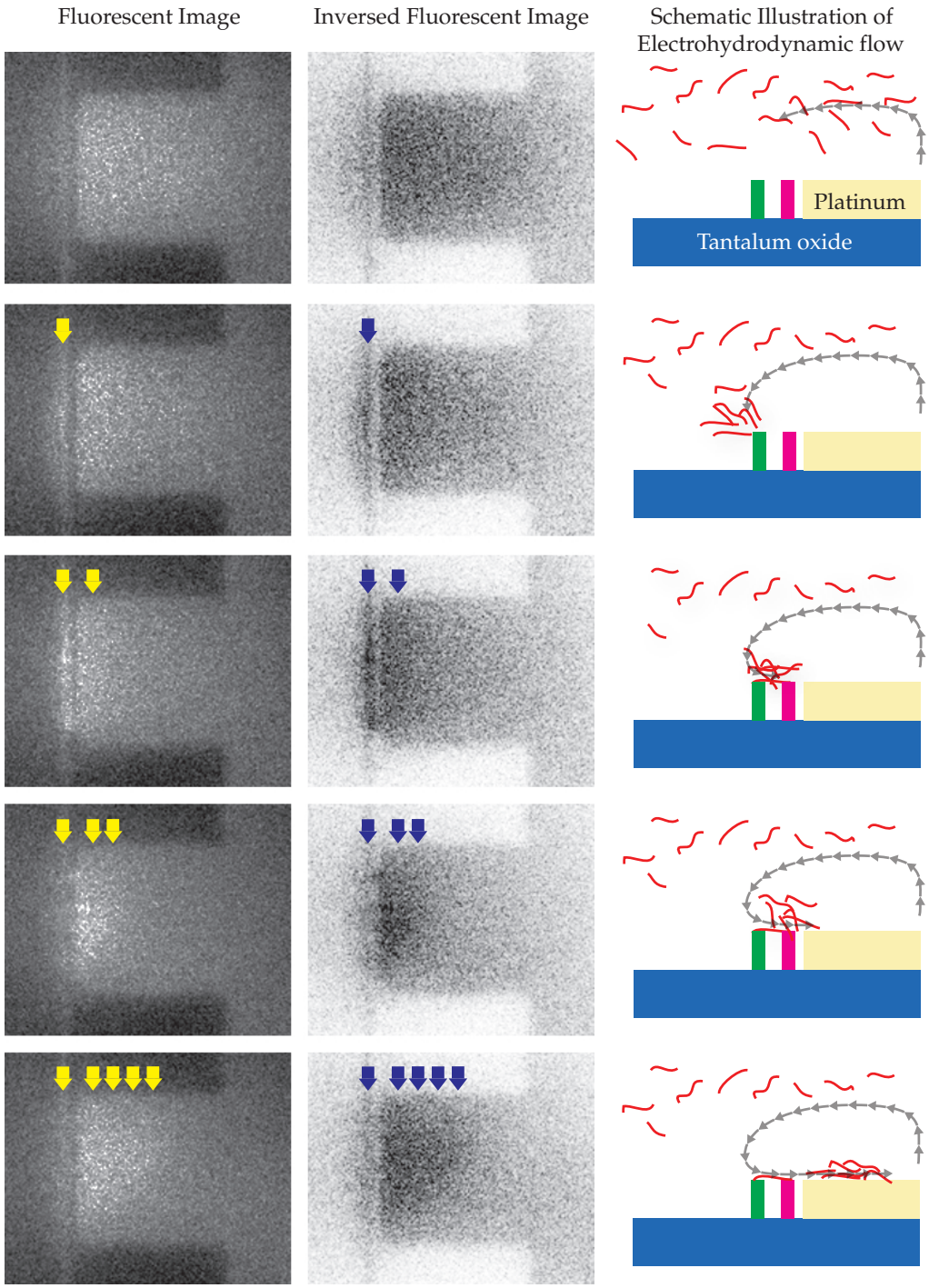

Figure 4.4:
Alignment of thiol-biotin bifunctionalized pUC19 DNA by electrohydrodynamic flow at 200 Hz ($2V_{p-p}$). The flow of DNA was denoted by block arrows. On the right is an schematic illustration showing the DNA (red lines) following the electrohydrodynamic flow (grey arrows).

Dielectrophoretic alignment of DNA (fig 4.5) on a pointed electrode with a lower surface area shows shape dependent behaviour irrespective of applied frequency.

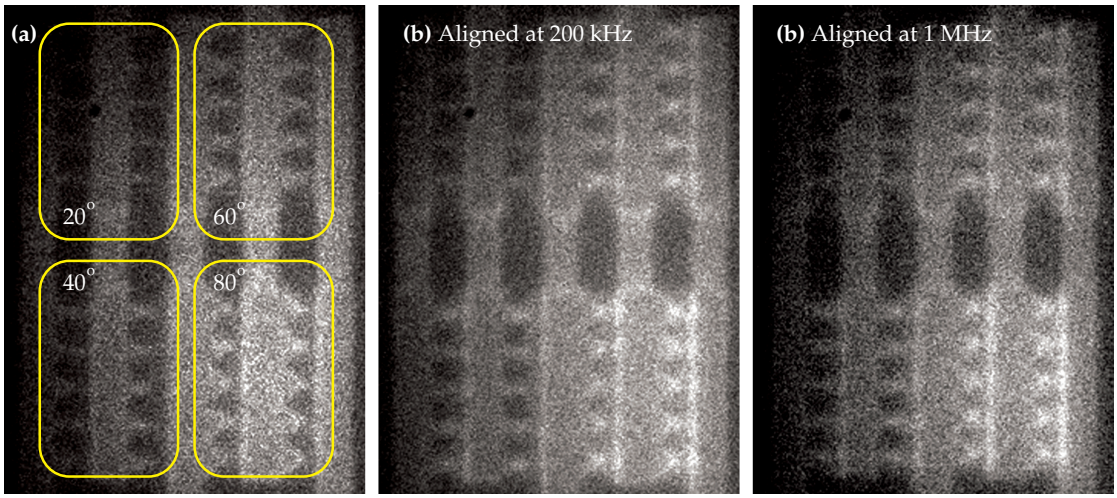

Figure 4.5:
(a) Pointed electrode geometry with varying angles. Alignment of thiol-biotin bifunctionalized pUC19 DNA by dielectrophoresis at $2V_{p-p}$ seen as bright spot at the pointed end, **(b)** 200 kHz, and **(c)** 1 MHz.

Glutaraldehyde Fixing

The resolution of fluorescence imaging was not sufficient to observe single DNA molecule due to the working distance limited by the experimental setup and low optical resolution. Hence, in order to facilitate visualization of DNA in SEM, the DNA was fixed with glutaraldehyde. Figures 4.6b and 4.6c show large amount of DNA being aligned at the electrode tip and a single or few DNA molecules were seen aligned at the electrode tip, respectively. The glutaraldehyde in the absence of DNA could not bridge the electrode gap (fig 4.6a). This technique requires a very delicate washing step to visualize aligned DNA with a high probability.

SEM
Scanning Electron Microscopy

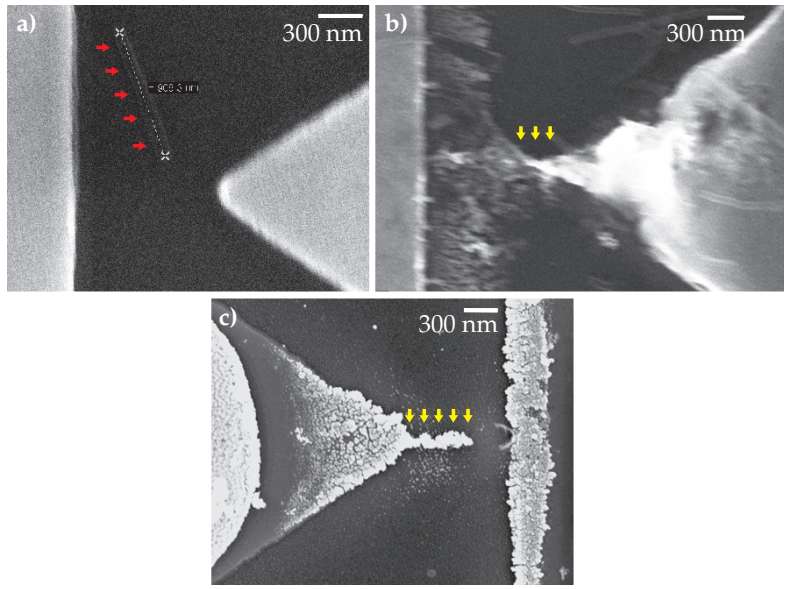

Figure 4.6: Electro micrograph of DNA fixed with gluteraldehyde. **(a)** control experiment without DNA and red arrow indicates the gluraldehyde polymer, **(b)** DNA bridging the electrode gap (arrows), **(c)** Single or few DNA molecules were aligned at the electrode.

Silver Ion Metallization

To effectively visualize DNA in SEM, the aligned DNA was metalized by reducing silver ions.[1] In figure 4.7, one end of DNA molecule was bound to gold surface, the other end was free and unbound to SiO_2. This shows that the biotin is not an efficient anchoring molecule on SiO_2 surface. So silane was considered as an anchoring molecule instead of biotin.[2]

[1] K. Keren et al., Science **297**, 72 (2002)

[2] A. Kumar et al., Nucleic Acids Res. **28**, e71 (2000)

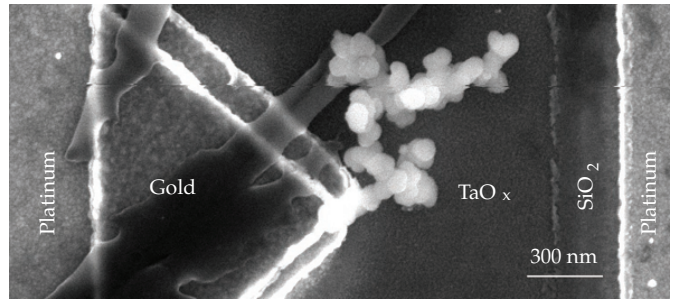

Figure 4.7: Electron micrograph of DNA metallized by reducing silver ions. The bifunctionalized DNA found immobilized only to gold surface.

4.1.2 *DNA Bifunctionalized with Thiol and Silane*

In this DNA bifunctionalization procedure pUC19 plasmid DNA was amplified with 5′ thiol forward primer and 5′ amino reverse primer. The silane molecule (APTES) was coupled to the amino end of DNA with the help of hetro bifunctional cross linkers as mentioned in methods (fig 3.4). The silane molecule is very unstable in aqueous solution especially at basic pH. Hence the linking method was performed in a non-aqueous solution [3]. The thiol group was activated with DTT, desalted and suspended in 25mM MES buffer pH 5.8. At this pH, silane is stable enough for performing the stretching/aligning experiments in aqueous solution. After alignment, the DNA was visualized in SEM by metallization of palladium ions,[4] because the process was easier to control the rate of metallization compared to silver ions.

APTES
3-aminopropyltri ethoxysilane

[3] A. Kumar et al., Nucleic Acids Res. **28**, e71 (2000)

[4] J. Richter et al., Adv. Mater. **12**, 507 (2000)

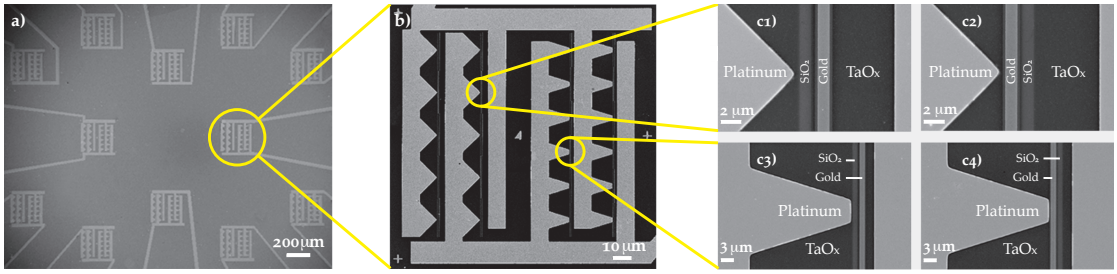

Figure 4.8:
SEM image of fabricated electrode for aligning DNA: **a)** Chip with twelve electrode regions, **b)** Individual electrode region and **c)** Magnified view of pointed and tappered-flat electrode. In both **c1** and **c3**, SiO_2 layer was placed in proximity to the platinum electrode followed by the gold layer. Conversely, in **c2** and **c4**, gold was placed in proximity to the platinum electrode.

Figure 4.8a shows a chip consisting of twelve electrode regions to maintain the same experimental condition during metallization procedure irrespective of applied frequency and voltage to each one of them. Every electrode region (fig 4.8b) consists of a pointed and tapered flat electrode[5] and gold - SiO_2 surface to their proximity (fig 4.8c). The gap between gold - SiO_2 surfaces where varied between 500 - 800 nm with a step size of 50 nm.

[5] K. E. Sung et al., Anal Chem. **78**, 2939 (2006)

The efficiency of orientation defined alignment and immobilization of DNA between gold - SiO_2 surface were achieved by applying 100 kHz (fig 4.9a) and 1 MHz (fig 4.9b) frequencies. The nature of DNA alignment shows the absence of DNA binding to TaO_x surface. DNA terminals lacking either silane (fig 4.10a) or gold (fig 4.10b) failed to bind to their specific surfaces leading to a free unbound DNA and this convinces that the specificity and stability of thiol - silane binding to gold and SiO_2 can be a very good strategy for aligning and orientating DNA over varying distances.

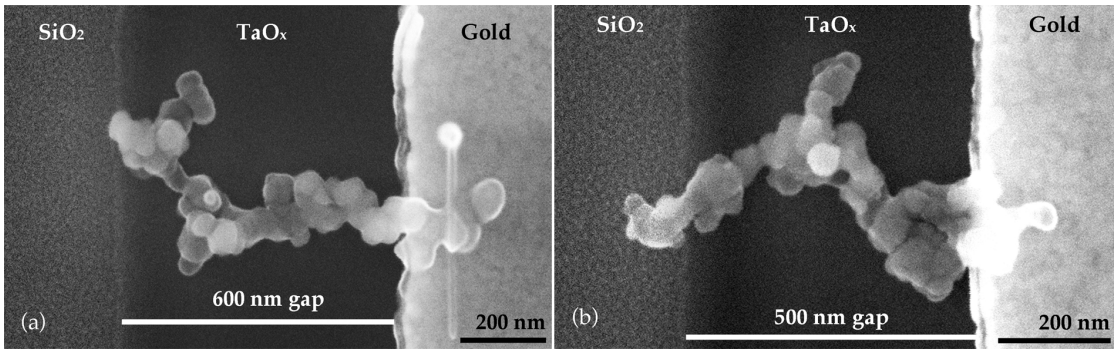

Figure 4.9: SEM image of metallized DNA alignment at **(a)** 100 kHz; 2 V_{p-p} for 5 min and **(b)** 1 MHz; 2 V_{p-p} for 5 min. The DNA was seen fixed between the gold and SiO_2 islands.

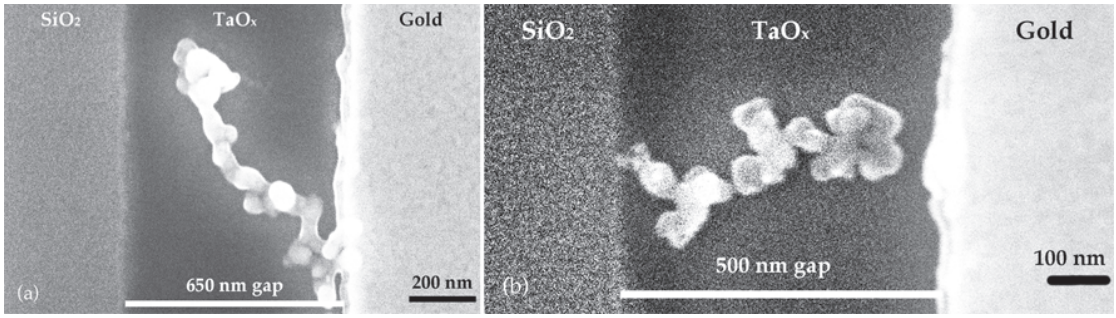

Figure 4.10: SEM image of Metallized DNA: DNA functionalized only with **(a)** thiol (100 kHz; 2 V_{p-p} for 5 min) and **(b)** silane (50 Hz; 2 V_{p-p} for 5 min).

Statistical Analysis

An analysis of 100 SEM images of metalized DNA on the gold and SiO_2 surface shows that around 25% of DNA single molecules

were aligned and immobilized between the gold and SiO_2 layer. Another 50 - 60% of molecules were either bound to gold or SiO_2. The rest of the molecule agglomerate at the edge of the electrode. In principle, most of the DNA in coiled state bind covalently at one end (gold or SiO_2) prior to an applied electric field. The function moiety at the free end of DNA will form covalent linkage to the other surface during stretching and gets aligned. The probability of an alignment is also affected by the proximity effect. Since the width of the binding surface is 1µm, a 890 nm long coiled DNA bind to either gold or SiO_2 at a location far away from opposite surface, then the alignment is not sustained.

4.2 *Synthesis of Homopolymer DNA*

4.2.1 *Synthesis of 239bp DNA*

The first building block of 239bp homopolymer DNA was synthesized by annealing two long oligos followed by extension with klenow fragment. The 239bp DNA fragment was gel eluted and ligated into pGEM-T vector. The ligated mix was then transformed into E.coli JM109. Clones were obtained and confirmed by sequencing. The plasmid which carried 239bp DNA fragment was used as template for further experiments.

4.2.2 *Synthesis of 773bp DNA*

The 773bp DNA fragment was synthesized by concatemerization of three 239bp DNA fragments (fig 4.11a). In order to facilitate the ordered concatemerization, each 239bp DNA was amplified with primers containing specific restriction endonuclease sites at the terminal ends as illustrated in figure 3.9.

The amplified fragments (A, B & C) were digested with kpnI and HindIII endonucleases (fig 4.11b) and ligated with T4 DNA ligase (fig 4.11c). The target 773bp DNA was gel eluted from the ligated product (fig 4.11d & e) and used as template.

The gel isolated 773bp DNA fragment was stabilized by cloning into pJET1.2/blunt ^{TM} vector and transformed in to E.coli JM109. Clones were screened by colony PCR using vector specific primers (fig 4.12a). Positive clones were inoculated in LB media with100µg/ml

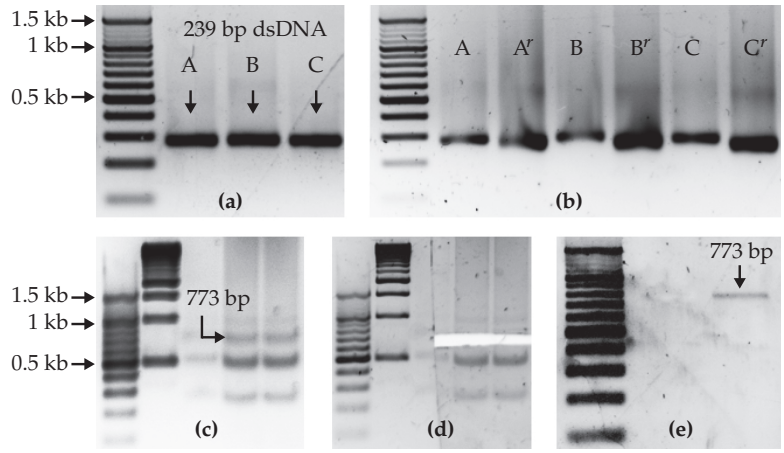

Figure 4.11: Steps involved in synthesis of 773bp:
(a) Synthesis of 239bp fragments with specific restriction sites, **(b)** Restricted with XbaI & Kpn2I (A^r, B^r & C^r), **(c)** Ligated with T_4 DNA ligase, **(d)** 773 bp was gel eluted and **(e)** Gel eluted DNA.

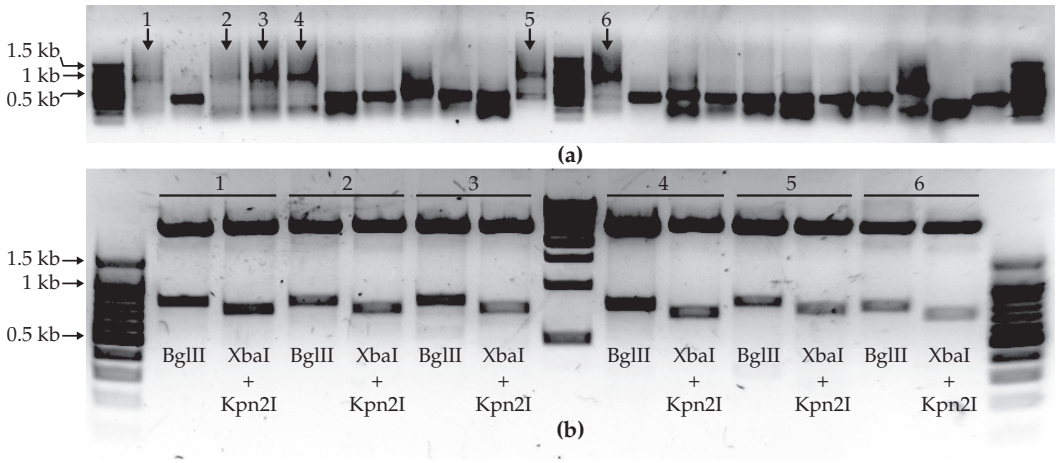

Figure 4.12: Confirmation of positive clones by **(a)** PCR amplification with specific primers, **(b)** Plasmid restricted with BglII (insert release) and XbaI & Kpn2I (773bp specific).

ampicillin and plasmid DNA were isolated. The Plasmids were restricted with BglII and XbaI+kpn2I and the presence of insert was confirmed by their respective sizes of 850bp and 773bp (fig 4.12b).

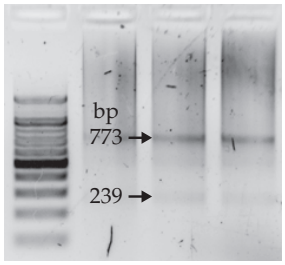

Figure 4.13: Amplification of 773bp using plasmid as template

The plasmid DNA was amplified with specific primers yielded a desired 773bp along with DNA of various lengths (fig 4.13). Hence the insert was released from the plasmid with BglII (fig 4.14a) and used as template to yield a highly homogeneous amplified product (fig 4.14b).

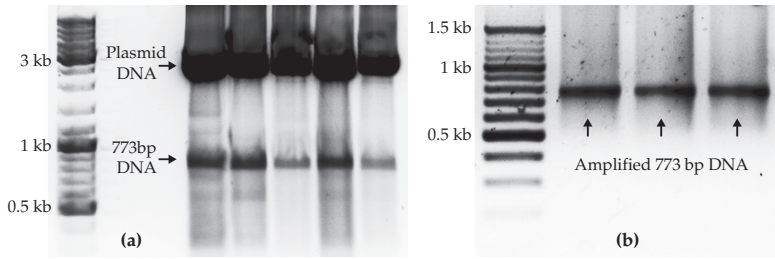

Figure 4.14: Isolation and amplification of 773bp: **(a)** Insert DNA released from plasmid by BglII and **(b)** PCR amplified 773bp DNA.

4.2.3 *Rolling Circle Amplification*

The DNA insert in the bacterial clones was unstable due to the nature of sequence with highly repeated pattern triggering a process called recombination. Hence further proliferation of clones containing 773bp DNA was not feasible and an *in vitro* method called Rolling Cycle Amplification was used for the mass production of 773bp template DNA. The plasmid containing 773bp DNA insert was amplified by Phi29 DNA polymerase (fig 4.15a) as described in table 3.6. The amplified product was restricted with BglII to release the insert DNA (fig 4.15b) and was used as a template.

recombination
A process by which genetic material is broken and joined to other genetic material

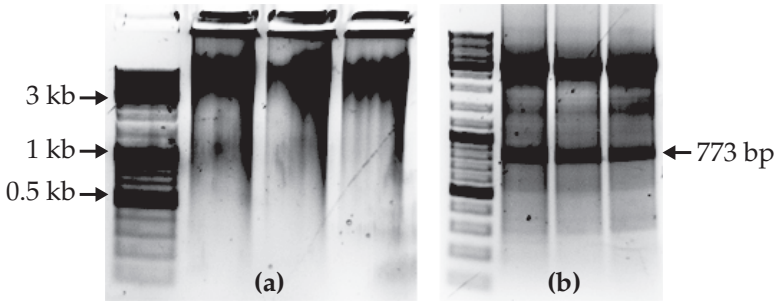

Figure 4.15: **(a)** Rolling circle amplification of plasmid containing insert DNA and **(b)** 773bp DNA released by BglII.

4.2.4 *Synthesis of DNA with Specific Insertion Sequences*

To understand the behavior of DNA polymerase activity with specific sequence, the sequence was inserted into the 773bp homopolymer DNA. This is achieved by amplifying the 239bp DNA with primer containing sequences such as, transcription termina-

tors (ropB1 & exoP) and transcription regulator (ExpR low affinity and high affinity) regions.

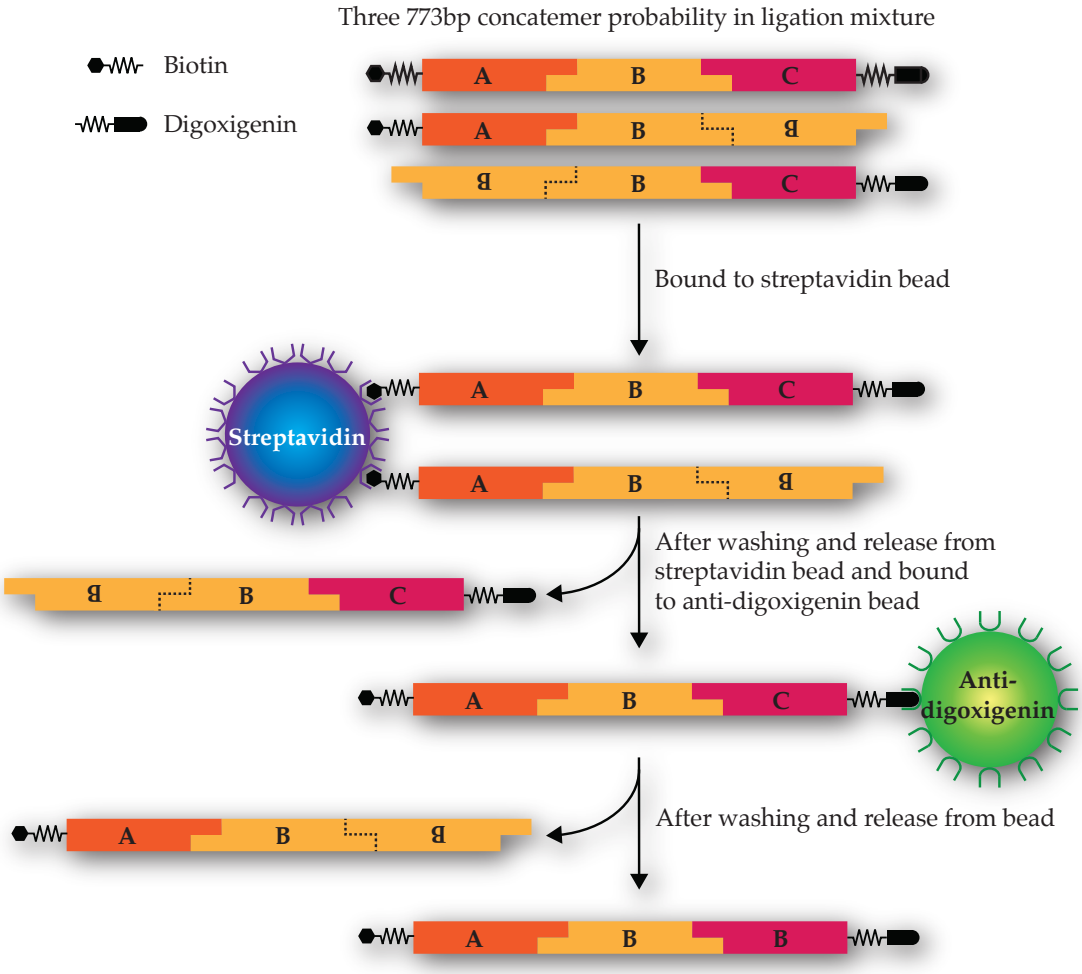

Figure 4.16: Illustration of *in vitro* selection an stabilization technique for concatemerizing DNA fragments.

A new technique was developed to synthesize homopolymer DNA with specific inserted sequence to circumvent the problems associated with cell based amplification (i.e., recombination in host cell). An overview of this new technique was illustrated in figure 4.16. In a ligation mixture (fig 4.11), the probability of an

A-B-C trimer at 773bp was around 33% along with other combinations such as A-B-B and B-B-C trimers. In principle, out of the three 239bp monomers namely, A, B & C, the monomer A & C were tagged during PCR amplification with biotin and digoxigenin at one end, respectively.

As a first step, the gel eluted ligation mixture at 773bp was bound with a streptavidin bead, which captures biotin tagged DNA and the mixture was washed to remove the B-B-C trimer lacking a biotin tag. The DNA fragment captured with streptavidin bead was released and bound with anti-digoxigenin bead. The trimer A-B-B lacking digoxigenin molecule was removed during the washing procedure. Finally the trimer A-B-C was recovered by releasing it from the bead.

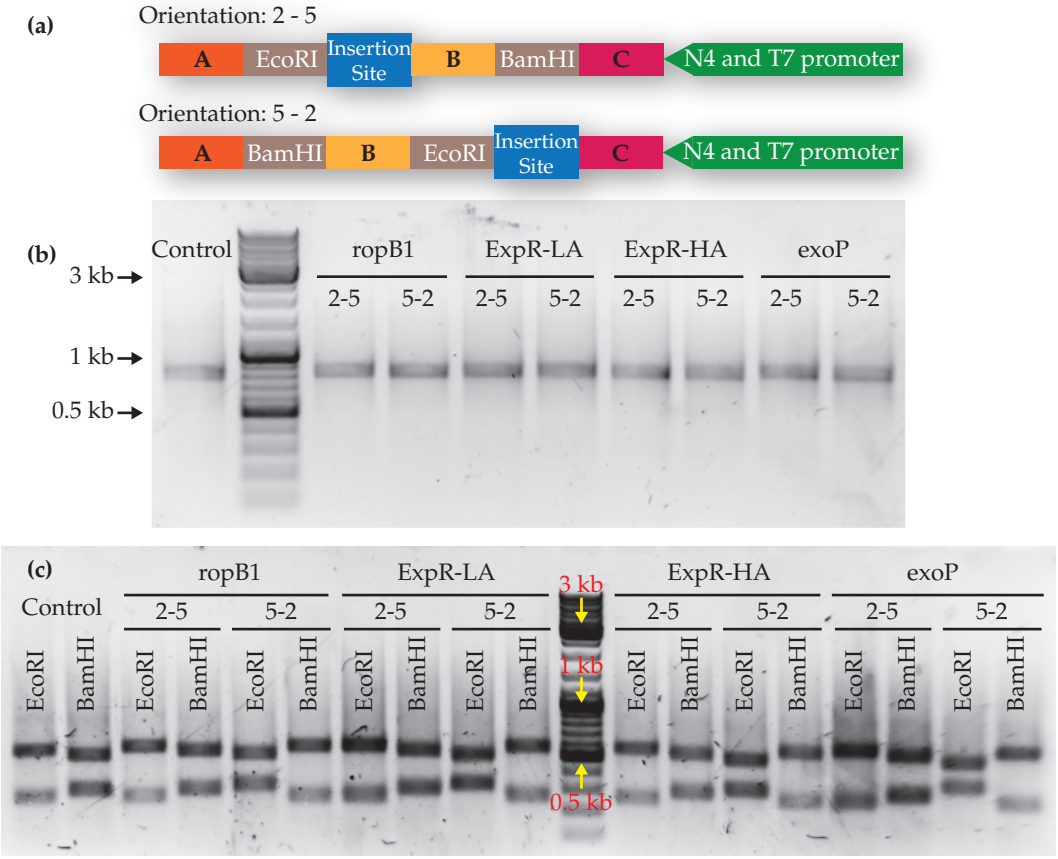

Figure 4.17:
Gel image of DNA with inserted sequence: **(a)** Illustration explaining the orientation nomenclature for inserted sequence, **(b)** PCR product of 773bp DNA with inserted sequence, and **(c)** Restriction analysis of DNA with inserted sequence by EcoRI & BamHI.

The specific sequences were inserted at two different locations (fig 4.17a) between A-BC and AB-C to compare the difference in enzyme activity during experiment and were named 2-5 and 5-2, respectively. The figure 4.17b shows the purity of DNA amplified using the template synthesized by this technique. The restriction analysis of the amplified DNA containing specific insertion sequences confirms the proper orientation of DNA trimers (fig 4.17c).

The **ropB1** inserted DNA (838bp) restricted with *EcoRI* and *BamHI* yielded 583 & 255bp, 517 & 321bp in **2-5** orientation and 494 & 344bp, 583 & 255bp in **5-2** orientation respectively. Similarly, restriction of DNA with **exoP** sequence (865bp) by *EcoRI* yielded 610 & 255bp **(2-5)**, 494 & 371bp **(5-2)** and *BamHI* yielded 544 & 321bp **(2-5)**, 610 & 25 bp **(5-2)**.

The **ExpR-LA** & **-HA** inserted DNA (842bp) restricted with *EcoRI* and *BamHI* yielded 587 & 255bp, 521 & 321bp in **2-5** orientation and 494 & 348bp, 587 & 255bp in **5-2** orientation respectively. Control DNA (without insertion) restricted with *EcoRI* yielded 560 255bp and *BamHI* yielded 494 321bp.

4.3 *Real time analysis of DNA/RNA polymerase activity on homo polymer DNA*

The proposed new technique is fluorescence analysis of DNA protein interaction based on hybridization of molecular beacons with ssDNA. The back-bone of this technique is a DNA template consisting of highly repeated sequence i.e., complementary only to molecular beacon. An overview of this technique is illustrated in figure 4.18. Initially the ssDNA is hybridized with molecular beacon and primer. In the presence of 4 dNTPs, the polymerase extends the primer to synthesize the complementary strand. During this course of complementary strand synthesis, the moving polymerase peels-off the hybridized molecular beacon leading to the decrease in total fluorescence, because the fluorophore and quencher are held in proximity by the molecular beacon in the absence of a complementary DNA. Hence the rate of total fluorescence reduction is directly proportional to the rate of polymerase movement (fig 4.18).

primer
is a short nucleic acid polymer

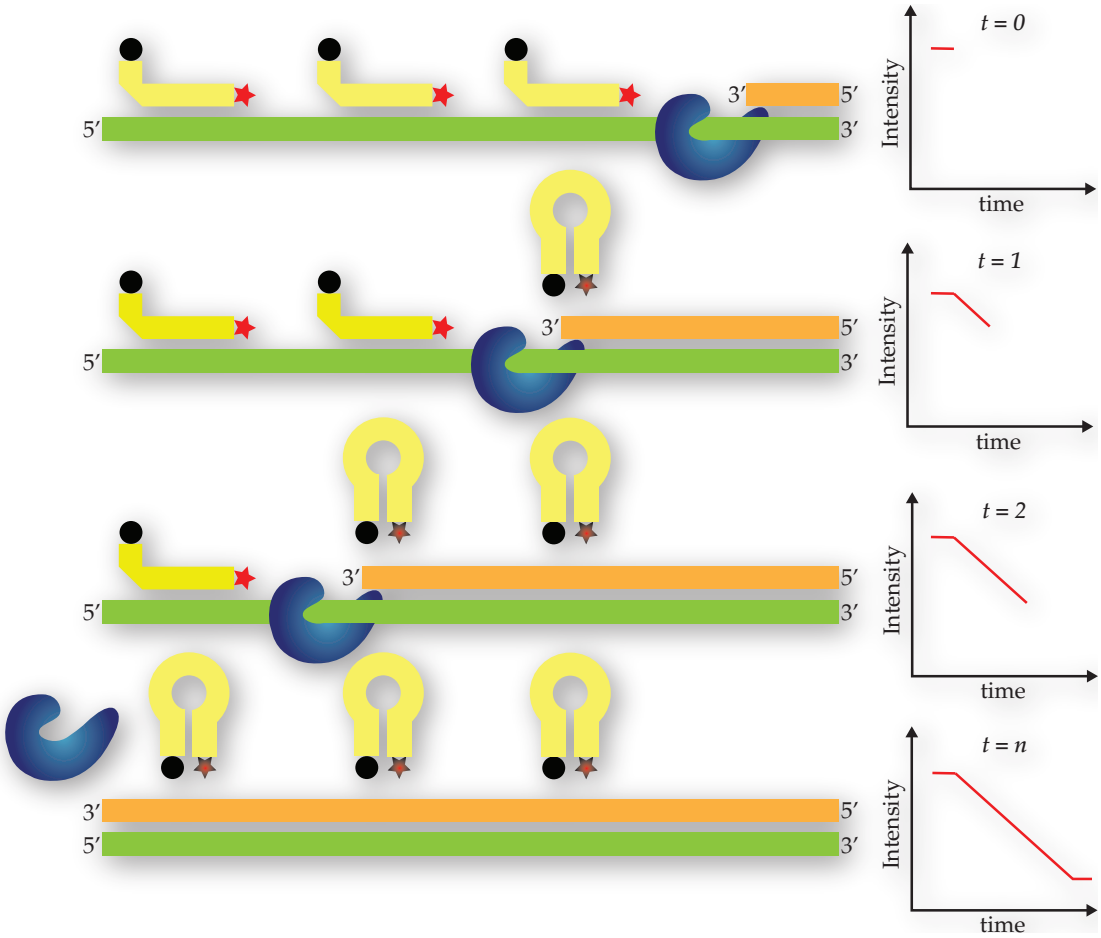

Figure 4.18:
Schematic Illustration of molecular beacon based realtime DNA-Protein interaction studies. The molecular beacons were removed from the target ssDNA by the polymerase during the primer extension leading to decrease in total fluorescence.

4.3.1 *Optimization of Realtime Fluorescence Method*

This new technique requires optimization of many basic parameters such as *instrumental stability*, *injection sequence of reaction component*, *reproducibility*, *enzyme saturation limit* and *molecular beacon characteristics*, which are explained below.

Injection Sequence of reaction component

The synthesis of DNA by polymerase requires few basic components such as nucleotides, primer and ssDNA template. The ssDNA was quantified by UV spectroscopy and cross verified by titration with molecular beacon (fig 4.19).

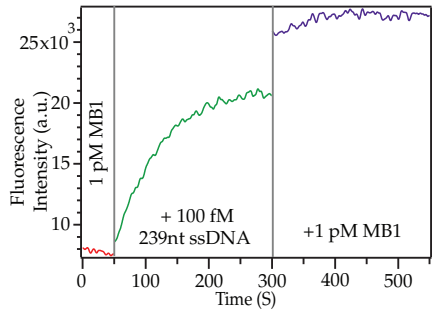

Figure 4.19:
Titration of 100 fM ssDNA with molecular beacon to determine the saturation limit.

The correct injection sequence of the reaction components were determined as shown in figure 4.20. The primer had to be annealed to the ssDNA before the injection of the polymerase else no activity was observed even in the presence of all four dNTPs (fig 4.20a). The polymerase requires all the 4 dNTPs to start the extension process (fig 4.20b).

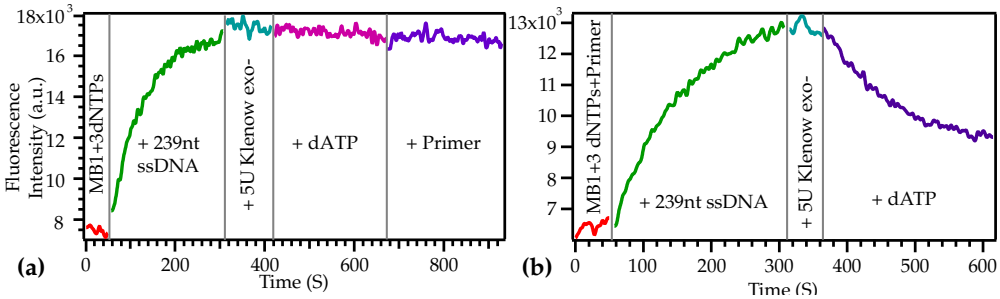

Figure 4.20:
Sequence of component injection for polymerase activity: **(a)** No polymerase activity and **(b)** Polymerase activity

Reproducibility

Experiments involving identical parameters were performed more than once to confirm the reproducibility in the rate of fluorescence reduction among them as shown in figure 4.21.

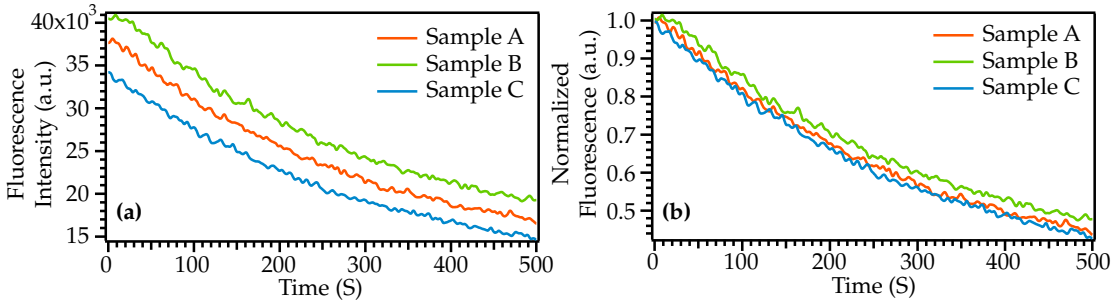

Figure 4.21:
Experimental reproducibility: **(a)** Raw fluorescent data as a function of detection time and **(b)** Normalized fluorescent data.

Saturation Limit

Analyzing the activity of DNA polymerase in bulk solution requires all of them to start extending the template DNA at the same time. This was achieved by determining the saturation limit of the polymerase for a given template concentration. The rate of fluorescence decrease with respect to enzyme concentration was shown in figure 4.22. For a 100 fM template concentration, 20 unit of enzyme was sufficient to nearly oversaturate the reaction.

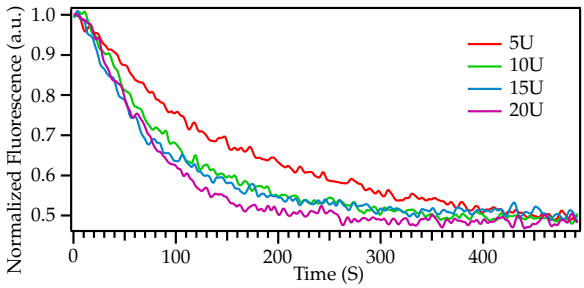

Figure 4.22:
Determination of polymerase concentration to oversaturate 100 fM ssDNA.

Molecular beacon characterization

The specificity of the molecular beacon designed for the real time analysis was shown in figure 4.23a. The molecular beacon

was incubated with different DNA such as lambda phage genome, pUC19 plasmid, 239bp dsDNA, and 239nt ssDNA under same conditions. The increase in total fluorescence was observed only in the presence of 239nt ssDNA due to hybridization of molecular beacon. The absence of an increase in fluorescence for DNA from other sources shows the specificity of the designed molecular beacon.

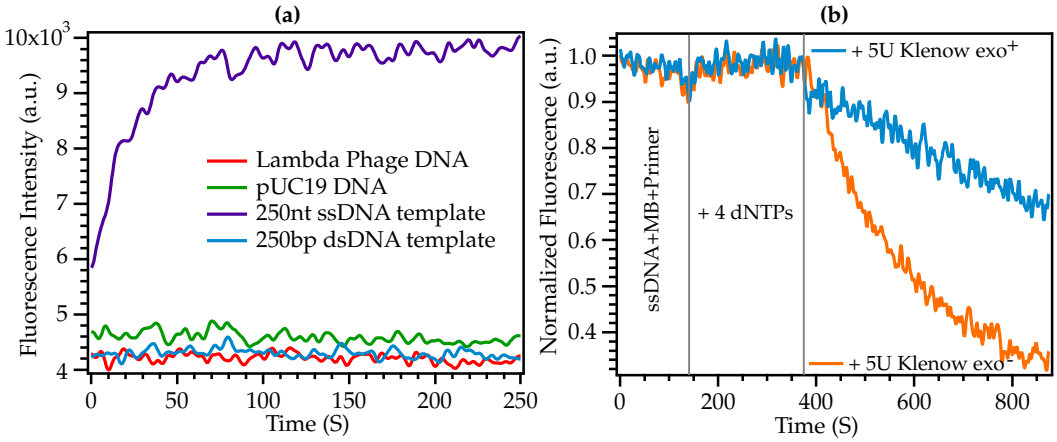

Figure 4.23: **(a)** Specificity of molecular beacon and **(b)** susceptibility of phosphodiester and resistance of phosphothioate backbone by exonuclease activity.

The molecular beacon made up of phosphodiester backbone could be susceptible to $3\prime \rightarrow 5\prime$ exo nuclease activity of the polymerase, because it may cleave the fluorophore or quencher from/of the beacons. In this experiment (fig 4.23b), the rate of decrease in fluorescence was higher for Klenow exo- compared to exo+ under the same conditions. In order to prevent the degradation of molecular beacon by exonuclease activity of polymerase, a phosphothioate backbone was preferred for further experiments.

4.3.2 *Analysis of DNA Polymerases*

Generally, enzymes have a very robust activity and highly dependent on many factors, such as temperature, Mg^{2+} ion concentration (in case of DNA polymerases), and other reaction components for successful conversion of substrate to product. A bacterial origin *E.coli* DNA polymerase I and a viral origin T7 DNA polymerase were used as model enzyme to demonstrate the newly de-

veloped molecular beacon based real time fluorescence technique. This realtime method was also used for monitoring T7 and N4 RNA polymerase activity.

To understand the temperature dependent activity, both the DNA polymerases were measured at temperatures 5^oC below optimal, and 5^oC above optimal. Similarly, magnesium ions act as a co-factor for polymerase activity and hence the activity is directly related to Mg^{2+} ion concentration in the reaction mixture. The EDTA was used as a chelating agent to reduce the Mg^{2+} ion concentration in the reaction buffer to validate the enzymatic activity. The activities of the two DNA polymerases under altered experimental conditions are given below.

EDTA
Ethylenediaminetetraacetic acid

E.coli DNA Polymerase I

The temperature dependent activity (fig 4.24) was measured at 32, 37 & 42^oC shows a near linear behavior of polymerase activity. In case of Mg^{2+} ion dependence (fig 4.25a), the ions were quenched by adding EDTA. The polymerase showed a reduced activity, when 25% of Mg^{2+} ions (12.5% EDTA) were quenched compared to native buffering conditions. At 50% (25% EDTA) and 75% of Mg^{2+} ion (37.5% EDTA) quenching, the polymerase retained a minimal and no activity, respectively. Figure 4.25b shows the activity of polymerase on DNA inserted with exoP, ropB1 or ExpR-LA and ExpR-HA sequence in the absence of ExpR or Acyl-homoserine lactone activated ExpR protein.

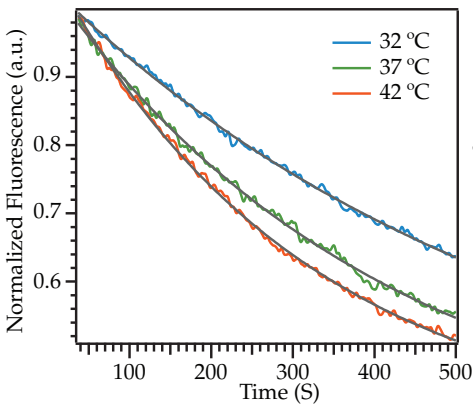

Temparature(°C)	Fit parameter τ (seconds)
32	604.53 ± 8.09
37	411.31 ± 4.16
42	311.79 ± 1.85

Figure 4.24: Temperature dependent activity of *E.coli* DNA polymerase I (scattered lines) fit with an exponential function (straight lines) (eqn 3.1).

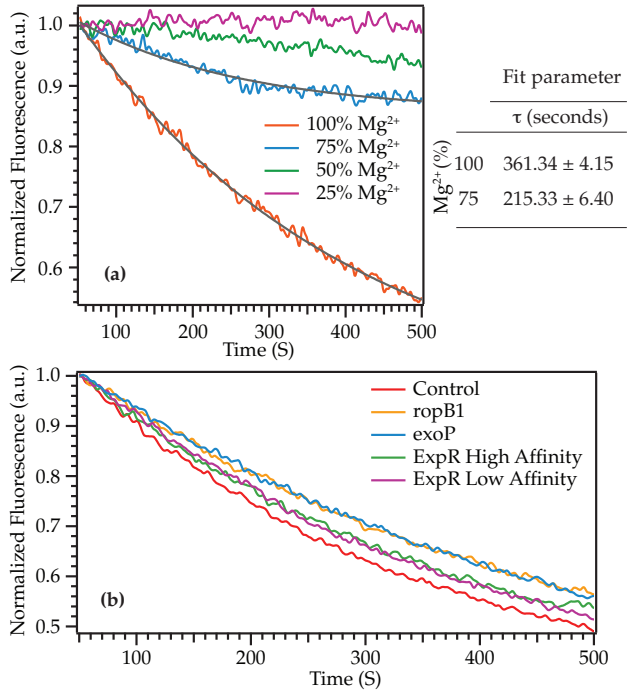

Figure 4.25: Activity of *E.coli* DNA polymerase I with respect to: **(a)** Mg^{2+} ion dependence, **(b)** Effect of inserted DNA sequence

T7 DNA Polymerase

The temperature dependent activity (fig 4.26a) was measured at 32, 37 & 42^{o}C shows an exponential decay of fluorescent intensity. In case of Mg^{2+} ion dependence (fig 4.26b), a complete loss of activity was observed when 25% of Mg^{2+} ions (12.5% EDTA) were quenched. Hence, the activity was measured at lower quenching rates of 6.25% (3.125% EDTA) & 12.5% (6.25% EDTA) along with no quenching control reaction. The temperature dependent activity was again measured at reduced polymerase speed by quenching 12.5% of Mg^{2+} ions (fig 4.26c). Figure 4.27 shows the activity of polymerase on DNA inserted with exoP, ropB1 or ExpR-LA and ExpR-HA sequence in the absence of ExpR or Acyl-homoserine lactone activated ExpR protein.

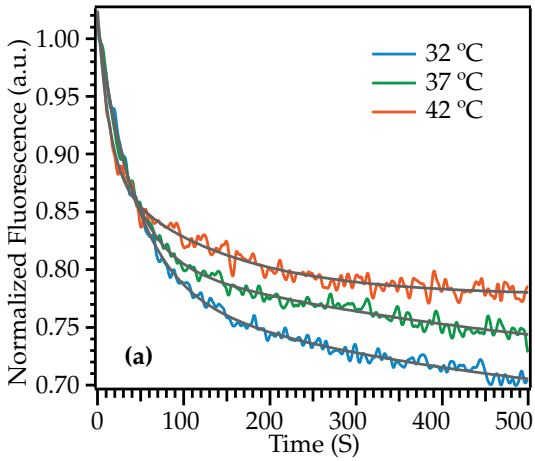

Temparature(°C)	Fit parameters	
	τ_1 (seconds)	τ_2 (seconds)
32	45.244 ± 0.854	470.15 ± 69.4
37	35.869 ± 0.669	572.64 ± 99
42	13.817 ± 0.489	135.60 ± 4.1

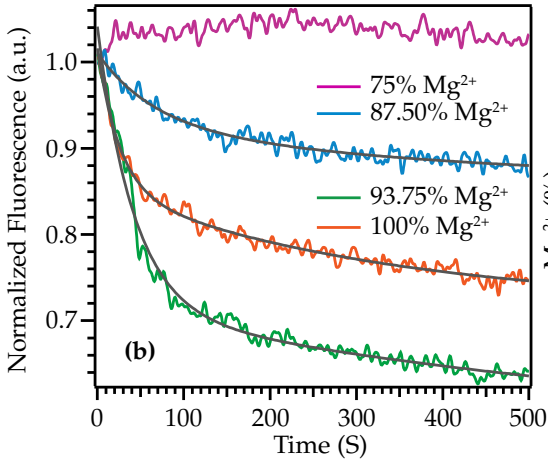

Mg^{2+} (%)	Fit parameters	
	τ_1 (seconds)	τ_2 (seconds)
100	25.146 ± 0.818	324.08 ± 23.9
93.75	42.579 ± 0.0003	1121.6 ± 1.05e-5
87.5	64.154 ± 9.61	379.11 ± 222

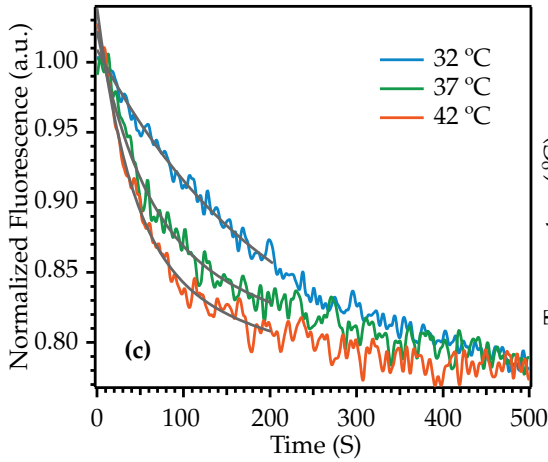

Temparature(°C)	Fit parameters	
	τ_1 (seconds)	τ_2 (seconds)
32	202.12 ± 7.78 e+04	163.57 ± 4.73 e+04
37	49.806 ± 94	102.53 ± 381
42	35.597 ± 18.9	87.119 ± 89.5

Figure 4.26:
Activity of T7 DNA polymerase with respect to: **(a)** Temperature, **(b)** Mg^{2+} ion dependence, and **(c)** Temperature dependent activity with 87.5 % Mg^{2+} ions.

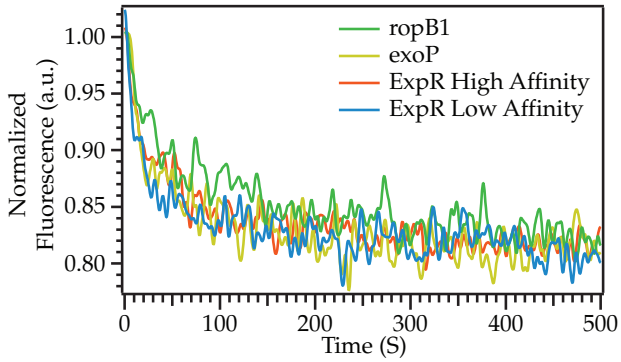

Figure 4.27: Effect of inserted DNA sequence on T7 DNA polymerase activity.

4.3.3 *Analysis of RNA Polymerases*

The activity of T7 and N4 virion RNA polymerases were monitored using molecular beacon based DNA-Protein interaction method. Promoters specific for these polymerases were inserted at the terminal of 773bp homopolymer DNA. Both ssDNA and dsDNA were used as template for T7 RNA polymerase, whereas ssDNA was used as template for N4 polymerase. Figure 4.28a and b, shows the activity of T7 polymerase on dsDNA and non-specific binding of N4 virion polymerase with molecular beacon.

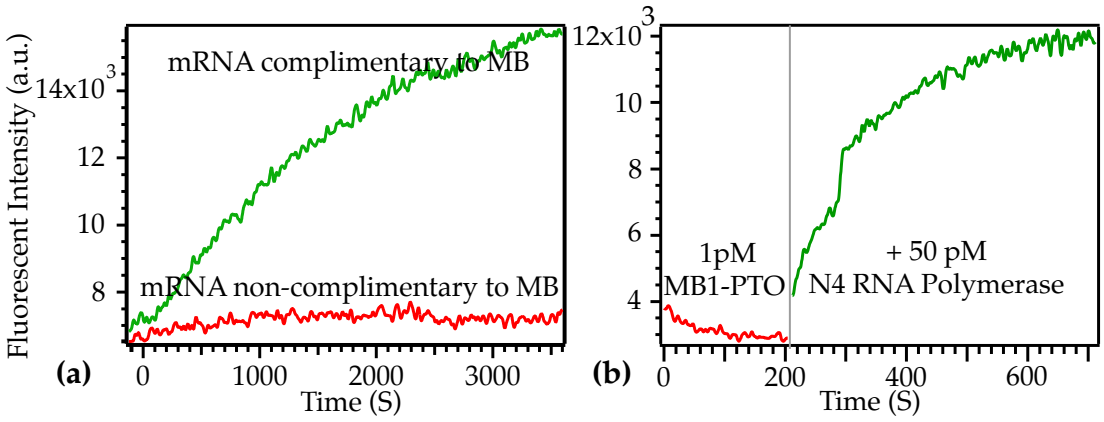

Figure 4.28: *In vitro* transcription of homopolymer DNA: **(a)** Transcription of ds-DNA by T7 RNA polymerase yielding RNA in sense and anti-sense to molecular beacon and **(b)** Activity of N4 virion RNA polymerase

5
Discussion

Different techniques were developed during the course of this study to recreate the enactment of DNA-protein interaction *in vitro*. This chapter reiterates those experimental techniques in detail including an explanation and compared with relevant literature to highlight the novelty behind it. The chapter contains four sections, namely *Alignment of DNA*, *Synthesis of Homopolymer DNA*, *Molecular-Beacon Characteristics Polymerase Activity*, *Conclusion* and *Outlook*

5.1 Alignment of DNA

The alignment of DNA in this study was performed using the electrokinetic force because of the advantage of its control over the spatial location of the DNA molecule being aligned. The number of aligned molecules could be modulated from single DNA strands to few hundreds of molecules in one experiment by adjusting the DNA concentration in the bulk solution.

5.1.1 Immobilization and Visualization of DNA

Immobilization of aligned DNA to a surface is an essential tool for the advancement of DNA based biomedical devices.[1] At below physiological pH, the native DNA terminals denature and the exposed nitrogen-containing nucleobases bind to the surface at acidic pH,[2] but this technique is limited since most of the DNA binding protein becomes inactive at below physiological pH. DNA

[1] M. Beier et al., Nucleic Acids Res. **27**, 1970 (1999)

[2] T. M. Herne et al., J. Am. Chem. Soc. **119**, 8916 (1997)

immobilization at physiological pH can be achieved by functionalizing the DNA either at terminal or internal using different chemistries. The nature of binding chemistry could be hydrophobic-hydrophobic interaction,[3] electro-static interaction[4] or covalent bonding.[5]

Covalent binding of DNA to the surface is significant for a device to withstand the assay procedure. Some of the covalent binding includes thiol binding to gold[6] and silane binding to silicon-dioxide surface.[7] Two binding chemistries were investigated for an orientation defined DNA alignment, namely (i) DNA functionalized with thiol at one end and biotin at the other end based on covalent and physical adsorption chemistries, respectively and (ii) DNA functionalized with thiol and silane at either ends based on covalent chemistry.

The aligned DNA was visualized by fluorescence microscopy and electron microscopy after gluteraldehyde fixing or metallization. DNA was metallized by reducing silver or palladium ion to facilitate high resolution imaging. Though AFM can be used for imaging aligned DNA without any modification, the surface roughness of tantalum oxide of around 5 nm proved impossible to image a DNA with 2 nm diameter.

The initial experiments were indeed performed with fluorescent DNA and observed in a fluorescence microscope. The full setup included a special constructed IC socket and a cover slit to allow an upside down observation. With this setup, it is not possible to use confocal microscopy and we were not able to obtain a qualitatively reasonable fluorescent image with an inverse fluorescent microscope.

5.1.2 *Alignment of DNA Functionalized with Thiol and Biotin*

The PCR amplification of pUC19 plasmid DNA with thiol-forward and biotin-reverse primer yielded a bifunctionalized DNA with a physical length of 890 nm. The thiol activated DNA was incubated with YOYO-1 dye at a ratio of 5:1 concentration for fluorescence imaging, dropped over the electrode surface, and closed with a cover slip to prevent the evaporation of solution. β-Mercaptoethanol was added to the DNA-dye solution to prevent photo-bleaching

[3] J. Allemand et al., Biophys J **73**, 2064 (1997)
[4] D. C. Schwartz et al., Science **262**, 110 (1993)
[5] E. Braun et al., Nature **391**, 775 (1998)
[6] V. Namasivayam et al., Anal. Chem. **74**, 3378 (2002)
[7] A. Kumar et al., Nucleic Acids Res. **28**, e71 (2000)

and minimize the evaporation induced turbulence.[8]

[8] J. Han et al., Anal. Chem. **74**, 394 (2002); and H.-Y. Lin et al., Nanotechnology **16**, 2738 (2005)

Alignment by Electrohydrodynamic Flow

DNA gets stretched and aligned with a local microscopic circular flow caused by movement of ions at the electrode surface in an applied non-uniform AC field.[9] The platinum electrode was fabricated with a characteristic size of 25 μm. The gold & SiO_2 layers acting as an anchoring surface for the bifunctionalized molecule, were fabricated in proximity to the platinum electrode with a gap of 500 nm between them. Figure 5.1 shows the electrohydrodynamic flow based alignment of DNA in dependence of the applied frrequency, in which the DNA follows the cyclic fluid motion generated by a non-uniform AC electric field. The rate of cyclic motion increases above the applied frequency of 100 Hz for the fabricated electrode geometry.

[9] H.-Y. Lin et al., Nanotechnology **16**, 2738 (2005)

The circular flow of the bulk solution is dependent on the applied frequency, electrode geometry and bulk solution properties. The torque of the flow increases proportionally with increase in surface area of the electrode. The speed of the flow depends on the applied frequency which causes the diffuse double layer formation creating a mass movement of bulk solution towards the electrode's edge. Pixel analysis of time-lapsed fluorescent image (fig 5.1 a&c) show the movement of DNA (peaks marked with green markers) along the electrode surface with highest intensity at the edge and gradually diffusing as the flow moves towards the center of the electrode. Stretched-alignment or trapping of DNA was observed at 100 Hz applied frequency at the electrode edge where the gold and SiO_2 was located (fig 5.1 b) compared to image at t=o.

Alignment by Dielectrophoresis

Dielectrophoresis is a translational motion of a particle due to interaction of an induced dipole with an electric field. It is widely used for trapping and manipulation of particles and biological materials such as viruses, bacteria, plant and animal cells.[10] Stretching of DNA by dielectrophoresis was first demonstrated by Washizu *et al.*[11]

[10] R. Pethig et al., Trends in Biotech. **15**, 426 (1997)

[11] M. Washizu et al., IEEE Trans on Industry Applications **31**, 447 (1995)

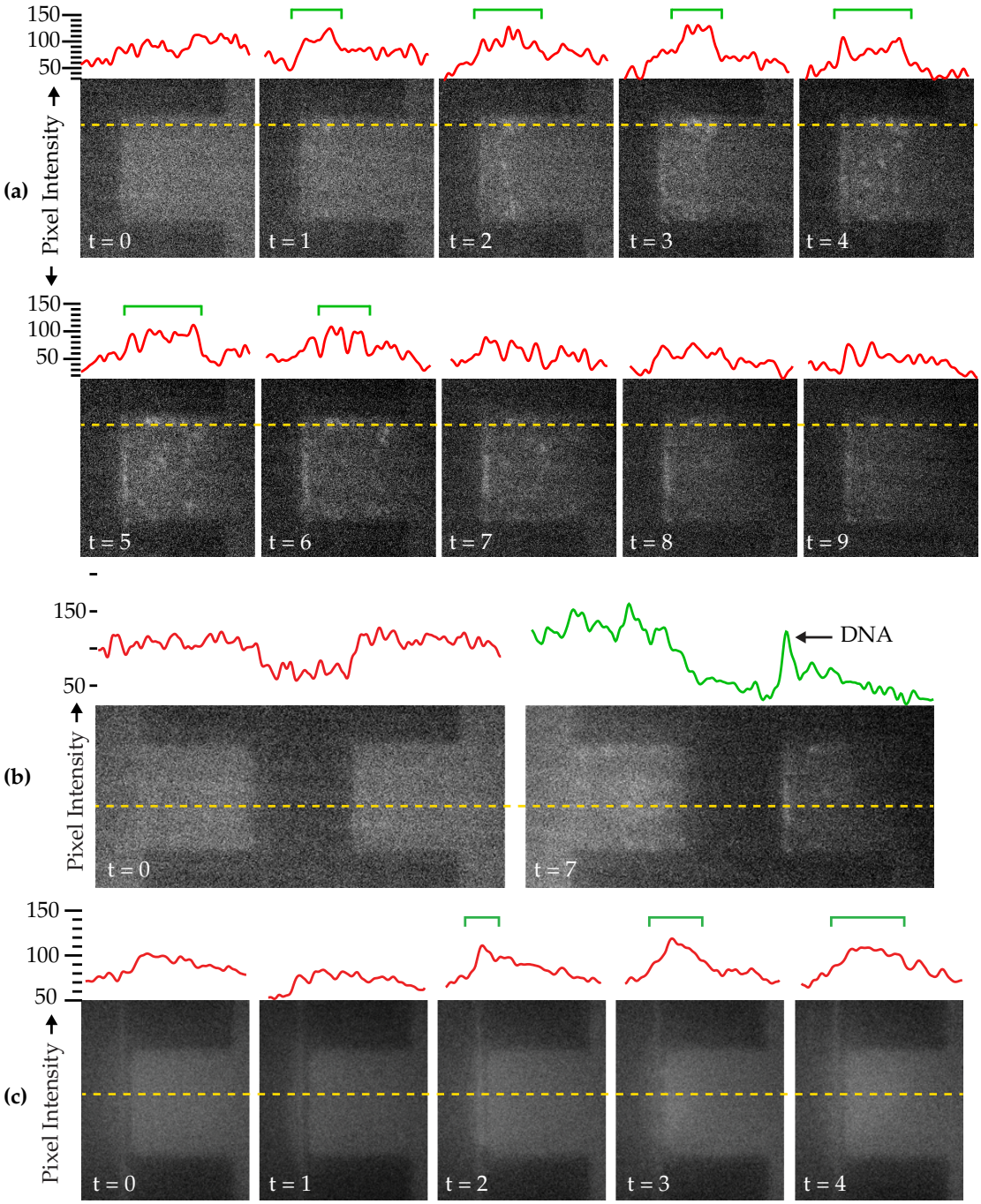

Figure 5.1:
Pixel analysis of image (yellow dotted line) shows the movement of DNA (green marker) over the electrode surface: **(a)** 100 Hz applied frequency, **(b)** DNA aligned at gold and SiO_2 surface (100 Hz; 2 V_{p-p}), and **(c)** 200 Hz applied frequency.

In this work, stretching of DNA was performed at the dielectrophoretic regime between 100 kHz and 1 MHz. The thiol-biotin bifunctionalized DNA was dropped on the pointed tip electrode (fig 4.2b) and stretched at an applied frequency of 200 kHz and 1 MHz. The geometrical angle of pointed electrode was varied at 20^o, 40^o, 60^o & 80^o to identify an optimal angle for efficient DNA alignment. Figure 5.2 shows the efficiency of DNA aligned/trapped at the electrode tip by image analysis.

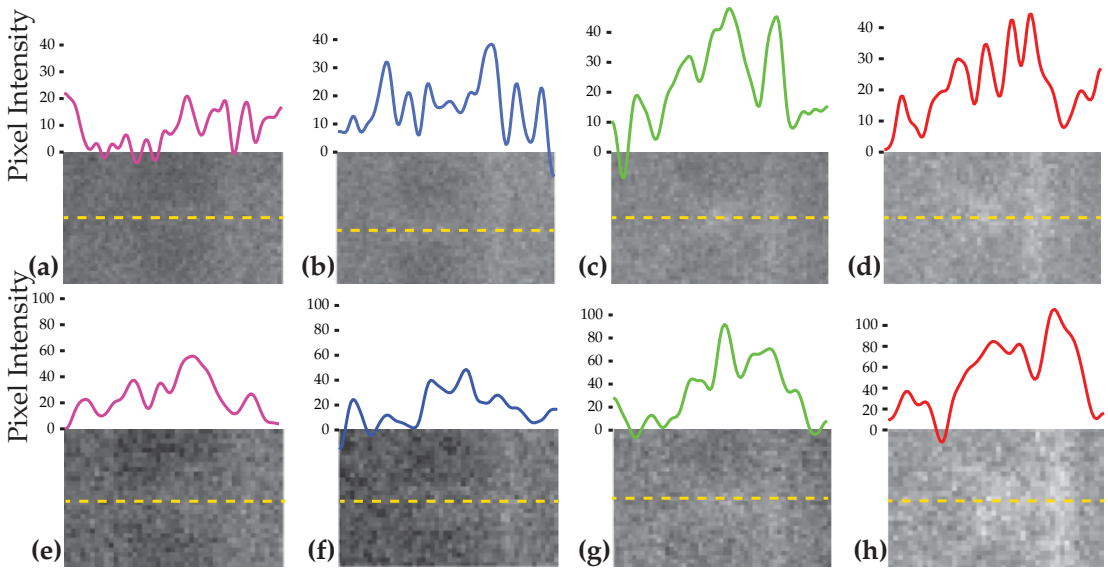

Figure 5.2: Alignment of DNA by dielectrophoresis at 200 kHz (a-d) and 1 MHz (e-h). Electrodes with varying angles 20^o (a&e), 40^o (b&f), 60^o (c&g) and 80^o (d&h) showed higher fluorescence at wider angles.

The image line plot shows the difference in pixel intensity between the initial and final time frame during the applied frequency. Electrodes with wider angle showed higher efficiency in aligning / trapping the DNA at applied frequencies of 200 kHz and 1 MHz.

The DNA visible at the desired electrode regions in the form of a bright fluorescence spots were not necessarily a conclusive evidence of DNA being aligned, due to the resolution limitation of the optical setup. After electrokinetic alignment, the DNA was cross-linked with glutaraldehyde or silver ion metallization to aid visualization in SEM.

SEM
Scanning Electron Microscope

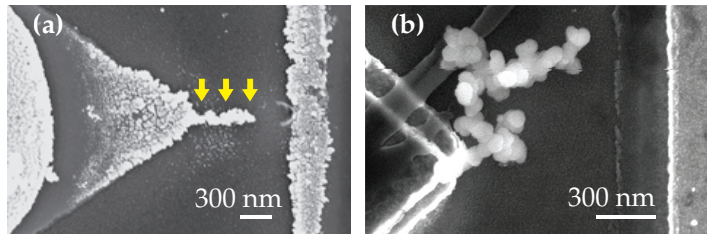

Figure 5.3: Electron microscopy image of **(a)** single/few DNA seen at electrode (yellow arrows) fixed by glutaraldehyde and **(b)** Single DNA molecule by slver ion metallization.

Figure 5.3a shows the single or few DNA aligned at the pointed electrode (yellow arrows). One possible explanation for visualizing DNA could be trapping of salts present in the reaction buffer by crosslinked molecules. Hence, the possibility of visualizing the aligned DNA directly depends on the washing procedure.

To find a more robust method for visualizing aligned DNA, the DNA was metalized by reducing silver ions. [12] Converting the DNA to a metallic wire makes it more stable during the washing procedure (fig 5.3b).

[12] K. Keren et al., Nano Lett. 4, 323 (2004)

Moreover in this work, the rate of metallization was not controllable to yield a consistent particle size. Figure 5.4 shows the different rate of metallization process between four experiments under the same conditions. The process of over-metallization could be caused either during aldehyde derivatization or reduction of silver ions.

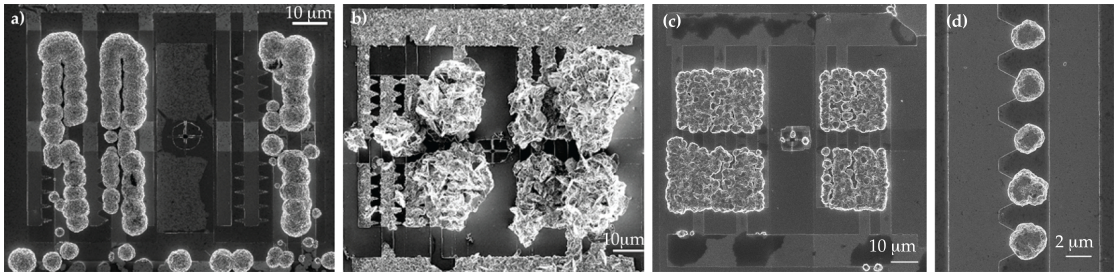

Figure 5.4: Electron microscopic image shows the inconsistent control over the silver metallization of DNA in different experiment with same procedure.

A single DNA molecule bifunctionalized with thiol and biotin was found to be immobilized only to gold surface (fig 5.3b). Whereas the biotin end of DNA failed to immobilize to the SiO_2 surface, which shows that biotin is not a suitable anchoring molecule.

5.1.3 *Alignment of DNA Functionalized with Thiol and Silane*

Immobilization of DNA terminals is important for sustaining an orientation defined alignment. Since the interaction between biotin and SiO_2 surface was not strong enough, a silane functional group was investigated to sustain the aligned DNA along with thiol group at the other end. To bifunctionalize the DNA with thiol and silane, the pUC19 plasmid was PCR amplified with thiol-forward and amino-reverse primers. The silane molecule was linked to the amino end of the DNA as described in figure 3.4. The DNA was metalized by reducing palladium ions[13] instead of silver ion metallization due to afore mentioned reasons. The produced palladium-DNA wires were stable similar to silver ion based metallization procedure. A better control on obtaining consistency in particle size during reduction of Pd^{2+} ions was found advantageous in this study.

[13] J. Richter et al., Adv. Mater. **12**, 507 (2000)

Figure 5.5 shows a palladium ion metalized DNA aligned at two different frequencies immobilized by terminal thiol and silane moieties. The DNA was immobilized only at the termini and the inter-terminal region was free from any interaction with the surface. The contour of aligned DNA was dependent on gap width, i.e., at wider gaps the contour was more linear (fig 5.5a) than in case of a narrower gap (fig 5.5b) and shows the free hanging nature of the immobilized DNA. The free hanging DNA between two points in the absence of an applied electric field will retain the standard B-structure of DNA.

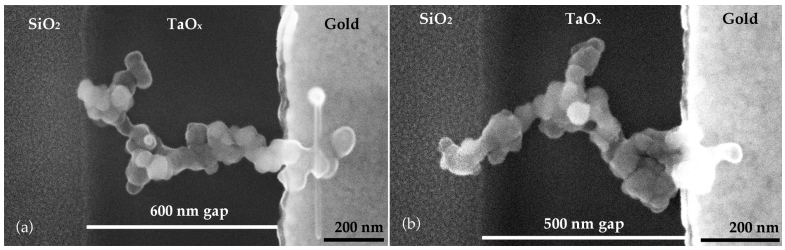

Figure 5.5: Electron microscopic image of metallized DNA alignment at **(a)** 100 kHz; 2 V_{p-p} for 5 min and **(b)** 1 MHz; 2 V_{p-p} for 5 min.

The specificity of binding chemistries were verified with a control experiment by functionalizing only one end of DNA, showing the specificity of thiol binding to gold and silane binding to

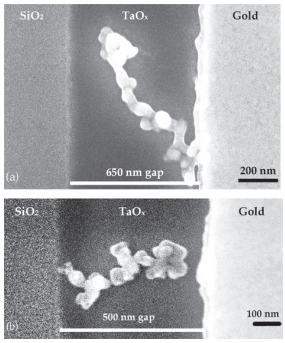

Figure 5.6: Electron microscopic image of Metallized DNA: DNA functionalized only with **(a)** thiol (100 kHz; 2 V_{p-p} for 5 min) and **(b)** silane (50 Hz; 2 V_{p-p} for 5 min)

SiO_2 surface (fig 5.6). The DNA was amplified by one modified primer and one unmodified primer. The thiol-only functionalized DNA (HS-DNA) bound to gold surface but not to SiO_2 (fig 5.6a). Similarly, the silane-only DNA (DNA-silane) bound only to SiO_2 surface (fig 5.6b). In both cases, the unmodified end of DNA retracted back to the immobilized end after stretching by an applied electric field.

In figure 5.6, it can be noted that the gap between gold and SiO_2 was less than 650 nm and due to the absence of an anchoring molecule at one end the stretching was not sustained. It is in perfect agreement with fluorescent data published by Namasivayam *et al.*,[14] where the thiol tagged DNA immobilizes on a gold electrode stretches, when an electric field was turned on and retracts back in the absence of an electric field (fig 5.7).

[14] V. Namasivayam et al., Anal. Chem. **74**, 3378 (2002)

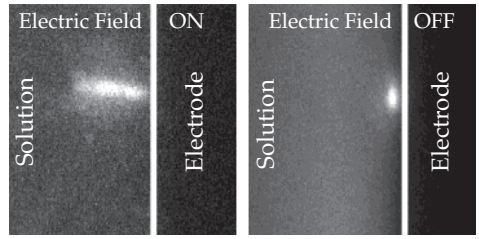

Figure 5.7: Fluorescent image of thiol-labeled DNA partly stretched under a electric field and recoils back and sticks to the right electrode electric field was switched off. Source: Namasivayam *et al.*, Anal. Chem. 74 (2002).

Based on the results, an optimal gap between gold and SiO_2 is directly dependent on the length of the DNA, physically a length of around 50 and 70 nm of DNA was required at both ends as spacers for efficient clamping. A lower gap resulted in an understretched but immobilized DNA and a higher gap led to a loss of clamping at one or both ends, so the DNA will either retract to its immobilized end or in to the solution, respectively. The gold and SiO_2 surface facilitate the anchoring of aligned DNA, but it is not clear, which event happens first i.e., immobilization or stretching, hence it could be deciphered that both are possible. First, the HS-DNA-Silane could bind either to gold or SiO_2 during the incubation process and gets stretched in the presence of an electric field gradient. Alternatively, the DNA would get immobilized during stretching[15] either to gold or SiO_2 placed in proximity to the platinum electrode due to the electrokinetic force, when an AC field is applied.

[15] H.-Y. Lin et al., Nanotechnology **16**, 2738 (2005)

5.1.4 *Compared to Literature*

DNA can be aligned by employing different methods such as optical tweezers, hydrodynamic force, confinement elongation, and electrokinetic force with its own pros and cons. One of the main advantage of electrokinetic technique is precise placement of DNA in a chip. DNA in an applied electric field becomes aligned or trapped (coiled state) depending on applied frequency, electrode dimension, bulk solution characteristics etc. Literature highlighting the process of stretching were discussed below due to its relevance in this work.

Namasivayam *et al.*,[16] demonstrated stretching of DNA between two electrodes like a bridge by immobilizing the thiol modified ends of λ phage DNA on a gold surface. The DNA was stretched at 1MHz applied frequency and was sustained only during the presence of an electric field. The bridged DNA retracted back to its immobilized end in the absence of electric field as show in figure 5.8.

[16] V. Namasivayam et al., Anal. Chem. **74**, 3378 (2002)

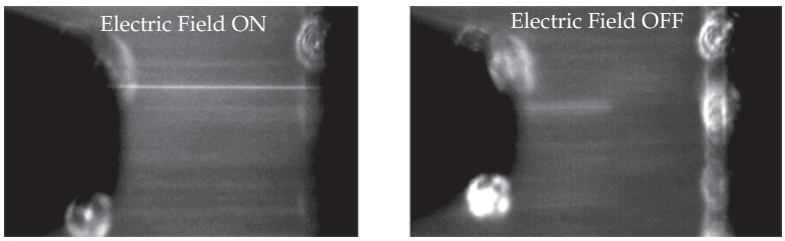

Figure 5.8: DNA fully stretched and bridged between the two electrodes recoils back to the pointed electrode in the absence of an electric field. Source: Namasivayam *et al.*, Anal. Chem. 74 (2002).

Aligned DNA was sustained in the absence of an electric field, but randomly orientated.[17] Lin *et al.*, reported the stretching and immobilization of λ phage DNA at the edge of a gold electrode by electrohydrodynamic flow without terminal modification. Dukkipati *et al.*, fabricated a floating electrode to assist immobilization of non-fuctionalized T2 phage DNA and sustained the stretching in the absence of electric field.

[17] H.-Y. Lin et al., Nanotechnology **16**, 2738 (2005); and V. R. Dukkipati et al., Appl. Phys. Lett. **90**, 083901 (2007)

Braun *et. al.*,[18] demonstrated orientation defined alignment and immobilization of λ phage genome by taking advantage of its cohesive termini as clamping sites (fig 5.10). The authors fabricated gold electrodes with a gap of 16 μm and wetted each elec-

[18] E. Braun et al., Nature **391**, 775 (1998)

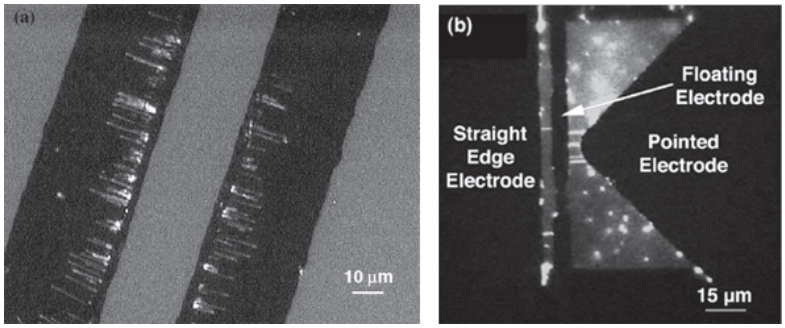

Figure 5.9: Sustained unoriented DNA stretched in the absence of electric field: **(a)** λ phage DNA Sand **(b)** T2 phage DNA, Source: Lin *et al.*, Nanotech. 16 (2005) and Dukkipati *et al.*, APL 90 (2007) respectively.

trode with different thiol functionalized oligo that are specifically complimentary to the λ phage cohesive termini. The DNA was dropped on the electrode surface and stretched by a flow perpendicular to the electrode induced by micropipette suction of the solution. Though the mode of stretching is not by electrokinetics, for the first time they demonstrated orientation defined alignment of DNA. At submicron dimensions precise placement of different anchoring molecules at both electrodes in form of droplets is an arduous task.

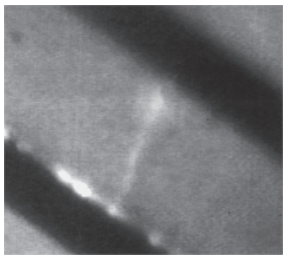

Figure 5.10: Orientationdefined stretching of λ DNA between gold electrodes. Source: Braun *et al.*, Nature (1998).

Incidenticaly, electrokinetic DNA stretching was mostly demonstrated with λ phage DNA and T2 phage DNA with a characteristic length of 16 μm and 55.8 μm, respectively. For the first time in this study, orientation defined stretching was demonstrated at submicron dimensions. This new method can be applied for gap distances from micrometers[19] to tens of nanometers[20] and therefore enabling orientation-defined alignment below the micrometer range. The orientation defined alignment is a very important aspect in the future of DNA based electronics, single molecule analysis and nano-transport systems.[21]

[19] V. R. Dukkipati et al., Appl. Phys. Lett. **90**, 083901 (2007)

[20] D. Porath et al., Nature **403**, 635 (2000)

[21] S. Sahu et al., Nano Lett. **8**, 3870 (2008)

5.2 *Synthesis of Homopolymer DNA*

The homopolymer DNA should contain binding sites for molecular beacon at regular intervals and specific primer binding sites for PCR based amplification only at the terminals. The template sequence must be unique and should have no homology with the

DNA from any natural source and should not form secondary structures in the single stranded state. Finally, there should be an insertion site for inserting the DNA sequence being studied for its role.

Figure 5.11 illustrates this salient features of the DNA template consisting of five specific sites for each molecular beacon (MB1 & MB2) placed alternatively and the specific sequence for adding restriction enzyme sites for concatemerization at the terminals. In a realtime DNA protein interaction experiment either one or both molecular beacons could be used.

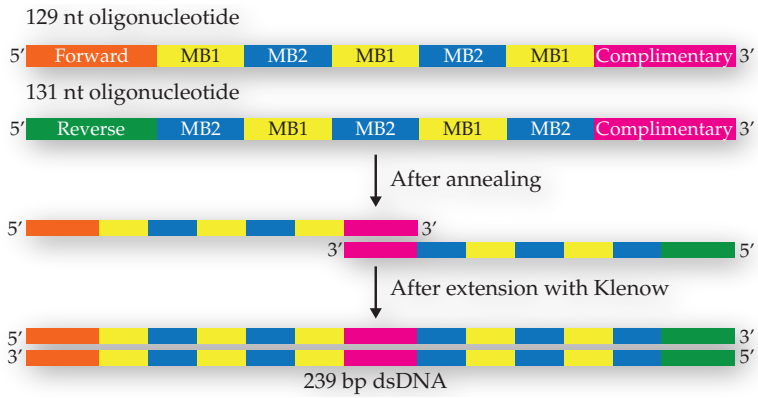

Figure 5.11: Illustration of sequence pattern in homopolymer DNA

5.2.1 *239 bp and 773 bp DNA*

The 239bp DNA was synthesized by annealing of two long oligonucleotides with a length of 129 nt and 131 nt. The annealed oligonucleotides were extended by Klenow fragment in the presence of 4 dNTPs. The 239bp product was separated from non extended oligonucleotides by agarose gel electrophoresis, cloned to plasmid, and transformed into *E.coli*.

nt
nucleotide

The plasmid with cloned DNA was distinguished from the self-circularized plasmid by blue/white screening method. In principle the blue color of the bacterial colony was formed due to the breakdown of chromogenic substrate X-Gal by an enzyme called β-galactosidase, which was induced by IPTG. In the presence of an inserted 239bp DNA, the activity of β-galactosidase

X-Gal
5-bromo-4-chloro-3-indolyl-β-D-galactopyranoside
IPTG
Isopropyl β-D-1-thiogalactopyranoside

was lost due to the structural changes in the protein leading to a white/colorless bacterial colonies. The presence of 239bp insert DNA in the white colonies was confirmed by PCR (fig 5.12a) and the plasmid of positive clones were harvested and used as template for increasing the length of homopolymer DNA.

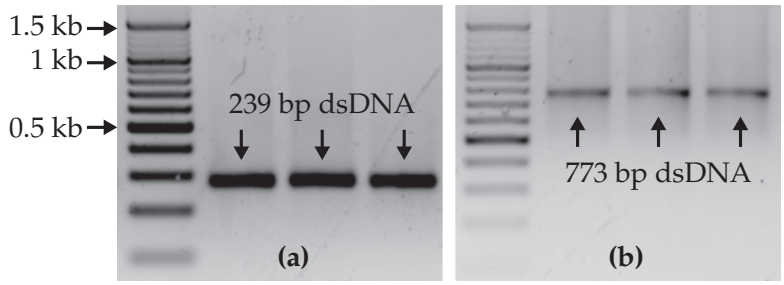

Figure 5.12: Homogeneity of PCR product: **(a)** 239bp DNA and **(b)** 773bp DNA

The 773bp DNA was synthesized by amplification and ligation of three 239bp fragments **A, B** & **C** (fig 5.12b) and cloned into pJET1.2/blunt vector instead of pGEMT vector because pJET1.2/-blunt contains a lethal gene (*eco47IR*) which prevents the growth of transformed *E.coli* containing self circularized plasmid. This method for selecting positive recombinants proved advantageous than blue/white screening. The presence of 773bp insert DNA in the positive clones was conformed by PCR using specific primers (fig 5.13) and the template for realtime analyses of polymerases was prepared by isolating the plasmid from positive clones.

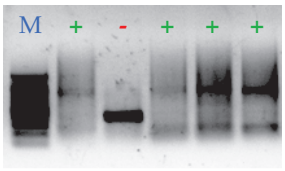

Figure 5.13: Presence of positive clones confirmed by PCR and M is marker

Amplification of 773bp DNA region from the plasmid yielded non-specific products along with a poor yield of target DNA. One possible reason for non-specific amplification could be due to recombination in host cell. Due to the nature of highly repeated sequence, the cell might remove the part of insert DNA by recombination leading to a non-homogeneous population of plasmid, i.e. not all plasmid will carry the same length of insert DNA. In order to overcome this problem the plasmid was restricted with BglII enzyme to release the insert. The target 773bp insert was gel eluted after electrophoresis and used as template for synthesizing 773bp by PCR. Figure 5.12b shows the homogeneous 773bp PCR product.

Further propagation of positive bacterial clones led to the increased instability of inserted 773bp DNA, which led to the scarcity of plasmid supply through cell based amplification for preparing 773bp template DNA. In an attempt to mass produce the 773bp template DNA the plasmid was amplified using *rolling circle amplification* procedure (fig 5.14).[22] In this procedure, the plasmid isolated from the positive clones during the initial experiments was amplified by Phi29 DNA polymerase. To release the 773bp insert DNA, the amplified reaction mixture was restricted with BglII and isolated by gel electrophoresis.

[22] F. B. Dean et al., Genome Res. **11**, 1095 (2001)

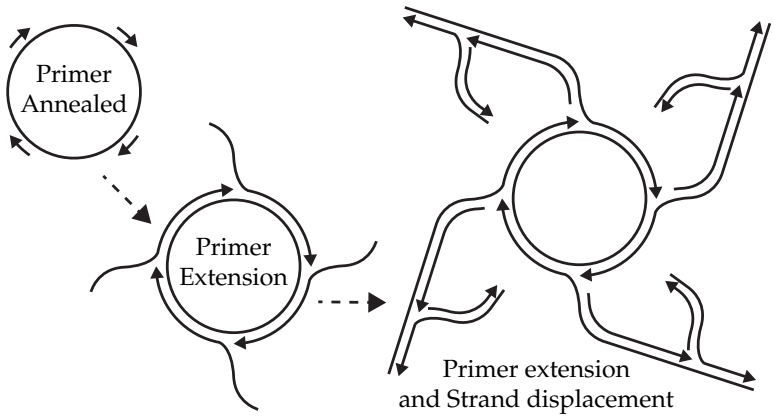

Figure 5.14:
Schematic illustration of rolling circle amplification.

5.2.2 *Synthesis of DNA with Specific Insertion sequences*

The processivity of polymerases depends on the complexity of the DNA sequence. To understand this behavior of polymerase on DNA with a specific sequence, DNA was inserted into the homopolymer template by an *in vitro* technique developed in this study. Since cell based amplification of DNA was not possible with the complexity of homopolymer DNA sequence, this technique was developed as explained in figure 4.16.

The technique was based on bifunctionalization of DNA with biotin and digoxigenin and the sequence to be inserted was designed in the primer that amplifies the 239bp DNA. The three subfragments of 773bp DNA were synthesized by amplifying 239bp

DNA with different combinations of primers. The fragments **A, B** & **C** were amplified with forward primers containing 5′-biotin, insert DNA sequence with EcoRI site and BamHI site and the reverse primers with EcoRI site, BamHI site and 5′-digoxigenin respectively.

The amplified fragments A, B & C were restricted with EcoRI and BamHI enzyme and ligated with T4 DNA ligase. The target DNA was separated and isolated by gel electrophoresis. The gel containing the DNA was treated with β-agarase until the agarose was digested. In this DNA solution three combination of fragments were possible **(A-B-C, A-B-B** & **B-B-C)**. Among the possible combinations, the fragment A-B-C was isolated by the following procedure.

The β-agarase treated DNA solution was incubated with My-One DYNA bead functionalized with streptavidin. In this step the fragments A-B-C and A-B-B binds to the bead because of biotin in sub unit A. The fragment B-B-C was removed during the washing procedure due to the lack of biotin. In the next step, the remaining fragments were released from streptavidin beads and incubated with digoxigenin functionalized polystyrene beads, where the fragment A-B-C binds to the bead and the unbound A-B-B fragment were removed by washing. Finally the A-B-C fragment was separated from other ligated probabilities and used as template for mass production of DNA for realtime analysis.

Insertion of Transcription Regulatory Sequences

The effect of transcription regulatory sequences such as promoter and protein binding regions on polymerase activity was analyzed by inserting those specific sequences into the homopolymer DNA in both 2-5 and 5-2 orientations. Two promoter regions **ropB1** (18 bp) & **exoP** (23 bp) and two protein binding regions **ExpR-LA** (22 bp) & **ExpR-HA** (22 bp) were inserted into the 773bp homopolymer DNA by *in vitro* technique. Restriction analyses of DNA by EcoRI and BamHI also confirmed the presence of inserted sequence in the correct orientation as expected (fig 4.17c). To analyze the role of inserted sequence by both DNA/RNA polymerases, promoters specific for N4 and T7 phage were incorporated at the start point (fig 4.17a).

LA
low affinity
HA
high affinity

5.3 *Molecular-Beacon Characteristics*

Since its invention, molecular beacons were extensively used due to their sequence specific interaction with single-stranded nucleic acids such as detection of PCR gene amplification products,[23] mutational analysis,[24] genotyping and allele discrimination,[25] clinical diagnosis,[26] oligonucleotide degradation studies,[27] DNA-RNA hybridization analysis,[28] real time visualization of hybridization in cells,[29] triplex DNA formation,[30] and DNA-protein interaction.[31]

In this work, shared-stem MB were used instead of conventional MB.[32] A conventional MB contains a target-specific probe domain between two complimentary arms that form the stem. In case of shared stem molecular beacons, one arm of the stem forms part of the target-specific probe domain (fig 5.15). Though shared-stem MB forms more stable duplexes with target molecules than conventional MB, the main strategy was to reduce the intermolecular fluorescence quenching between the target-bound adjacent molecular beacons.

[23] G. Leone et al., Nucleic Acids Res. **26**, 2150 (1998)
[24] A. S. Piatek et al., Antimicrob. Agents Chemother. **44**, 103 (2000)
[25] S. Tyagi et al., Nat. Biotechnol. **16**, 49 (1998)
[26] J. A. M. Vet et al., Proc. Natl. Acad. Sci. USA **96**, 6394 (1999)
[27] J. J. Li et al., Nucleic Acids Res. **28**, e52 (2000)
[32] A. Tsourkas et al., Nucleic Acids Res. **30**, 4208 (2002)

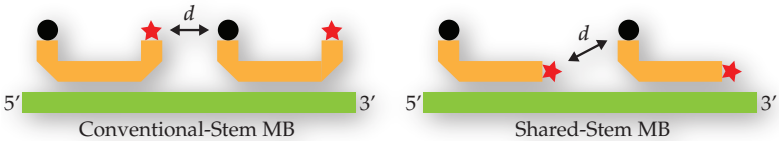

Figure 5.15: Illustration of conventional and shared-stem molecular beacon, where d is the distance

5.3.1 *Thermodynamics*

Understanding the thermodynamics of molecular beacons will facilitate the designing of MB with high target affinity, specificity, and binding kinetic rates. A molecular beacon in solution can have three phases: closed, bound-to target and random-coil. The sequence in the stem region determines the transition of phase between closed and random-coil. A stronger stem region ($\geq$ 6 nucleotide) would prevent random-coiling, but will also act as a competitor and prevent target hybridization. Hence the sequence of the duplex forming stem region has to be optimized for phase transition between open (presence of target) and closed (absence of target) but not random-coil by analyzing the change

in Gibbs free energy (ΔG) and melting temperature (T_M). Though there was no direct relationship between ΔG and T_M, they both provide more qualitative thermodynamic understanding, because they share the same principle components Enthalpy (ΔH) and Entropy (ΔS). The thermodynamic data of molecular beacon and target DNA was computed using *mfold* server: (http://mfold.rna.albany.edu/?q=mfold).[33]

[33] M. Zuker, Nucleic Acids Res. **31**, 3406 (2003)

$$\begin{aligned} \Delta G &= \Delta H - T \times \Delta S \\ T &= (\Delta H - \Delta G)/\Delta S \\ &When \quad \Delta G = 0, \\ T &= \Delta H/\Delta S = T_M \end{aligned} \tag{5.1}$$

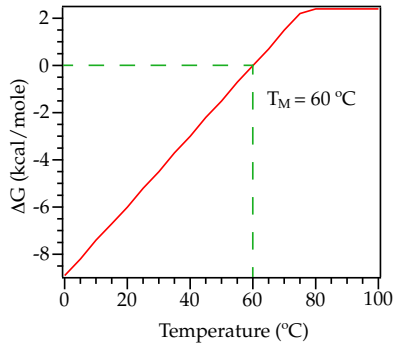

Figure 5.16: Stability of molecular beacon's stem region

Figures 5.17 a&b show the calculated probability dot plots of base-paring of molecular beacon (intramolecular interaction) and MB-template DNA respectively at different temperatures in the presence of 10 mM Na^+ and 10 mM Mg^{2+}. In a probability dot plot, a dot in row i and column j represents a base pair between the i^{th} and j^{th} bases, the *warm* colors represent high probability base pairs and *cool* colors represent low probability base pairs. Thermodynamic analysis of MB-MB interaction (fig 5.17a) shows the stability of the stem region in the absence of target DNA with a probability of $\geq$ 0.9 at 37 ^{o}C.

Similarly, MB-target interaction (fig 5.17b) shows a greater hybridization stability even at 50 ^{o}C with a probability of $\geq$ 0.95. Hence, a decrease in fluorescence during the experiment (at 37

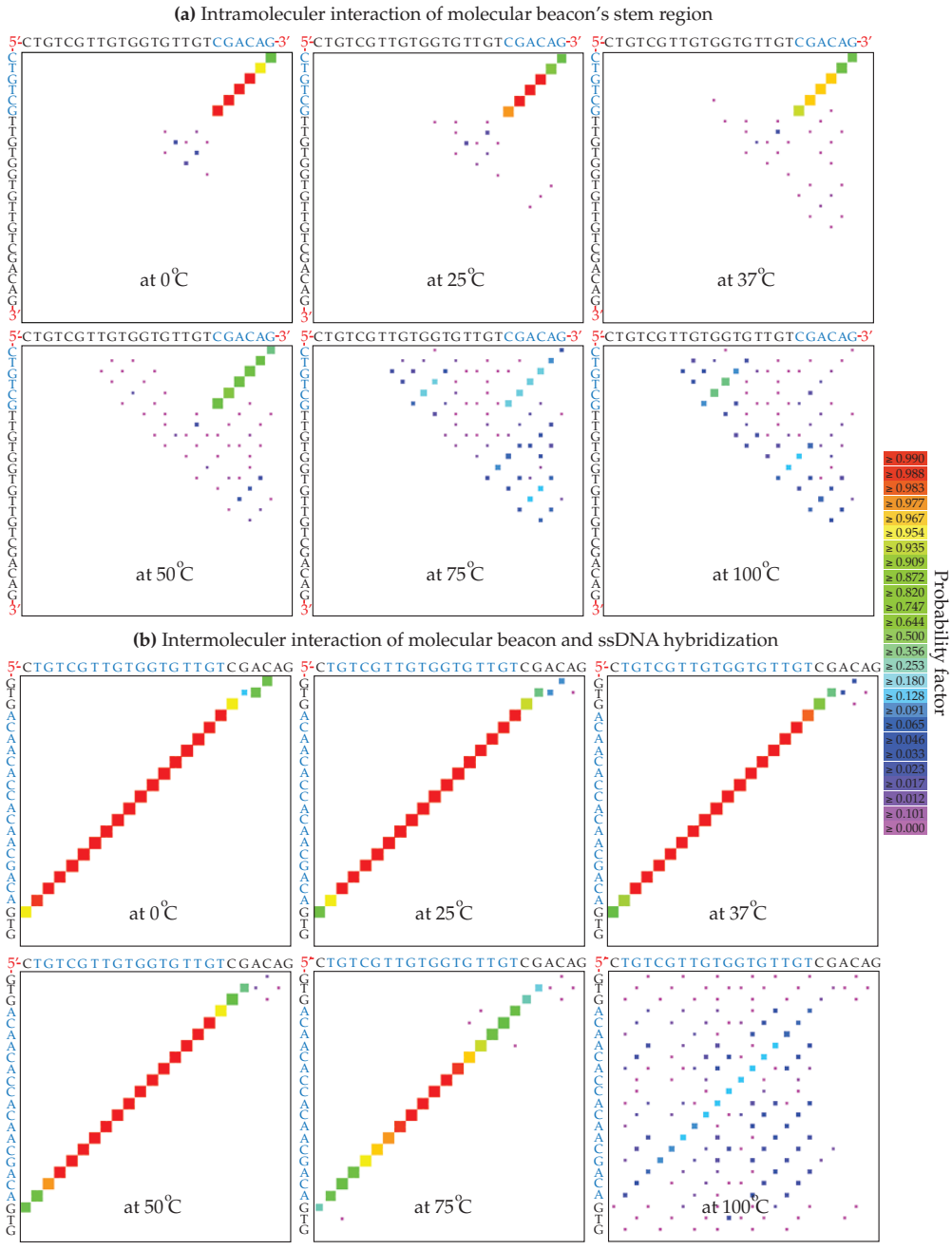

Figure 5.17:
Thermodynamic probability dot plot of nucleotide base-pairing at different temperatures for **(a)** MB stem stability and **(b)** MB-DNA stability. Bases printed in blue participate in hybridization. The warmer and cooler color represent higher and lower probability value, respectively.

^{0}C) directly represents the removal of molecular beacons by polymerase activity and not by thermal denaturation.

5.3.2 *Specificity and Stability*

Molecular beacon incubated with different DNA source such as phage, pUC19, 239bp dsDNA and 239nt ssDNA, increase in fluorescence only with 239nt ssDNA (fig 4.23a) shows the specificity of the molecular beacon towards the target DNA. The molecular beacon with phosphodiester backbone was found susceptible to $3\prime \rightarrow 5\prime$ and $5\prime \rightarrow 3\prime$ exo nuclease activity of the polymerase (fig 5.18).

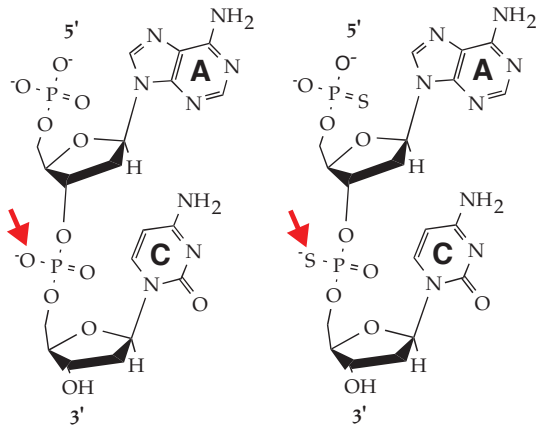

Figure 5.18: Chemical structure of molecular beacon backbone (red arrow): **(a)** Phosphodiester and **(b)** Phosphothioate.

To prevent the degradation and release of fluorophore/quencher from the molecular beacon, a MB with phosphothioate backbone (fig 5.18) was considered and it yield a better fluorescent decay profile compared to phosphodiester-MB (fig **??**b).

5.4 *Polymerase Activity*

5.4.1 *E. coli DNA Polymerase I*

A DNA-dependent DNA polymerase was discovered by Arthur Kornberg in 1950s. It is a 928 amino acid protein with a mass of 109 kDa possessing both $3\prime \rightarrow 5\prime$ (proof-reading activity) and

$5\prime \rightarrow 3\prime$ exonuclease activities along with polymerization domain. [34] DNA polymerase I is not the principal replicative enzyme in *E. coli* due to its slow catalytic rate of 10 - 20 nt s^{-1}, and the main role of this enzyme is to rectify the DNA damage.[35] A *E. coli* carrying mutant *pol A* gene that codes this polymerase still survives.[36] The fluorescent data was normalized at 37^{th} second and fit with an exponential function (eqn. 3.1). Two types of relative polymerase activities were calculated based on fluorescent data and curve-fitted data, where the curve-fitted data represents the global behavior of the polymerase activity.

The polymerase requires Mg^{2+} ion as co-factor for incorporation of nucleotides during polymerization and it is temperature dependent. The effects of temperature and Mg^{2+} ion concentration were studied using the molecular beacon based realtime fluorescent analysis. The temperature dependence was assayed at 37 ^{o}C, optimal temperature of enzyme, and $\pm$ 5 ^{o}C, i.e. 32 ^{o}C & 42 ^{o}C. Figure 5.19 a shows the temperature behavior of *E.coli* DNA polymerase I with a highest activity at 42 ^{o}C and lowest at 32 ^{o}C.

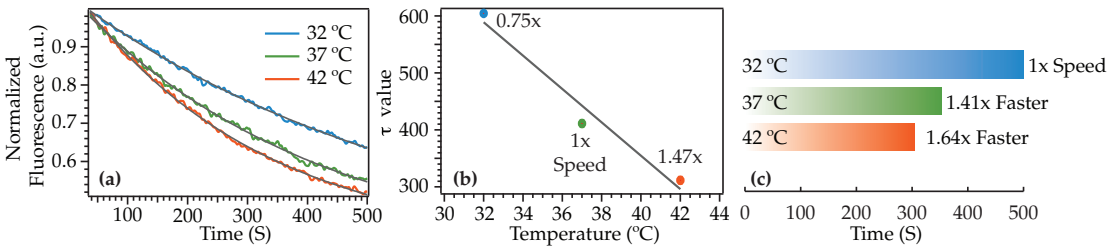

Figure 5.19: Temperature dependent activity of *E. coli* DNA polymerase I on 773 bp DNA: **(a)** Fluorescent data fit with an offset-exponential function, **(b)** τ value based relative speed, and **(c)** Fluorescent data based relative speed.

The calculated comparative speed of the polymerase is a ratio of time taken to reach a given fluorescent value. The enzyme was found to be 1.41$\times$ (37 ^{o}C) and 1.64$\times$ (42 ^{o}C) relatively faster compared to 32 ^{o}C, which was calculated based on the total fluorescent decay at 500^{th} second (fig 5.19c). Analysis of τ values obtained from exponential fit gives the relative speed of 0.75$\times$ at 32 ^{o}C and 1.47$\times$ faster at 42 ^{o}C than enzyme activity at 37 ^{o}C (fig 5.19b).

The activity of polymerase dependent on Mg^{2+} ion at 37 ^{o}C was studied by quenching the Mg^{2+} ion concentration by adding

[34] I. R. Lehman et al., J. Biol. Chem. **233**, 163 (1958); and M. J. Bessman et al., J. Biol. Chem. **233**, 171 (1958)

[35] H. Miller et al., Biochemistry **36**, 15336 (1997)

[36] P. D. Lucia et al., Nature **224**, 1164 (1969)

EDTA, where each molecule of EDTA can chelate to Mg^{2+} ions. The enzyme activity was measured for different Mg^{2+} ion concentrations such as 25%, 50%, and 75% by adding 12.5%, 25% and 37.5% EDTA respectively. The figure 5.20a shows the effect of Mg^{2+} ion concentration on enzyme activity. A total loss of activity was observed, when 75% of Mg^{2+} ions were quenched and retained minimal activity for 25% and 50% of Mg^{2+} quenched compared to a control reaction.

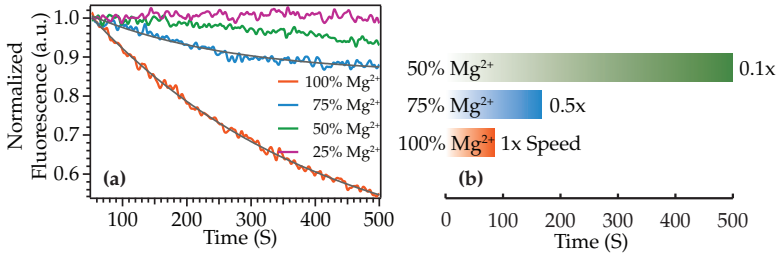

Figure 5.20: Mg^{2+} ion dependent activity of *E. coli* DNA polymerase I on 773 bp DNA: **(a)** Fluorescent data fit with an offset-exponential function and **(b)** Fluorescent data based relative speed.

The enzyme was found to have a relative speed of 0.1× and 0.5× at a Mg^{2+} ion concentration of 50% and 75%, respectively, compared to reaction mixture with 100% Mg^{2+} ion concentration (fig 5.20b).

The effect of inserted sequences on DNA polymerase movement given in figure 4.25 shows a categorical behavior in polymerase activity towards transcription terminators and regulators such as ropB1 & exoP and ExpR-LA & -HA compared to DNA without an insert sequence. This shows the DNA sequence related to transcription does not affect the DNA polymerase activity. since terminator sequences act at RNA and not at DNA level and from the folding energy it is unlikely that the stem-loop forms at DNA level if the DNA is double-stranded.

5.4.2 *T7 DNA Polymerase*

A DNA-dependent DNA polymerase responsible for replication of T7 phage DNA *in vivo* composed of a 1:1 complex of the viral T7 gene 5 protein and the *E. coli* thioredoxin with a mass of 80 kDa and 12 kDa respectively. This fast and highly processive enzyme

has an *in vivo* replication rate of 100 bases per second,[37] lacking 5′ → 3′ exonuclease domain, but the 3′ → 5′ exonuclease activity is approximately 1000-fold greater than that of Klenow fragment.[38] T7 DNA polymerase exhibits higher fidelity of nucleotide incorporation than bacteriophage T4 DNA polymerase[39] and is widely used for site-directed mutagenic studies.[40]

Similar to *E. coli* DNA polymerase I, they require Mg^{2+} ions as cofactor for synthesizing DNA. Hence, the temperature and Mg^{2+} ion dependent activity was assayed. The temperature dependence was assayed at 37 ^{o}C optimal temperature of the enzyme and $\pm$ 5 ^{o}C, i.e. 32 ^{o}C & 42 ^{o}C. Figure 5.21a shows the temperature dependent behaviour of T7 DNA polymerase with a highest activity at 32 ^{o}C and lowest at 42 ^{o}C. The fluorescent data was normalized at the zeroth second and fit with an two-exponential function (eqn. 3.2). Two types of relative polymerase activity were calculated similar to E.coli DNA polymerase I analysis.

[37] G. J. Wuite et al., Nature **404**, 103 (2000); and S. Tabor et al., J. Biol. Chem. **262**, 16212 (1987)

[38] J. Sambrook, *Molecular Cloning: A Laboratory Manual*ISBN 978-087969577-4, 3 ed. (CSHL Press, 2001)

[39] M. J. Englerz et al., J. Biol. Chem. **258**, 11165 (1983)

[40] K. Bebenek et al., Nucleic Acids Res. **17**, 5408 (1989)

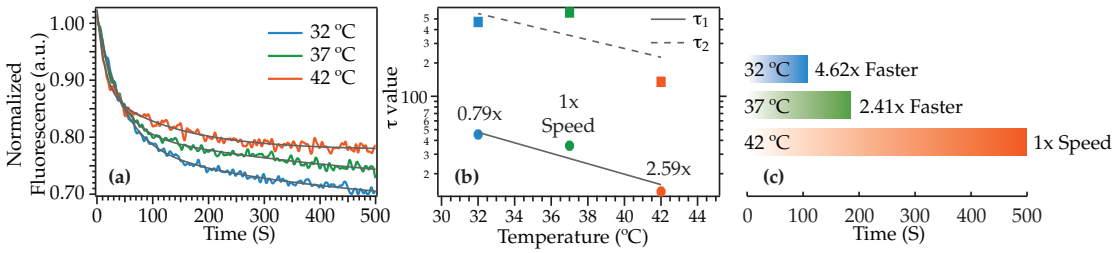

Figure 5.21: Temperature dependent activity of T7 DNA polymerase on 773 bp DNA: **(a)** Fluorescent data fit with an two offset-exponential function, **(b)** τ value based relative speed, and **(c)** Fluorescent data based relative speed.

Since T7 DNA polymerase has a very high catalytic rate, the values τ_1 & τ_2 shows two different events that occur during polymerization, hypothetically, τ_1 could represents the speed of polymerase and τ_2 could represent the rebinding to free DNA influenced by diffusion and concentration. At 32 ^{o}C the enzyme has a relative speed of 0.79$\times$ and 2.59$\times$ faster at 42 ^{o}C compared to τ_1 values at 37 ^{o}C (fig 5.21b). Based on the calculated fluorescent data at the 500^{th} second, the enzyme was found to be 2.41x (37 ^{o}C) and 4.62x (32 ^{o}C) relatively faster compared to 42 ^{o}C (fig 5.21c).

The activity of polymerase dependent on Mg^{2+} ion at 37 ^{o}C was studied by quenching the Mg^{2+} ion concentration by adding EDTA. The T7 DNA polymerase lost its complete activity when

25% of Mg^{2+} ion was quenched (fig 5.22a). Hence the experiments were carried out in the presence of 3.125% & 6.25% of EDTA which quenches 6.25% & 12.5% of Mg^{2+} ion concentration respectively. The enzyme was found to be 19.2x (3.125% EDTA) and 14.2x (no EDTA) relatively faster compared to 6.25% EDTA, which was calculated based on the total fluorescent decay at 500^{th} second (fig fig 5.22c). Analysis of τ_1 values obtained from two-exponential fit showed the relative polymerase speed of 0.59× and 0.39× for 93.75% and 87.5% Mg^{2+} ions, respectively, compared to the control experiment with 100% Mg^{2+} ion concentration(fig 5.22b).

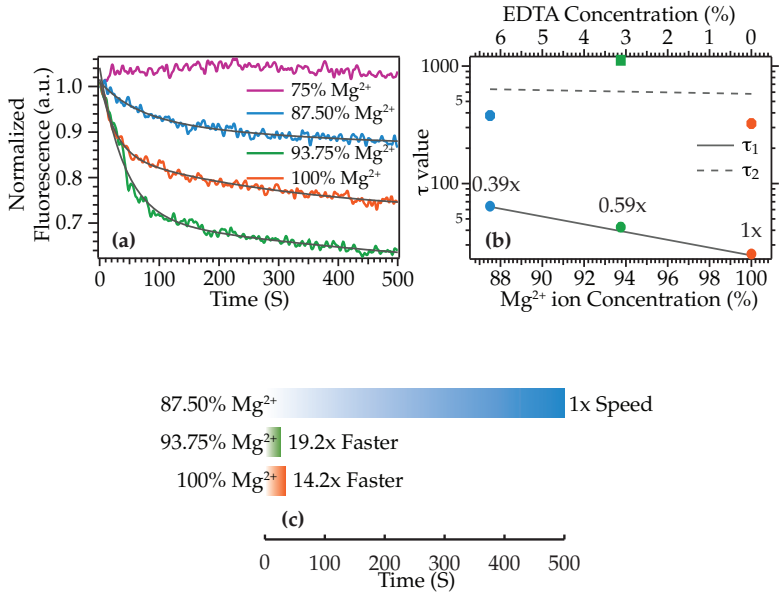

Figure 5.22: Mg^{2+} dependent T7 DNA polymerase activity at 37 ^{o}C: **(a)** Fluorescent data fit with an two offset-exponential function, **(b)** τ value based relative speed, and **(c)** Fluorescent data based relative speed.

In the figure 5.21a, an unusual polymerase behavior was observed with respect to temperature that was contradictory to *E.coli* DNA polymerase I, i.e. the total fluorescence decay was higher at 32 ^{o}C compared to 37 ^{o}C & 42 ^{o}C. Similarly, the fluorescence decay profile in the presence of 3.125% EDTA was higher than the control experiment without EDTA (fig 5.22a).

The possible reason for this unusual behavior could be due to delay between injection of polymerase into the reaction mixture and the start of measuring process, which is usually around 8 sec-

onds. This time-lag could lead to a loss of initial data points being recorded. To understand this problem, the temperature dependent activity was performed at reduced Mg^{2+} ion concentrations by adding 6.25% EDTA. Figure 5.23a shows the behavior of polymerase at 32 ^{o}C, 37 ^{o}C, and 42 ^{o}C. The trend of fluorescence decay was comparable to *E.coli* DNA polymerase I, where higher enzymatic activity was observed at 42 ^{o}C compared to 32 ^{o}C, moreover they all converged at 500^{th} second. The τ_1 based relative speed was found to be 0.24× and 1.4× for 32^{o}C and 42^{o}C, respectively, compared to activity at 37^{o}C (fig 5.23b). The enzyme was found to be 1.83× faster at 37 ^{o}C and 2.63× faster at 42 ^{o}C compared to 32 ^{o}C (fig 5.23c).

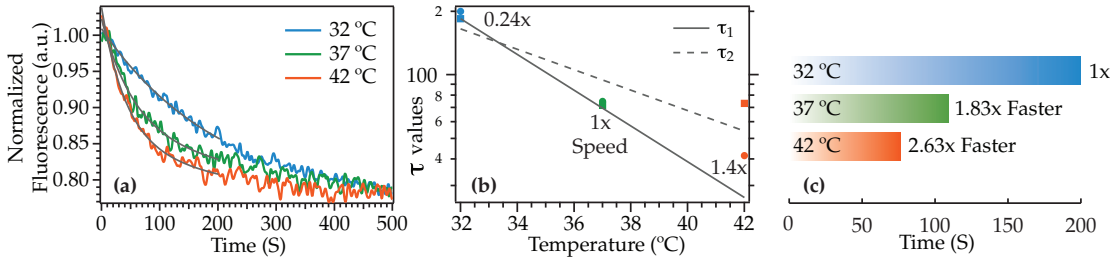

Figure 5.23: Temperature dependent T7 DNA polymerase activity at 37 ^{o}C with reduced Mg^{2+} ion concentration:**(a)** Fluorescent data fit with an two offset-exponential function, **(b)** τ value based relative speed, and **(c)** Fluorescent data based relative speed.

The effect of inserted sequences on DNA polymerase movement given in figure 4.26d shows no distinct pattern in polymerase activity towards transcription terminators and regulators such as ropB1 & exoP and ExpR-LA & -HA compared to DNA without an insert sequence.

5.4.3 *RNA Polymerases*

To investigate the applicability of the realtime molecular beacon based fluorescence method developed in this study for analyzing the behavior of RNA polymerases, promoters specific to T7 and N4 virion RNA polymerase were inserted at the terminals of the homopolymer DNA.

T7 RNA Polymerase

An extremely promoter-specific DNA-dependent RNA polymerase transcribes only DNA downstream of a T7 promoter at a very low error rate. This 99 kDA protein requires Mg^{2+} ions as cofactors. With a elongation speed of $\sim$230 nt s^{-1} compared to *E. coli* RNAP at $\sim$50 nt s^{-1}.[41] The T7 RNA polymerase requires a double stranded promoter for initiation of transcription, but can synthesize mRNA from a single stranded DNA template.

[41] M. Golomb et al., J. Biol. Chem. **249**, 2858 (1974); R. Sousa, Trends Biochem. Sci. **21**, 186 (1996); and L. Bai et al., Annu. Rev. Biophys. Biomol. Struct. **35**, 343 (2006)

Hence the movement of transcribing polymerase could be monitored by a decrease in fluorescence caused by closure of the molecular beacon. But unlike DNA polymerases, they release the transcribed mRNA from the ssDNA template instead of forming RNA-DNA hybrid, causing the removed molecular beacon to re-anneal to the homopolymer DNA. This re-annealing causes overall fluctuation in the fluorescence decay profile as illustrated in the figure 5.24.

The realtime analysis of the T7 RNA polymerase can be monitored using a double-stranded homopolymer DNA template.[42] The orientation of promoter region determines, which strand of DNA to be transcribed by the polymerase. The figure 4.28a shows an increase in fluorescence, when the transcribed mRNA was complimentary to molecular beacon. In the same homopolymer DNA, the positioning of promoter on the other end yielded an mRNA with same sequence as molecular beacon, hence, no increase in fluorescence was observed.

[42] S. A. E. Marras et al., Nucleic Acids Res. **32**, e72 (2004)

N4 Virion RNA Polymerase

To overcome the intrinsic property of T7 RNA polymerase releasing the mRNA transcript from DNA, realtime fluorescence based investigation of specific DNA sequences acting as transcription stoppers were analyzed using N4 virion RNA polymerase. It is a DNA-dependent RNA polymerase recognizing a single-stranded promoter region and leaves the transcribed mRNA to be hybridized to the single-stranded template DNA.[43] Figure 4.28b shows the non-specific binding of the polymerase to the molecular beacon resulting in an increased fluorescence in the absence of target homopolymer ssDNA. Hence, this polymerase is not suitable for molecular beacon based realtime experiments.

[43] C. Casoli et al., FEMS Microbiol. Lett. **4**, 167 (1978); M. Glucksmann-Kuis et al., Cell **84**, 147 (1996); L. L. Haynes et al., Cell **41**, 597 (1985); and K. Kazmierczak et al., EMBO Journal **21**, 5815 (2002)

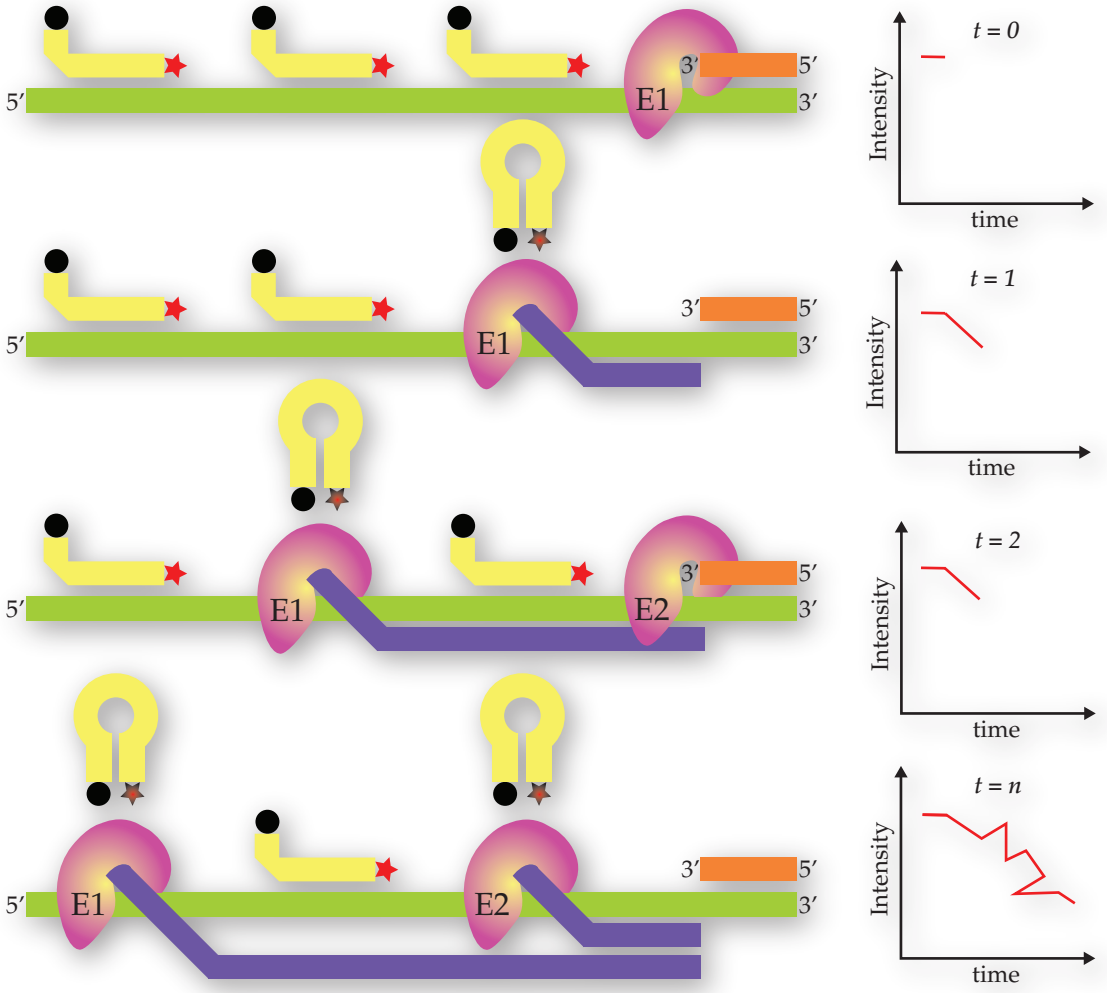

Figure 5.24:
Illustration of T7 RNA polymerase transcribing single-stranded homopolymer DNA. Trancription of one ssDNA by more than one polymerase causing fluctuations in fluorescence.

5.4.4 *Compared to Literature*

The biological processes involving DNA-Protein interactions such as replication transcription, recombination, and repair can be studied using a wide variety of techniques, namely band-shift assay, affinity chromatography, fluorescence analysis, and direct visualization of molecular events by confocal microscopy.

Molecular beacons are very promising candidates for realtime analysis of DNA-Protein interaction. They are extensively used in realtime PCR amplification for characterizing gene expression levels. Though it is termed realtime, the fluorescent data were recorded only after each cycle and not continuously during the course of amplification of the target gene.

Realtime monitoring of DNA protein interaction using molecular beacons was first reported by Li *et al.*,[44] demonstrating the binding of *E.coli* single-stranded binding proteins (SSB) to molecular beacons (fig 5.25a). The increase in fluorescence was observed continuously as a function of time. The same work group also reported an assay for monitoring enzymatic cleavage of ssDNA (fig 5.25b). The fluorescence enhancement was observed in molecular beacons due to enzymatic cleavage by single-strand specific nucleases.

[44] J. J. Li et al., Nucleic Acids Res. **28**, e52 (2000); and J. J. Li et al., Angew. Chem. Int. Ed. **39**, 1049 (2000)

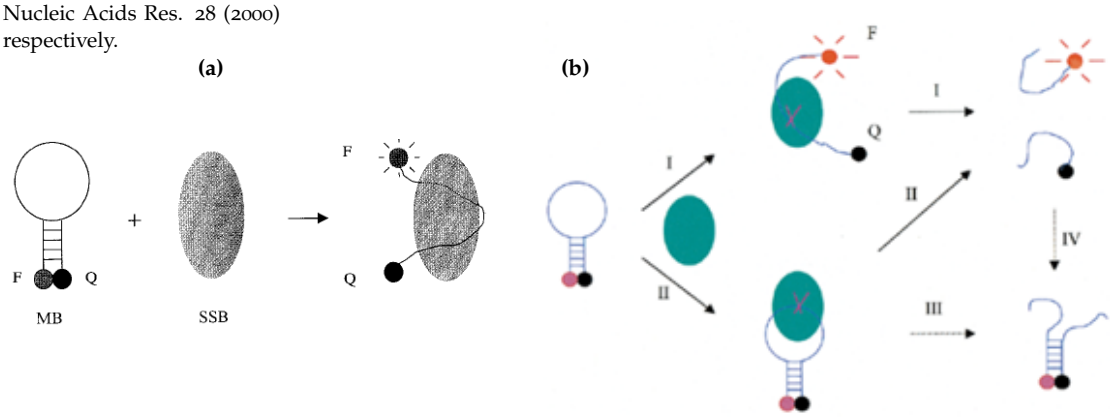

Figure 5.25: Interaction of proteins with molecular beacon: **(a)** Single-stranded binding protein interacting with MB and **(b)** Nuclease interacting with MB, Source: Li *et al.*, Angew. Chem. Int. Ed. 39 (2000) and Li *et al.*, Nucleic Acids Res. 28 (2000) respectively.

[45] S. A. E. Marras et al., Nucleic Acids Res. **32**, e72 (2004)

In vitro transcription measurements in realtime were reported by Marras *et al.*[45] It is a technique, where the fluorescence was

measured continuously. The molecular beacons were designed complimentary to the transcribed mRNA. They used molecular beacons possessing a 2′-*O*-methylribonucleotide backbone to prevent non-specific binding of RNA polymerases and consequent transcription causing increase in fluorescence.

Ma *et al.*,[46] demonstrated realtime monitoring of the DNA polymerase activity using molecular beacons as a template (fig 5.27). A short primer was annealed to the loop region of the molecular beacons. The increase in fluorescence was observed, when the primer is extended causing the fluorophore and quencher to be separated. This technique is limited by the length of the loop-region and physical size of the protein.

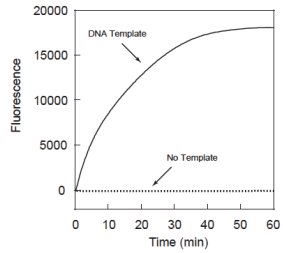

Figure 5.26: Realtime analysis of *in vitro* transcription. Source: Marras *et al.*, Nucleic Acids Res. 32 (2004).

[46] C. Ma et al., Analytical Biochemistry 353, 141 (2006)

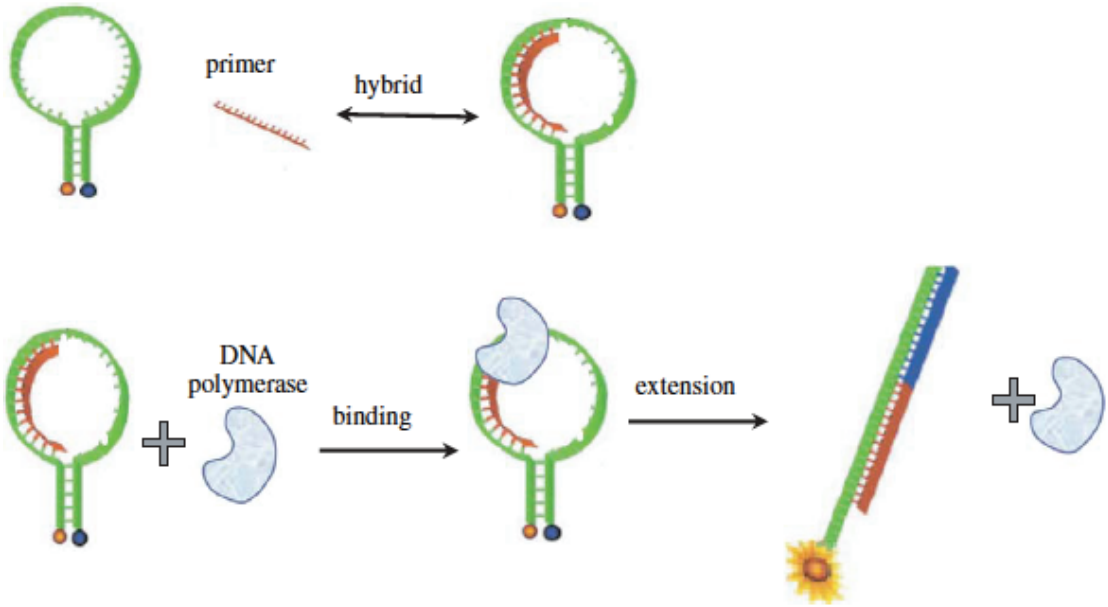

Figure 5.27: Realtime monitoring of DNA polymerase activity using molecular beacon as template. Source: Ma *et al.*, Anal. Biochem. 353 (2006).

The technique developed in this study overcomes this geometrical constraints by using a homopolymer DNA, that can accommodate molecular beacons at regular intervals throughout the sequence. Realtime monitoring of eukaryotic transcription involving association of many proteins requires template DNA with longer geometries, which is not possible with one molecular bea-

con acting as template. Hence the homopolymer DNA templated realtime analysis could be a novel platform for studying DNA-Protein interaction.

5.5 Conclusion

Orientation defined alignment of DNA could be achieved by a very specific binding chemistry. The ability of thiol binding to gold and silane binding to silicon dioxide was used for immobilization of DNA in an orientation defined manner just by dropping them on the electrode surface and applying an electric field. Terminal functionalization of DNA by thiol and silane can be achieved by PCR amplification using modified primers as described in this study, but also by ligation of modified oligonucleotide linker. This allows for functionalization of DNA fragments that cannot be generated by PCR because of their large size and makes orientation-defined alignment of large DNA molecules also feasible for the construction of physical maps. This way of bifunctionalization offers new options for orientation defined studies.

One of the main advantages of electrostatically floating island of gold layer is that it is not affected by the applied voltage. Else a 15 nm gold layer would vaporize immediately in an event of joule heating. Thereby, the DNA is not part of an electrostatic circuit of the whole stretching apparatus, but only subject to the AC stretching field. The number of DNA to be aligned and immobilized can be controlled not only by dilution of the DNA solution, but also by optimizing the size of gold and SiO_2 layers due to steric hindrance.

To analyze the realtime behavior of polymerase activity, a novel DNA template has been developed in this study and termed as *homopolymer DNA*. The homopolymer DNA was designed to contain specific sites for molecular beacons and concatemerization. A 239bp DNA consists of five molecular beacon sites was concatemerized to form a trimer (773bp) using restriction and ligation technique. Cell based amplification of homopolymer DNA was found highly unstable due to the degree of repeatedness in sequence. In order to overcome this, a new technique was developed to select and stabilize the desired homopolymer DNA *in vitro*. It

was based on bifunctionalization of DNA with biotin-digoxigenin and specifically captured with streptavidin and anti-digoxigenin beads. Specific sequences were inserted into the 773bp DNA (A-B-C) at two locations namely, A-BC & AB-C termed as 2-5 & 5-2 orientation, respectively. Transcription regulation regions such as ropB1, exoP, ExpR-LA and ExpR-HA were inserted into the 773bp homopolymer DNA and confirmed by restriction analysis. Single-stranded DNA was prepared from dsDNA to serve as template for realtime DNA-protein interaction studies by alkaline melting of DNA. The *in vitro* stabilization technique could be used to synthesize and stabilize any length of DNA, subject to the processivity of the DNA polymerase during amplification.

The molecular beacon based realtime analysis of the polymerase movement on homopolymer DNA was demonstrated with *E.coli* DNA polymerase I and T7 DNA polymerase. A shared stem molecular beacon was designed to increase the distance between fluorophore and quencher of two neighboring MBs. Thermodynamic analysis of MB showed a stable stem formation in the absence of target DNA at 37 ^{o}C and hybridization with a target DNA above 50 ^{o}C. The MB with phosphothioate backbone was useful in preventing degradation by exonuclease activity of polymerases. An enzyme concentration of 20 units was found sufficient to oversaturate 100 fM ssDNA template. The effect of temperature and Mg^{2+} ion concentration were demonstrated for *E.coli* and T7 DNA polymerases.

The fluorescent data corresponding to the activity of *E.coli* and T7 DNA polymerase were fit with one- and two-exponential functions. The temperature dependent activity was found higher at 42 ^{o}C and lower at 32 ^{o}C for both the enzymes, considered to be above (+5 ^{o}C) and below (-5 ^{o}C) the optimal temperature respectively. In Mg^{2+} ion dependent experiments, the *E.coli* DNA polymerase retains the activity until 50% of Mg^{2+} ions were quenched. Comparatively, T7 DNA polymerase was found highly susceptible to fluctuations in Mg^{2+} ion concentration, leading to a complete loss of activity when 25% of Mg^{2+} ions were quenched. The activity of DNA polymerase was not drastically affected by the presence of inserted transcription stopping and regulatory sequences except a minor shift in global fluorescence decay profile.

T7 and N4 virion RNA polymerases were used to demonstrate the real time monitoring of *in vitro* transcription by MB fluorescent method. T7 RNA polymerase based analysis requires dsDNA as template with specific promoter, whereas non-specific binding of N4 virion RNA polymerase with MB resulted in increase in fluorescence. Hence N4 virion RNA polymerase was not considered for realtime *in vitro* transcription analysis.

5.6 Outlook

The techniques developed for this study such as, orientation defined alignment of DNA, synthesis of homopolymer DNA and realtime analysis of DNA-Protein interaction using molecular beacon, have been employed in investigation of biomolecular processes at a single molecular level. In this work, the molecular beacon based realtime DNA-Protein interaction analysis was demonstrated in bulk solution. But this technique could be implemented for single molecule analysis using confocal microscopy for direct observation of molecular events. Though analysis of *in vitro* transcription of ssDNA template by T7 RNA polymerase was not possible to be demonstrated in bulk solution, in single molecular analysis the movement of polymerase can be directly observed by removal and reannealing of MB to the template DNA producing an on/off fluorescent signal (fig 5.28a).

Movement of two different proteins can be recreated using orientation defined alignment of homopolymer DNA and molecular beacon based realtime DNA-Protein analysis. In this method, the DNA and RNA polymerase will simultaneously replicate and transcribe the same DNA strand from either ends, respectively. Two molecular beacons with distinctive fluorophores will be used as reporters and each MB will bind specifically only to half length of the template DNA (fig 5.28c).

The advantage of orientation defined alignment of DNA can be used as molecular nano-wires upon metallization. The intrinsic electronic property of DNA can be investigated since the termini are bound to the surface by a covalent linkage (fig 5.28d).

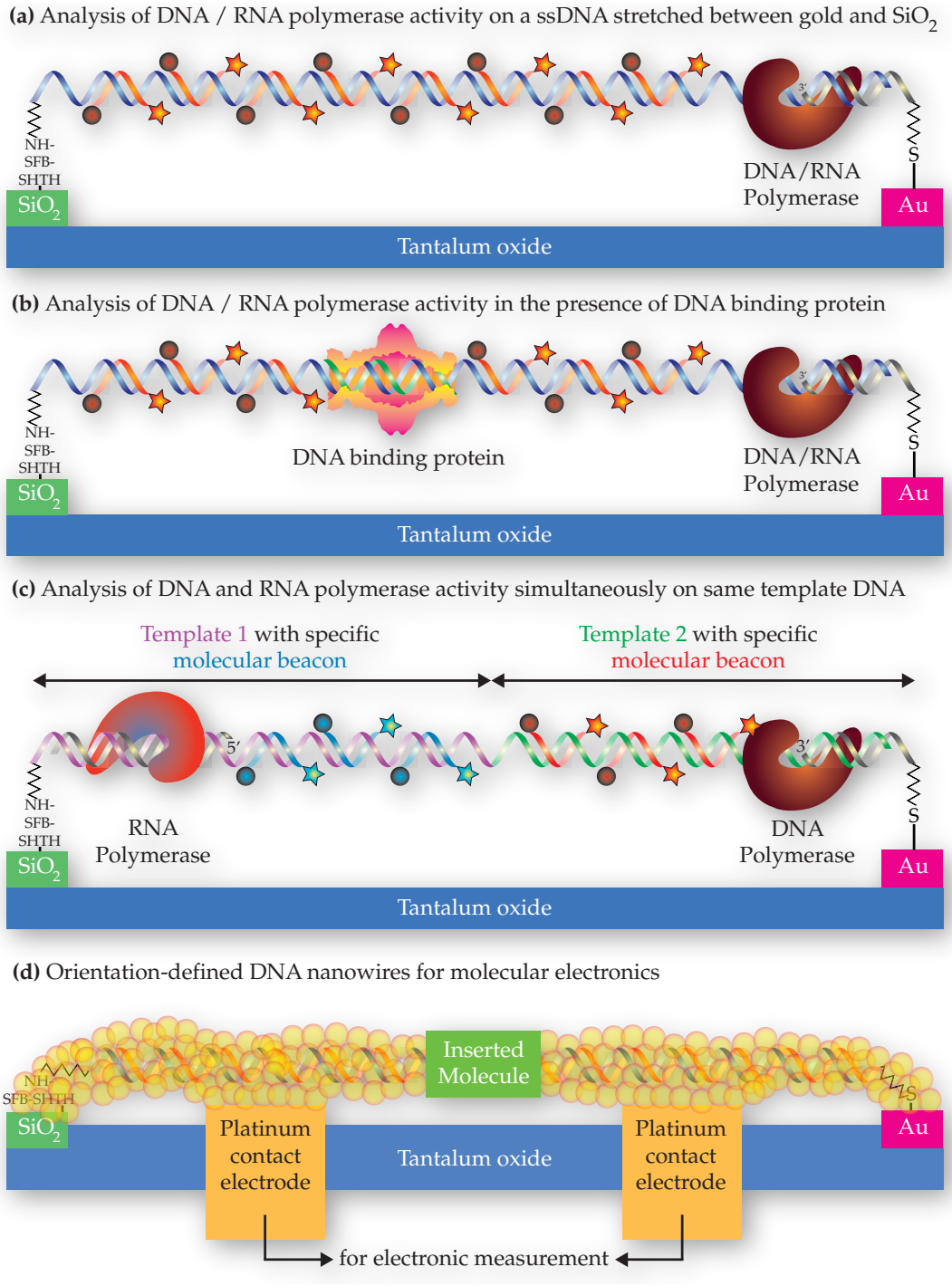

Figure 5.28:
(a-c) Schematic illustration of Confocal microscopy based real-time analysis of single molecule DNA-Protein interaction using homopolymer DNA and molecular beacons, and **(d)** DNA templated molecular nanowires for molecular electronics - An outlook.

6
Summary

A novel platform for studying DNA-Protein interaction in real-time at single-molecule level requires development of three key techniques namely, orientation-defined alignment of DNA, synthesis of homopolymer DNA and the study of DNA-Protein interaction at the macroscopic level.

The DNA was bifunctionalized with thiol-biotin and thiol-silane chemistries. Functionalization with thiol-biotin was straightforward, the DNA was PCR amplified with thiol-forward primer and biotin-reverse primer. Conversely, linking thiol-silane to the DNA termini was a multi-step procedure where the DNA was PCR amplified with thiol-forward and amine-reverse primer and the silane (APTES) was linked to the amino end of the DNA by hetero-bifunctional cross-linkers. The DNA with terminal functional groups was aligned between gold and SiO_2 surface (500-800 nm) using electrokinetic force (50 Hz-1 kHz and 100 kHz-1 MHz) generated by platinum electrode and visualized in scanning electron microscope after palladium ion metallization. The thiol-biotin chemistry was found ineffective in immobilizing the DNA between gold and SiO_2 surface, particularly biotin binding to SiO_2, whereas efficient immobilization of DNA termini was observed with thiol-silane chemistry. The 890 nm long pUC19 DNA with thiol-silane was effectively aligned and immobilized between a gap of 500-600 nm width.

A DNA containing molecular beacon binding sites at regular intervals was termed as *homopolymer DNA* and synthesized by annealing two oligo nucleotides yielding a 239 bp DNA build-

ing block. A 773 bp DNA was synthesized by concatemerizing three monomers of 239 bp DNA (A-B-C) using restriction and ligation. A new technique was developed to select, stabilize and store the homopolymer DNA *in vitro* for mass production of template ssDNA for realtime studies. It is based on affinity principle where the monomer 'A' was tagged with biotin, an untagged 'B' monomer and digoxigenin tagged 'C' monomer were restricted and ligated to yield a trimer. A trimer with proper orientation A-B-C was isolated from the ligation mixture by sequential binding and elution with streptavidin and anti-digoxigenin beads.

To demonstrate the concept of molecular beacon based real-time analysis, the temperature and Mg^{2+} ion dependent activity of *E.coli* DNA polymerase I and T7 DNA polymerase were investigated. A linear fluorescent decay profile was observed for temperature dependent *E.coli* DNA polymerase I activity i.e., compared to 37 ^{o}C, an activity of 1.31$\times$ decrease or increase was observed at 32 ^{o}C and 42 ^{o}C, respectively. Similarly for Mg^{2+} ion dependent activity at 37 ^{o}C, a residual activity was observed until 50% of Mg^{2+} ions were quenched. Compared to control experiment (100% Mg^{2+} ion) a 0.4$\times$ slower activity was observed for 25% of Mg^{2+} ion concentration. Unlike *E.coli* DNA polymerase I, the T7 DNA polymerase shows a high rate of activity at a double exponential scale and very sensitive to changes in temperature and Mg^{2+} ion concentration. The activity increases to 2.59$\times$ faster at 42 ^{o}C compared to optimum temperature. A total loss of activity was observed when 25% of Mg^{2+} ions were quenched. The activity of DNA polymerases was not affected by the presence of transcription -termination and -regulation sequences. This method can also be used for analysing RNA polymerase activity by using dsDNA and ssDNA as templates for bulk reaction and single molecule fluorescence measurement, respectively.

7
Reference

A

Allemand J., Bensimon D., Jullien L., Bensimon A., and Croquette V. pH-dependent specific binding and combing of DNA, *Biophys J.* **73:** 2064 (1997).

Antony T., Thomas T., Sigal L. H., Shirahata A., and Thomas T. J. A Molecular Beacon Strategy for the Thermodynamic Characterization of Triplex DNA: Triplex Formation at the Promoter Region of Cyclin D1, *Biochemistry* **40:** 9387 (2001).

Ashkin A., Dziedzic J. M., Bjorkholm J. E. and Chu S. Observation of a single-beam gradient force optical trap for dielectric particles, *Optics Lett.* **11:** 288 (1986).

B

Bai L., Santangelo T. J., and Wang M. D. Single-Molecule Analysis of RNA Polymerase Transcription, *Annu. Rev. Biophys. Biomol. Struct.* **35:** 343 (2006).

Baumgarth B., Bartels F.W., Anselmetti D., Becker A., and Robert R. Detailed studies of the binding mechanism of the *Sinorhizobium meliloti* transcriptional activator ExpG to DNA, *Microbiol.* **151:** 259 (2005).

Bebenek K., and Kunkel T. A. The use of native T7 DNA polymerase for site-directed mutagenesis, *Nucleic Acids Res.* **17:** 5408 (1989).

Beier M., and Hoheisel J. D., Versatile derivatisation of solid support media for covalent bonding on DNA-microchips, *Nucleic Acids Res.* **27:** 1970 (1999).

Bensimon A., Simon A., Chiffaudel A., Croquette V., Heslot F., and Bensimon D. Alignment and sensitive detection of DNA by a moving interface, *Science* **265:** 2096 (1994).

Bertani G. Studies on lysogenesis. I. The mode of phage liberation by lysogenic *Escherichia coli*. *J. Bacteriol.* **62:** 293 (1951).

Bessman M. J., Lehman I. R., Simms E. S., and Kornberg A. Enzymatic Synthesis of Deoxyribonucleic Acid: II. General properties of the reaction, *J. Biol. Chem.* **233:** 171 (1958).

Bhalla V., Bajpai R. P., and Bharadwaj L. M. DNA electronics, *EMBO reports* **4:** 442 (2003).

Braun E., Eichen Y., Sivan U., and Ben-Yoseph G. DNAtemplated assembly and electrode attachment of a conducting silver wire, *Nature* **391:** 775 (1998).

C

Casoli C., Manini M., and Pesce A. N4 virion RNA polymerase: A zinc metalloenzyme, *FEMS Microbiol. Lett.* **4:** 167 (1978).

D

Dean F. B., Nelson J. R., Giesler T. L., and Lasken R. S. Rapid Amplification of Plasmid and Phage DNA Using Phi29 DNA Polymerase and Multiply-Primed Rolling Circle Amplification, *Genome Res.* **11:** 1095 (2001).

Dimaki M., and Bøggild P. Dielectrophoresis of carbon nanotubes using microelectrodes: a numerical study, *Nanotechnology* **15:** 1095 (2004).

Dukkipati V.R., and Pang S.W. Precise DNA placement and stretching in electrode gaps using electric fields in a microfluidic system, *Appl. Phys. Lett.* **90:** 083901 (2007).

E

Englerz M. J., Lechnerg R. L., and Richardson C. C. Two Forms of the DNA Polymerase of Bacteriophage T7, *J. Biol. Chem.* **258:** 11165 (1983).

F

Falibert F., *et al.* The Composite Genome of the Legume Symbiont *Sinorhizobium meliloti, Science* **293:** 668 (2001).

Fang X., Li J. J., and Tan W. Using Molecular Beacons To Probe Molecular Interactions between Lactate Dehydrogenase and Single-Stranded DNA, *Anal. Chem.* **72:** 3280 (2000).

G

Glucksmann-Kuis M., Dai X., Markiewicz P., and Rothman-Denes L. B. *E. coli* SSB Activates N4 Virion RNA Polymerase Promoters by Stabilizing a DNA Hairpin Required for Promoter Recognition, *Cell* **84:** 147 (1996).

Golomb M., and Chamberlin M. Characterization of T7- specific Ribonucleic Acid Polymerase: IV. RESOLUTION OF THE MAJOR IN VITRO TRANSCRIPTS BY GEL ELECTROPHORESIS, *J. Biol. Chem.* **249:** 2858 (1974).

Gueroui Z., Place C., Freyssingeas E., and Berge B. Observation by fluorescence microscopy of transcription on single combed DNA, *Proc. Natl. Acad. Sci. USA* **99:** 6005 (2002).

H

Han J., and Craighead H. G. Characterization and Optimization of an Entropic Trap for DNA Separation, *Anal. Chem.* **74:** 394 (2002).

Haynes L. L., and Rothman-Denes L. B. N4 virion RNA polymerase sites of transcription initiation, *Cell* **41:** 597 (1985).

Herne T. M., and Tarlov M. J. Characterization of DNA Probes Immobilized on Gold Surfaces, *J. Am. Chem. Soc.* **119:** 8916 (1997).

Hershey A., and Chase M., Independent functions of viral protein and nucleic acid in growth of bacteriophage, *J. Gen. Physiol.* **36:** 39 (1952).

K

Kazmierczak K., Davydova E., Mustaev A., and Rothman-Denes L. The phage N4 virion RNA Polymerase catalytic domain is related to single-subunit RNA polymerases, *EMBO J.* **21:** 5815 (2002).

Keren K., Berman R. S., and Braun E. Patterned DNA Metallization by Sequence-Specific Localization of a Reducing Agent, *Nano Lett.* **4:** 323 (2004).

Keren K., Krueger M., Gilad R., Ben-Yoseph G., Sivan U., and Braun E. Sequence-Specific Molecular Lithography on Single DNA Molecules, *Science* **297:** 72 (2002).

Kim Z., Kim K. S., Kounovsky K. L., Chang R., Jung G. Y., de-Pablo J. J., Jo K., and Schwartz D. C. Nanochannel confinement: DNA stretch approaching full contour length, *Lab Chip* **11:** 1701 (2011).

Krishnan M., Mönch I., and Schwille P. Spontaneous Stretching of DNA in a Two-Dimensional Nanoslit, *Nano Lett.* **7:** 1270 (2007).

Kumar A., Larsson O., Parodi D., and Liang Z. Silanized nucleic acids: a general platform for DNA immobilization, *Nucleic Acids Res.* **28:** e71 (2000).

Kuo T.-C., Streamlined method for purifying singlestranded DNA from PCR products for frequent or highthroughput needs, *BioTechniques* **38:** 700 (2005).

L

Lehman I. R., Bessman M. J., Simms E. S., and Kornberg A. Enzymatic Synthesis of Deoxyribonucleic Acid: I Preparation of substrates and partial purification of an enzyme from *Escherichia coli*, *J. Biol. Chem.* **233:** 163 (1958).

Lehnman I. R. DNA Ligase: Structure, Mechanism, and Function, *Science* **186:** 790 (1974).

Leone G., van Gemen B., Schoen C. D., van Schijndel H., and Kramer F. R. Molecular beacon probes combined with amplification by NASBA enable homogeneous, real-time detection of RNA, *Nucleic Acids Res.* **26:** 2150 (1998).

Li J. J., Fang X., Schuster S. M., and Tan W. Molecular Beacons: A Novel Approach to Detect Protein-DNA Interactions, *Angew. Chem. Int. Ed.* **39:** 1049 (2000).

Li J.J., Geyer R., and Tan W. Using molecular beacons as a sensitive fluorescence assay for enzymatic cleavage of singlestranded DNA, *Nucleic Acids Res.* **28:** e52 (2000).

Lin H.-Y., Tsai L.-C., Chi P.-Y., and Chen C.-D. Positioning of extended individual DNA molecules on electrodes by nonuniform AC electric fields, *Nanotechnology* **16:** 2738 (2005).

Liu X., and Tan W. A Fiber-Optic Evanescent Wave DNA Biosensor Based on Novel Molecular Beacons, *Anal. Chem.* **71:** 5054 (1999).

Lucia P. D., and Cairns J. Isolation of an *E. coli* Strain with a Mutation affecting DNA Polymerase, *Nature* **224:** 1164 (1969).

M

Ma C., Tang Z., Wang K., Tan W., Li J., Li W., Li Z., Yang X., Li H., and Liu L. Real-time monitoring of DNA polymerase activity using molecular beacon, *Anal Biochem.* **353:** 141 (2006).

Marras S. A. E., Gold B., Kramer F. R., Smith I., and Tyagi S. Real-time measurement of *in vitro* transcription, *Nucleic Acids Res.* **32:** e72 (2004).

McIntosh M., Meyer S., and Becker A. Novel *Sinorhizobium meliloti* quorum sensing positive and negative regulatory feedback mechanisms respond to phosphate availability, *Molecular Microbiol.* **74:** 1238 (2009).

Miller H., and Grollman A. P., Kinetics of DNA Polymerase I (Klenow Fragment Exo-) Activity on Damaged DNA Templates: Effect of Proximal and Distal Template Damage on DNA Synthesis, *Biochemistry* **36:** 15336 (1997).

N

Namasivayam V., Larson R. G., Burke D. T., and Burns M. A. Electrostretching DNA Molecules Using Polymer- Enhanced Media within Microfabricated Devices, *Anal. Chem.* **74:** 3378 (2002).

Nasser W., Bouillant M.L., Salmond G., and Reverchon S. Characterization of the *Erwinia chrysanthemi* expl-expR locus directing the synthesis of two N-acyl-homoserine lactone signal molecules, *Molecular Microbiol.* **29:** 1391 (1998).

Neuman K. C., and Block S. M. Optical trapping, *Rev. Sci. Instrum.* **75:** 2787 (2004).

P

Pethig R., and Markx G. H. Applications of dielectrophoresis in biotechnology, *Trends in Biotechnol.* **15:** 426 (1997).

Piatek A. S., Telenti A., Murray M. R., El-Hajj H., Jacobs W. R., Kramer F. R., and Alland D. Genotypic Analysis of Mycobacterium tuberculosis in Two Distinct Populations Using Molecular Beacons: Implications for Rapid Susceptibility Testing, *Antimicrob. Agents Chemother.* **44:** 103 (2000).

Porath D., Bezryadin A., de Vries S., and Dekker C. Direct measurement of electrical Direct measurement of electrical transport through DNA molecules, *Nature* **403:** 635 (2000).

R

Reichmanis E., and Novembre A. E. Lithographic resist materials chemistry, *Annu. Rev. Mater. Sci.* **23:** 11 (1993).

Reisner W., Morton K. J., Riehn R., Wang Z. M., Yu Z., Rosen M., Sturm J. C., Chou S.Y., Frey E., and Austin R. H. Statics and Dynamics of Single DNA Molecules Confined in Nanochannels, *Phys. Rev. Lett.* **94:** 196101 (2005).

Richter J., Mertig M., Pompe W., Mönch I., and Schackert H. K. Construction of highly conductive nanowires on a DNA template, *Appl. Phys. Lett.* **78:**536 (2001).

Richter J., Seidel R., Kirsch R., Mertig M., Pompe W., Plaschke J., and Schackert H. K. Nanoscale Palladium Metallization of DNA, *Adv. Mater.* **12:** 507 (2000).

Riehn R., Lu M., Wang Y.-M., Lim S. F., Cox E. C., and Austin R. H. Restriction mapping in nanofluidic devices, *Proc. Natl. Acad. Sci. USA* **102:** 10012 (2005).

S

Sahu S., LaBean T. H., and Reif J. H. A DNA Nanotransport Device Powered by Polymerase Φ29, *Nano Lett.* **8:** 3870 (2008).

Sambrook J. Molecular Cloning: A Laboratory Manual, 3 ed. ISBN 978-087969577-4, (CSHL Press, 2001).

Schwartz D. C., Li X., Hernandez L. I., Ramnarain S. P., Huff E. J., and Wangt Y.-K. Ordered Restriction Maps of Saccharomyces cerevisiae Chromosomes Constructed by Optical Mapping, *Science* **262:** 110 (1993).

Smith S. B., Finzi L., and Bustamante C. Direct Mechanical Measurements of the Elasticity of Single DNA Molecules by Using Magnetic Beads, *Science* **258:** 1122 (1992).

Sokol D. L., Zhang X., Lu P., and Gewirtz A. M. Real time detection of DNA-RNA hybridization in living cells, *Proc. Natl. Acad. Sci. USA* **95:** 11538 (1998).

Sousa R. Structural and mechanistic relationships between nucleic acid polymerases, *Trends Biochem. Sci.* **21:** 186 (1996).

Strick T. R., Croquette V., and Bensimon D. Single-molecule analysis of DNA uncoiling by a type II topoisomerase, *Nature* **404:** 901 (2000).

Sung K. E., and Burns M. A. Optimization of dielectrophoretic DNA stretching in microfabricated devices, *Anal. Chem.* **78:** 2939 (2006).

T

Tabor S., Huber H. E., and Richardson C. C. *Escherichia coli* thioredoxin confers processivity on the DNA polymerase activity of the gene 5 protein of bacteriophage T7, *J. Biol. Chem.* **262:** 16212 (1987).

Tsourkas A., Behlke M. A., and Bao G. Structure-function relationships of shared-stem and conventional molecular beacons, *Nucleic Acids Res.* **30:** 4208 (2002).

Tuukkanen S., Kuzyk A., Toppari J. J., Häkkinen H., Hytönen V. P., Niskanen E., Rinkiö M., and Törmä P. Trapping of 27 bp - 8 kbp DNA and immobilization of thiol-modified DNA using dielectrophoresis, *Nanotechnology* **18:** 295204 (2007).

Tyagi S., and Kramer F. R. Molecular Beacons: Probes that Fluoresce upon Hybridization, *Nat. Biotechnol.* **14:** 309 (1996).

Tyagi S., Bratu D. P., and Kramer F. R. Multicolor molecular beacons for allele discrimination, *Nat. Biotechnol.* **16:** 49 (1998).

V

Vet J. A. M., Majithia A. R., Marras S. A. E., Tyagi S., Dube S., Poiesz B. J., and Kramer F. R. Multiplex detection of four pathogenic retroviruses using molecular beacons, *Proc. Natl. Acad. Sci. USA* **96:** 6394 (1999).

W

Wang Y. M., Tegenfeldt J.O., Reisner W., Riehn R., Guan X.-J., Guo L., Golding I., Cox E. C., Sturm J., and Austin R. H. Single-molecule studies of repressor-DNA interactions show long-range interactions, *Proc. Natl. Acad. Sci. USA* **102:** 9796 (2005).

Washizu M., Kurosawa O., Arai I., Suzuki S., and Shimamoto N. Applications of Electrostatic Stretch-and-Positioning of DNA, *IEEE Trans on Industry Applications* **31:** 447 (1995).

Wuite G. J., Smith S. B., Young M., Keller D., and Bustamante C. Single-molecule studies of the effect of template tension on T7 DNA polymerase activity, *Nature* **404:** 103 (2000).

Y

Yanisch-Perron C., Vieira J., and Messing J. Improved M13 phage cloning vectors and host strains: nucleotide sequencing of the M13mp18 and pUC9 vectors, *Gene* **33:** 103 (1985).

Z

Zuker M. Mfold web server for nucleic acid folding and hybridization prediction, *Nucleic Acids Res.* **31**, 3406 (2003).

8
Appendix

The 239bp DNA fragment was synthesized by annealing two oligonucleotides given below. The red, blue, green color represents specific sequence for PCR amplification, molecular beacon and annealing of two oligonucleotides, respectively.

129nt Forward Template (5′ → 3′)

5′-AGATAGTAGCAAATACCACAACACCACCACgtgACAACACCACAACGACAgtgTACCACAACACCACCACgtgACAACACCACAACGACAgtgTACCACAACACCACCACACGTGTCTTGTACTTCCCGTC-3′

131nt Reverse Template (5′ → 3′)

5′-GACACGACAACCATGTCGTTGTGGTGTTGTcacGTGGTGGTGTTGTGGTAcacTGTCGTTGTGGTGTTGTcacGTGGTGGTGTTGTGGTAcacTGTCGTTGTGGTGTTGT-GACGGGAAGTACAAGACACGT-3′

PCR Primers for Homopolymer DNA Synthesis

The forward (A_xF) and reverse (A_xR) primers used for concatemerization of 239bp contains a restriction site at the 5′ end of the sequence (red) and followed by template annealing sequence (green). The list of primers used for homopolymer DNA synthesis is given in table 8.1.

Table 8.2 enlists the primers with specific insertion sequence denoted by underlined bases. The primers named AR-N4P contains N4 virion promoter sequence and AR-T7P-N4P contains both T7

and N4 promoter region. The ssDNA template for realtime analysis was prepared by amplifying template DNA with biotin-tagged M13 Forward and unmodified AR-N4P or AR-T7P-N4P reverse primer.

List of Forward Primers

Name	RE site	Sequence (5′ → 3′)
A_1F-NotI	XbaI	AAAAAGCGGCCGCACG**TCTAGA**TAGTAGCAAATACCA
A_2F-NotI	KpnI	AAAAAGCGGCCGCACG**GGTACC**TAGTAGCAAATACCA
A_3F-NotI	HindIII	AAAAAGCGGCCGCACG**AAGCTT**TAGTAGCAAATACCA
A_4F-NotI	BamHI	AAAAAGCGGCCGCACG**GGATCC**TAGTAGCAAATACCA
A_5F-NotI	EcoRI	AAAAAGCGGCCGCACG**GAATTC**TAGTAGCAAATACCA
AF-control	NotI	AAAAAGCGGCCGCAC

List of Reverse Primers

Name	RE site	Sequence (5′ → 3′)
A_1R-AscI	KpnI	AAAAAGGCGCGCCATG**GGTACC**ACGACAACCATGTCG
A_2R-AscI	HindIII	AAAAAGGCGCGCCATG**AAGCTT**ACGACAACCATGTCG
A_3R-AscI	Kpn2I	AAAAAGGCGCGCCATG**TCCGGA**ACGACAACCATGTCG
A_4R-AscI	BamHI	AAAAAGGCGCGCCATG**GGATCC**ACGACAACCATGTCG
A_5R-AscI	EcoRI	AAAAAGGCGCGCCATG**GAATTC**ACGACAACCATGTCG
AR-control	AscI	AAAAAGGCGCGCCAT

Table 8.1:
List of primer for hompolymer DNA synthesis. The bases denoted in red are restriction sites and bases in green denotes the template complimentary sequence.

List of Primers with insertion sequence

Name	RE site	Sequence (5′ → 3′)
AF-M13F		GTTTTCCCAGTCACGACTAGTAGCAAATACCA
AF-exoP	EcoRI	AAACGGAATTCCGAAAGGCCGCGCCACTTGTGCGCG GCCTAGTAGCAAATACCA
AF-ropB1	EcoRI	AAACGGAATTCCGAAAGGCCGGGGCGACCCGGCCTA GTAGCAAATACCA
AF-ExpR-HA	EcoRI	AAACGGAATTCCGAAACCCCCACAAATTTATTGGGAA ATAGTAGCAAATACCA
AF-ExpR-LA	EcoRI	AAACGGAATTCCGAAACCCCCACAAATCTATTGTGAA ATAGTAGCAAATACCA
AR-N4P		ATCTTCATTAAGAAGCTCCGCTTCTTTTGGACGACAAC CATGTCG
AR-T7P-N4P		AAAAAGCGGCCGCACGTAATACGACTCACTATAGGGA GACCACCATGGATCTTCATTAAGAAGCTCCGCTTCTTTTG

Table 8.2:
List of primers with insertion sequence. The bases denoted in red are EcoRI sites, underlined bases refers to the specific insertion sequence, and green denotes the template complimentary sequence.

9
List of Publications

Research Article

Venkatesh A.G., Herth S., Becker A., and Reiss G. Orientation-defined alignment and immobilization of DNA between specific surfaces. *Nanotechnology,* **22(14):** 145301 (2011).

Sebastian A., Venkatesh A.G., and Markx G. H. Tissue engineering with electric fields: Investigation of the shape of mammalian cell aggregates formed at interdigitated oppositely castellated electrodes. *Electrophoresis,* **28(21):** 3821 (2007).

Venkatesh A.G., and Markx G.H. On the height of cell aggregates formed with positive dielectrophoresis. *J. Phys. D: Appl. Phys.* **40:** 106 (2007).

Conference Proceeding and Highlights

Venkatesh A.G., Herth S., Becker A., and Reiss G. Functional groups orientate DNA binding across sub-micron gap. *Nanotechweb.org* April 12, 2011.

Venkatesh A.G., Herth S., Becker A., and Reiss G. Orientation defined stretching and immobilization of DNA by AC electrokinetics. *DPG - Regensburg (Germany),* March 22 - 26, 2010.

Venkatesh A.G., Herth S., Becker A., Huetten A., and Reiss G. Orientation defined stretching and fixing of DNA by AC volt-

age induced electro-osmotic Flow. *Biosensors 2008 - Shanghai (China),* May 14 - 16, 2008.

Venkatesh A.G., Herth S., Becker A., Huetten A., and Reiss G. Orientation defined stretching and fixing of DNA by AC voltage induced electro-osmotic flow. *DPG - Berlin (Germany),* February 25 - 29, 2008.

Sebastian A., Venkatesh A.G., Buckle A.M., and Markx G.H. Tissue engineering with electric fields: Investigation of the shape of mammalian cell aggregates formed at interdigitated oppositely castellated electrodes. *Electrostatics 2007, Oxford (UK),* March 25 - 29, 2007.

Carney L., Buckle A.M., Sebastian A., Venkatesh A.G. and Markx G.H. Tissue engineering with electric fields: microfabrication of haematopoietic stem cell microniches. *British Society of Rheology 2006 Annual Meeting, Manchester (UK),* December 11 - 12, 2006.

Venkatesh A.G., and Markx G.H. What is the maximum size of cell aggregates which can be formed with positive dielectrophoresis? *Biodielectrics: Theories, Mechanisms and Applications, Leicester (UK),* April 10 - 12, 2006.

10
Acknowledgement

First, I would like to thank Prof. Dr. Günter Reiss for giving me the opportunity to do my Ph.D. in his group and his inspiring fine thoughts behind the experimental principles, invaluable guidance and discussions made this thesis possible.

I am deeply grateful to my advisor Dr. Simone Herth for her supervision and encouragement throughout the course of this study. Her continuous support was essential in progress and success of my research work. And I am privileged for being her first doctoral student.

I thank Prof. Dr. Anke Becker for her intellectual support, encouragement and enthusiasm in this research work from day one. I feel grateful to Prof. Dr. Walter Arnold and Prof. Dr. Karl-Josef Dietz for providing their lab facility for my research work at very crucial juncture when I was left with no lab space.

I would also like to acknowledge Prof. Dr. Walter Pfeiffer and Prof. Dr. Peter Reimann for agreeing to be part of my examination committee. I thank International Office for STIBT fellowship in the last phase of my research work.

Dr. Karsten Rott and Dr. Camelia Albon for teaching the nuances of electron-beam lithography during my initial days. A special mention to Mrs. Aggi Windmann for assisting with all kind of official procedures during my stay in Germany. I want to express my gratitude to Dr. Jan-Michael Schmalhorst and all the colleagues from D2-Physics, W0-Genetics lab, W5-Plant Biology Lab, and G01-CeBiTec for their fruitful discussions, for sharing the lab and for a great help.